Ruamāhanga Airborne Aquifer Mapping Project: Phase 2 Hydrogeological Model

RL Kellett
DT Berhe
P Scadden
TR Sahoo
JM Lee
F Sanders
AL Kirkby
M Herpe
AF Boyes

GNS Science Consultancy Report 2025/23
June 2025

DISCLAIMER

This report has been prepared by the Institute of Geological and Nuclear Sciences Limited (GNS Science) exclusively for and under contract to Greater Wellington Regional Council. Unless otherwise agreed in writing by GNS Science, GNS Science accepts no responsibility for any use of or reliance on any contents of this report by any person other than Greater Wellington Regional Council and shall not be liable to any person other than Greater Wellington Regional Council, on any ground, for any loss, damage or expense arising from such use or reliance.

Use of Data:

Date that GNS Science can use associated data: 01 July 2025

BIBLIOGRAPHIC REFERENCE

Kellett RL, Sahoo TR, Kirkby AL, Berhe DT, Lee JM, Herpe M, Scadden P, Sanders F, Boyes AF. 2025. Ruamāhanga Airborne Aquifer Mapping Project: Phase 2 Hydrogeological Model. Lower Hutt (NZ): GNS Science. 61 p. Consultancy Report 2025/23.

CONTENTS

FIGURES

TABLES

EXECUTIVE SUMMARY

The Ruamāhanga Airborne Aquifer Mapping Project is a multi-year initiative (2022–2025) jointly funded by the Kānoa Regional Economic Development and Investment Unit (Kānoa), Greater Wellington Regional Council (GWRC), Masterton District Council, Carterton District Council and South Wairarapa District Council. The project utilises airborne electromagnetic surveying technology (SkyTEM) to improve groundwater resource potential mapping and 3D modelling of the spatial extent of the aquifers within the Ruamāhanga Catchment in the Wairarapa Valley. The project is managed by GWRC on behalf of the group that provided funding. GNS Science (GNS) undertook technical support of the acquisition and leadership of the processing and interpretation.

Phase 1 of the project involved processing the SkyTEM data through to the stage of developing resistivity models. It included a series of workshops that reviewed the SkyTEM models compared to existing borehole and other geophysical data. This phase of the project resulted in the delivery of a report and an archive of the SkyTEM data and models. Phase 2 of the project is a detailed interpretation of the resistivity data and the development of a hydrogeological model through a series of tasks.

Task 1 is a review of the Quaternary, Tertiary and Mesozoic basement geology, and existing geological and hydrogeological models to identify the different elements of the hydro-stratigraphy. This framework is then used to generate a layered model that divides the strata into three discrete hydrogeological units and a basement unit. The top layer (HU-1) includes the Holocene deposits present in the river valleys, and Holocene and Late Pleistocene gravel on the uplifted terraces across the valley. It also includes finer-grained sediments in the Lake Wairarapa area. The layer is typically 10–50 m thick (maximum ~70 m). The second layer (HU-2) includes older Quaternary gravel deposits and their finer-grained equivalents. The layer is typically 100–300 m thick (maximum ~500 m).

Below this unit the strata are more likely to be consolidated sediments, and HU-3 includes mostly Pliocene and Miocene sandstone, mudstone and limestone. These units outcrop on the hills around the edges of the basin and can be mapped dipping under the Quaternary section. Very few boreholes have tested these Tertiary sediments for their groundwater potential, but in some cases the SkyTEM resistivity values indicated that they could be aquifers. The Tertiary rocks were also mapped in published interpretations of the geology of the Wairarapa from seismic surveys.

The greywacke exposed in the footwall of the Wairarapa Fault (Tararua and Remutaka ranges), the eastern hills (Aorangi Range) and faulted blocks in the centre of the basin (Tiffin Hill and Te Maire Ridge) is composed of indurated sandstone, mudstone and breccia with low groundwater potential.

Task 2 focussed on correlating the SkyTEM resistivity with the QMAP geology and borehole lithologies. A range of resistivity facies are defined that can, in turn, be classified into zones with different Aquifer Potential. Aquifer Potential (AP) is defined as the likelihood that the interval contains water bearing geological units (low AP is a confining layer, high AP is a good aquifer). The output of Task 2 is a 3D model that comprises the SkyTEM resistivity value, classified resistivity value (15 levels), classified hydrogeological unit (HU-1, 2, 3 or Basement), and an associated AP value for all SkyTEM measurements points (147,601) extending from ground surface to the depth of investigation (approximately 300 m).

Task 3 included building a 3D model of a pilot area in the central Wairarapa Valley and presenting it to a group of stakeholders using a web-mapping product (JS Map Server). Following a review of the pilot project, the entire SkyTEM survey area was modelled using the same approach.

The project has generated a series of products that can be used by groundwater professionals, policy makers and administrators of groundwater allocations, landowners and other interested groups to develop more local-scale groundwater assessments. These products include grids of the hydrogeological units (elevation and thickness), 3D models of the hydrogeological model in Leapfrog software, and a web-based mapping tool that can present the model in cross-sections and pseudo-boreholes.

1.0 Introduction

The Ruamāhanga Airborne Aquifer Mapping Project is a three-year initiative jointly funded by the Kānoa Regional Economic Development and Investment Unit (Kānoa, formerly the Provincial Growth Unit), Greater Wellington Regional Council (GWRC), Masterton District Council, Carterton District Council and South Wairarapa District Council. The project was originally designed to begin in 2019 and conclude in 2022. Delays due to COVID-19 meant that the project started in 2022. The project applies Airborne Electromagnetic (AEM) survey technology (SkyTEM) to improve the understanding of the hydrogeological units in the Ruamāhanga Catchment. The goal is to develop a more detailed groundwater resource-potential map and provide input for the next generation of 3D groundwater flow models within the Wairarapa Valley. To execute the project, GWRC engaged SkyTEM Australia to collect the AEM data and GNS Science (GNS) to process and interpret the data.

The area covered by the survey included low-lying areas in southern Wairarapa (Lake Onoke, Lake Wairarapa and a small section offshore), five urban centres (Featherston, Martinborough, Carterton, Greytown and Masterton) and some elevated areas around the edges of the basin (Figure 1.1). In this report we refer to the area covered by the survey as the Ruamāhanga Catchment, recognising that it is only the portion of the catchment that lies in the floor of the Wairarapa Valley. For reference, a map with all of the key locations discussed in this report is shown in Figure 1.2.

Phase 1 of the project was completed in June 2024 with the delivery of a resistivity model developed from the AEM data to GWRC (Kellett et al. 2024). Phase 2 is the development of a hydrogeological model and web-based mapping product. This phase of the project commenced in July 2024.

The current report oulines the methodology used to develop the hydrogeological model. Hydrogeological interpretation of resistivity models is a process of translating resistivity values (typically represented by the unit ohm.m) to categorical or numerical values of more immediate use to a hydrogeologist. The numerical values present in a resistivity model are a function of complex relationships between bulk lithology, porosity, grain size and sorting, mineralogical content, such as clay and permeability, and groundwater properties, such as salinity. Supporting local information is therefore required to help interpret the resistivity models.

The report has four aims:

1. Provide a summary of the current geological and hydrogeological models in the Ruamāhanga Catchment.
2. Provide an overview of the conceptual geological model used as a framwork for a revised hydrogeological model.
3. Give a detailed description of the steps taken to develop the hydrogeological model from the SkyTEM resistivity model.
4. Describe the products delivered to GWRC as the outputs of Phase 2.

The report is structured in the following way:

- Section 2 describes the SkyTEM resistivity model used as the basis for the hydrogeological model.
- Section 3 presents the background geological information and describes the conceptual geological model.
- Section 4 summarises the previous hydrogeological models, including their limitations and the need for a revised model.
- Section 5 discusses the borehole data used to support the SkyTEM interpretation.

- Section 6 outlines the process used to establish a set of relationships between electrical resistivity and the lithological and hydrogeological properties of the units, which is critical to developing the improved model.
- Section 7 presents the improved hydrogeological model with a description of the products. The concepts of the Hydrogeological Unit, adapted from previous SkyTEM interpretation projects is used to build the layered structure. The Aquifer Potential is the ultimate output of this component of the project, and its derivation is described in this section. The web-based mapping application being used to publicise results is also described in this section.
- Section 8 summarises the results of phase 2 of the project.
- Section 9 makes recommendations as to the value of these products for a range of users.

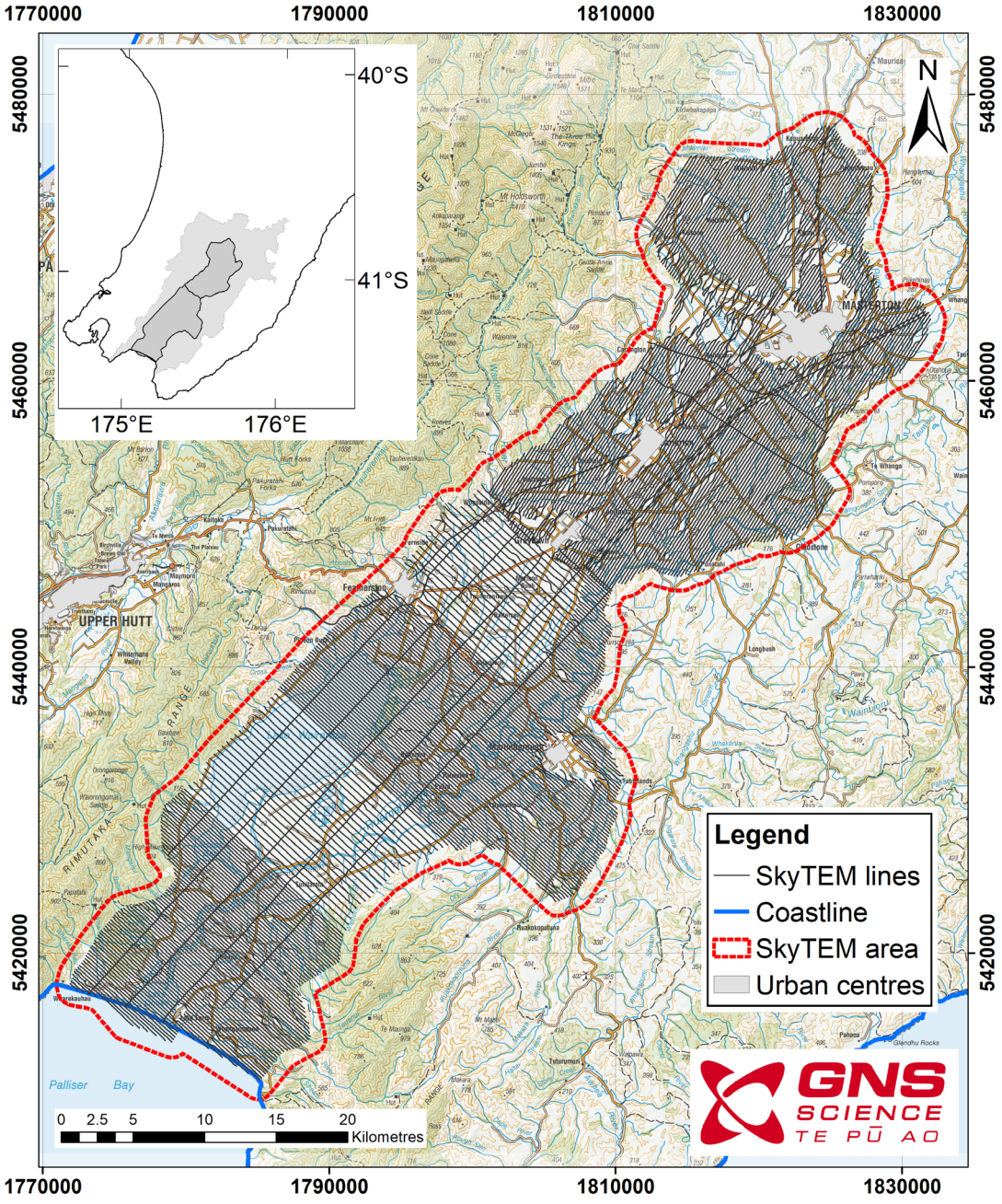

Figure 1.1 Location map of the Ruamāhanga Airborne Aquifer Mapping Project area. The inset map shows the lower North Island and the location of the survey area (dark grey) within the Ruamāhanga Catchment (light grey). The main map shows the SkyTEM flight lines.

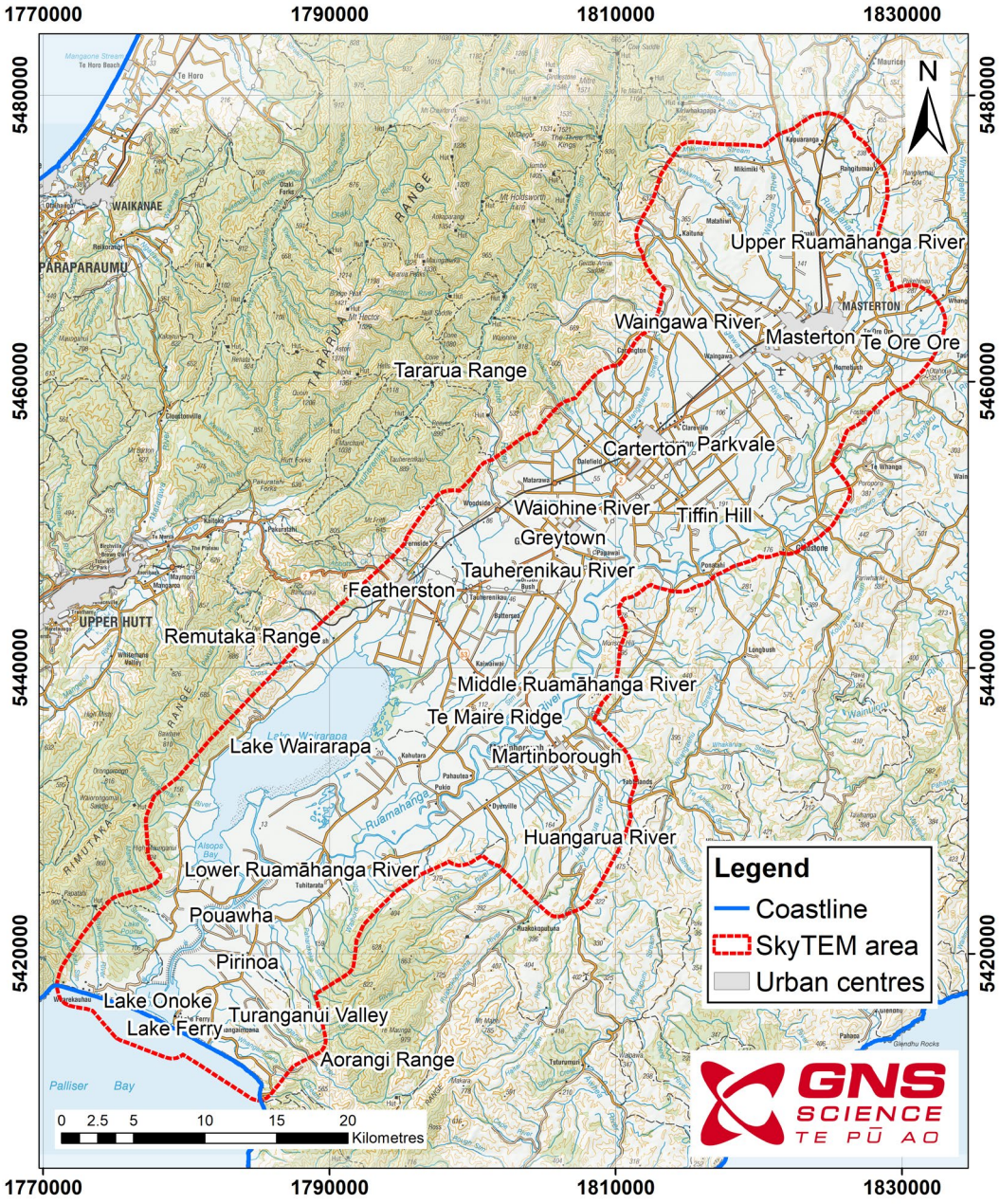

Figure 1.2 Location map of the Ruamāhanga Airborne Aquifer Mapping Project area, including towns, rivers and other key areas discussed in this report.

Throughout both phases of the project, the following software have been used to develop the models:

- Seequent AGS Workbench™ (Workbench): The SkyTEM resistivity model.
- Seequent Leapfrog™ (Leapfrog): The conceptual geological model, the hydrogeological model and the aquifer potential model.
- ALT WellCAD™ (Wellcad): Borehole lithology logs.
- JS Map Server: Display of hydrogeological model and supporting borehole and geological data.

Workbench provides the tools for processing and inverting the AEM data (Phase 1). Leapfrog provides the tools for interpreting borehole geological data, AEM resistivity data in both pseudo-borehole and 3D geophysical model format. More detailed geological interpretation of the boreholes was undertaken in WellCAD. The final models are exported in a range of formats required by GWRC and published on the web using the GNS-developed JavaScript (JS) Map Server. These outputs are discussed in Section 7.

2.0 SkyTEM Airborne Electromagnetic Resistivity Model

2.1 Smooth and Sharp Resistivity Models

The resistivity models produced as part of Phase 1 (Kellett et al. 2024) consist of 147,601 1D models collected into a 3D network of resistivity values. The models were generated using a spatially constrained inversion process that resulted in two outputs:

1. Smooth model: 40 layers with a vertical constraint that imposes a gradual change between layers resulting in smooth changes across layer boundaries.
2. Sharp model: 40 layers with a vertical constraint that maintained a constant resistivity in each layer until the model misfit demanded a larger jump in resistivity, resulting in sharp changes across layer boundaries.

The processing and inversion procedures followed the standard workflow developed by Rawlinson et al. (2021) and Auken et al. (2015), and are described in detail in Sections 3 and 4 of Kellett et al. (2024).

The 1D models at each sounding location can be presented in three main file formats:

3. Pseudo-borehole format with a collar, survey and interval file. This format is suitable for 3D geological modelling software, such as Leapfrog. The smooth and sharp models are represented by separate files. The advantage of this format is that it maintains the individual layered models. The disadvantage is that the gaps between survey lines are more obvious in the models.
4. Average resistivity in a layer format for both smooth and sharp models stacked as layers below ground surface. The data are interpolated onto a regular grid and the layering is discretised more finely to allow smooth lateral changes. The advantage of this approach is that it efficiently represents a model across the entire valley. The disadvantage is that it ignores the structural relationships between low lying areas and the elevated areas at the edges of the model.
5. Average resistivity in a layer format for both smooth and sharp model stacked as layers relative to mean sea level. The data are interpolated onto a regular grid and the layering is discretised more finely to allow smooth lateral changes. The advantage of this approach is that it can be loaded into the 3D workstation and interpreted alongside other geological data. The disadvantage is that it requires many layers to represent the model from the northern area that is >200 m above sea level (masl) and the coastal area at 0 masl with the same vertical resolution.

The pseudo-borehole format is easily loaded into any 3D geological modelling software (Figure 2.1). The stacked average resistivity formats require integration into a cube or voxel model to be imported into Leapfrog (Figure 2.2). The 3D models of resistivity can be truncated at depth using the Depth of Investigation (DOI) data to represent the resolution of the SkyTEM data (Christiansen and Auken 2012). The resistivity data are presented in a range of colour schemes to highlight different aspects of the models. The typical colour ramp is shown in Figure 2.3. This colour bar was chosen during a series of workshops in Phase 1 of the project (Kellett et al. 2024). Red colours represent low-resistivity materials and blue colours represent high-resistivity materials.

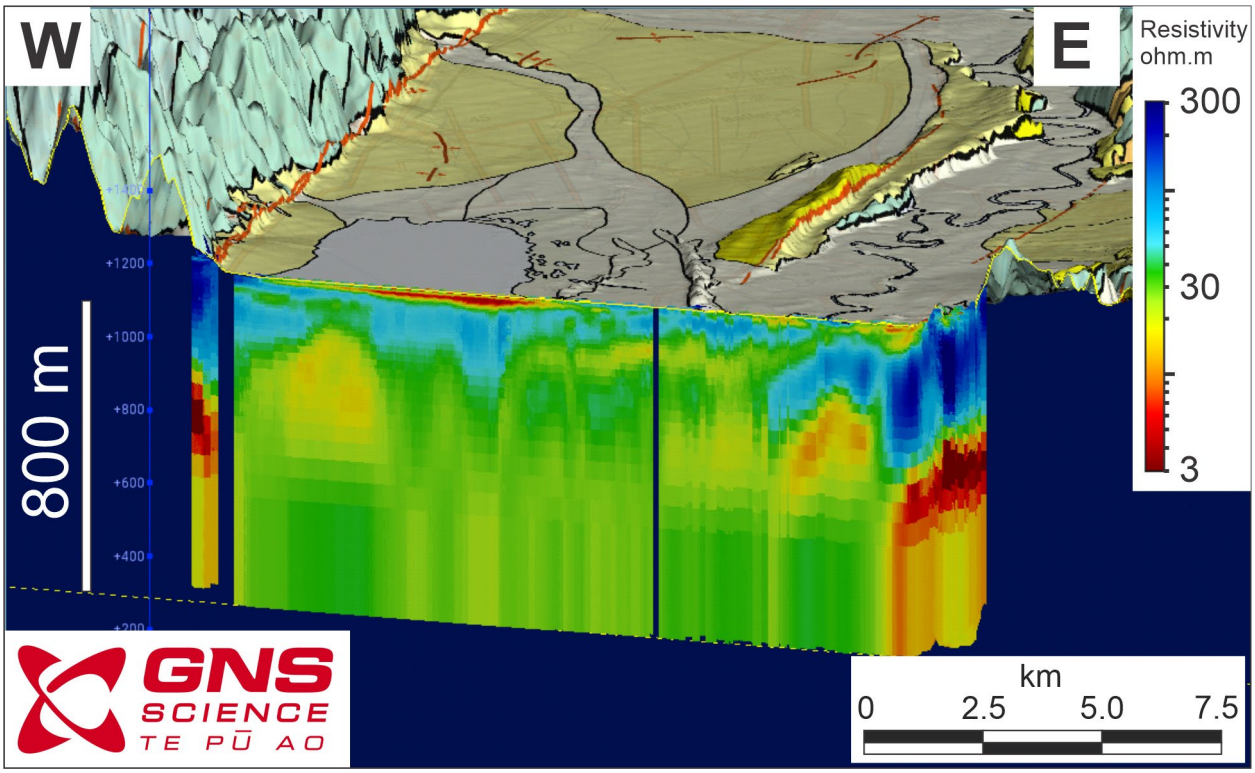

Figure 2.1 The smooth resistivity model presented as a pseudo-borehole data set in Leapfrog. The section is a 250-m-wide slice through the pseudo-borehole dataset. Vertical exaggeration is 8x. The view is to the north. The topography is shown with the 1:250 000 Geological Map of New Zealand dataset (Heron 2023) draped on the ground surface.

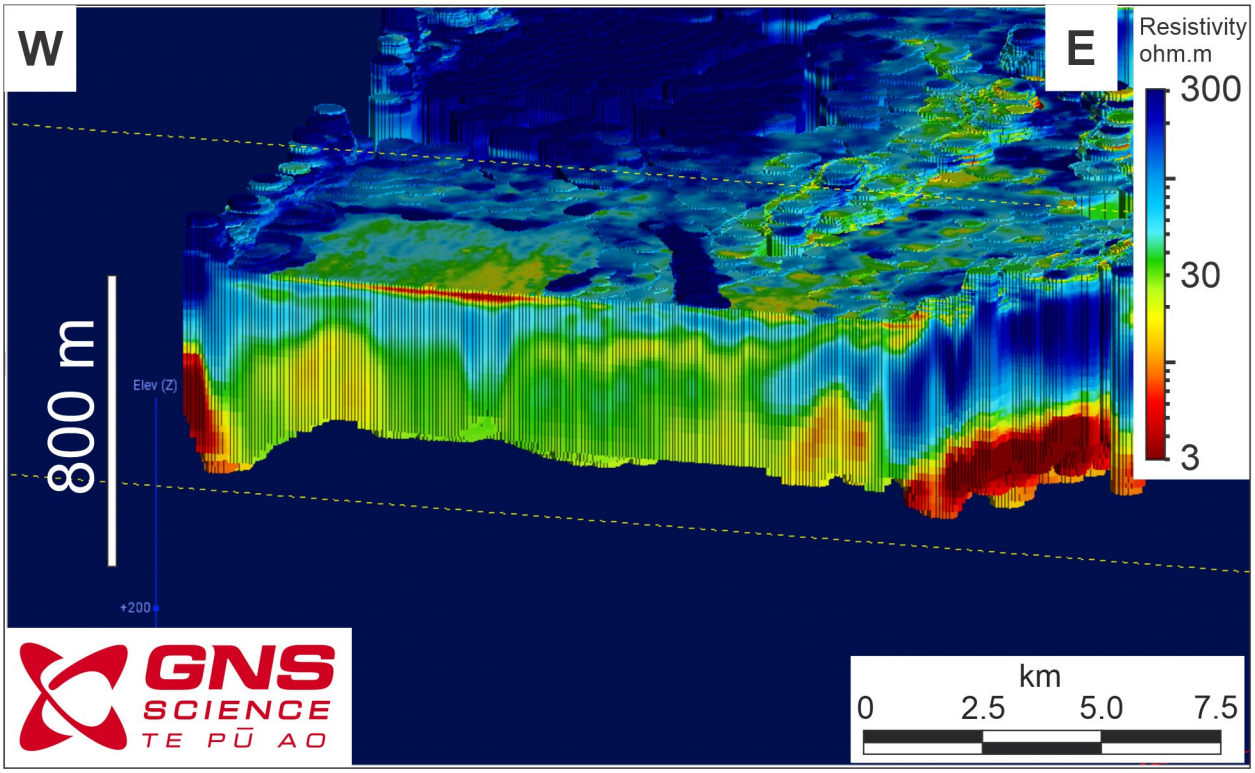

Figure 2.2 The smooth resistivity model presented as an interpolated 3D volume in Leapfrog. The topography is not shown in order to reveal the extents of the model. The same face is exposed as in Figure 2.1. The data are truncated at depth by the DOI. The vertical exaggeration is 8x. The view is towards the north.

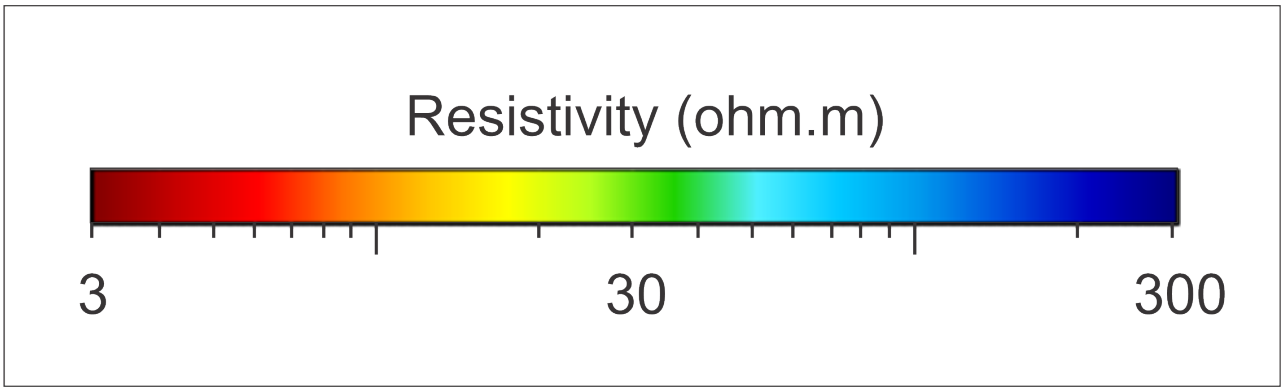

Figure 2.3 The colour ramp used to represent the electrical resistivity data. The values increase on a logarithmic scale from 3 to 300 ohm.m.

3.0 Conceptual Geological Model

This section summarises the geological framework for the Wairarapa Valley, describing previous work, surface geology, stratigraphy and ages, and interpretations of key cross-sections. These data are used to constrain the subsurface interpretation of the SkyTEM data. The map of geological units represents what can be mapped at the surface, and extending these lithological layers to depth requires a detailed knowledge of the spatial variations in the thickness of the specific units. This information can be implied from the outcrop patterns but can only be accurately modelled from a combination of drilling and geophysical interpretations. The conceptual geological model has been used as a major input into the definition of the four hydrogeological units defined in Section 7.

3.1 Previous Work and Data Sources

Comprehensive descriptions of the geology for the Wairarapa Valley with a groundwater focus have been provided in Begg et al. (2005). Gyopari and McAlister (2010a, 2010b, 2010c) describe the hydrogeological potential of the geological units for the lower, middle and upper parts of the Wairarapa Valley, and provided geological cross-section interpretations based on borehole data and knowledge of geological processes. However, the cross-sections are limited to providing interpretation of the geology to around 50–100 m depth due the lack of deeper borehole depths. Begg has produced several reports that contain detailed cross-sections and interpretations for the lower part of the valley south of Lake Wairarapa, which are also limited to 100 m depth (Begg 2020; Begg JG [date unknown] and included in Kellett et al. 2022).

Begg et al. (2005) divided the geology in the Wairarapa Valley into five units, which are based primarily on rock relationships and geological history but do provide some reference for the properties relevant for hydrogeology (Table 3.1). We include an overview of the five units in this report to provide the context for our conceptual model. The various lithologies within each unit reflect facies changes. The groupings for these units help provide a broader context to understanding their distribution based on knowledge of their depositional history. The hydrogeological properties of the lithologies that Begg et al. (2005) assigned to Units 1 to 5 are summarised below, but discussed in more detail in Section 6.

Unit 1 is the Mesozoic basement commonly seen in outcrop as greywacke (mudstone and sandstone). This unit has limited capacity to store groundwater through joints and fault planes (see Section 6 for more detail). We consider this unit to be hydrogeological basement in parts of the study area. However, the unit is important in the hydrogeological context because rock eroded from this unit by the rivers and streams is the source of the gravel that is deposited on the plains of the Wairarapa Valley.

Begg et al. (2005) indicates that most of the conglomerate, sandstone, mudstone and limestone lithologies within Unit 2 have little or no capacity to store groundwater as the porosity is low. However, the younger conglomerate and sandstone in Unit 3 are potential aquifers, depending on their thickness, structure and any confining lithologies that lie above and below them.

The likelihood of the gravel in Unit 4 being an aquifer is good but may be limited by the finer-grained silt and clay content. Younger gravel (Unit 5) has the highest potential of being a significant source of groundwater.

Table 3.1 A summary of the rock unit groups from Begg et al. (2005). Figure 3 in Begg et al. (2005) shows a simplified map of the distribution of these units.

	Name	Age (Ma)	Materials
Unit 5	Late Quaternary	<0.128	Alluvial gravel, sand, silt, minor swamp deposits
Unit 4	Early to Middle Quaternary	2.3–0.128	Alluvial gravel, sand, minor silt and minor swamp deposits
Unit 3	Palliser and Onoke groups	25–2.3	Sandstone, siltstone, mudstone, limestone and minor conglomerate
Unit 2	Mangapurupuru Group, Glenburn Formation, Tinui and Mangatu groups	100–25	Conglomerate, sandstone, mudstone, limestone
Unit 1	Torlesse composite terrane, Pahaoa Group	230–120	Hard sandstone and mudstone (greywacke)

3.2 Geological Framework

Since the Begg et al. (2005) report, the geological mapping has been updated and shown in Figure 3.1. The main source for surface geology is from the 1:250 000 Geological Map of New Zealand dataset (Heron 2023). The geological map, also referred to as QMAP, consolidates the work of Begg and Johnston (2000), Lee and Begg (2002), Nicol et al. (2002) and Cape et al. (1990). Updated fault information from lidar mapping has been included (Coffey and Litchfield 2023; Morgenstern et al. 2024), as well as the addition of the Bidwill Fault just east of Te Maire Fault (Cape et al. 1990; Seebeck et al. 2022).

The geological map in Figure 3.1 shows the units that are used for the remainder of this report, further subdividing the Begg et al. (2005) Units 3, 4 and 5. The legend for the geological map is shown in Figure 3.2. The stratigraphic section clearly indicates that the gravel content is higher in the Quaternary units.

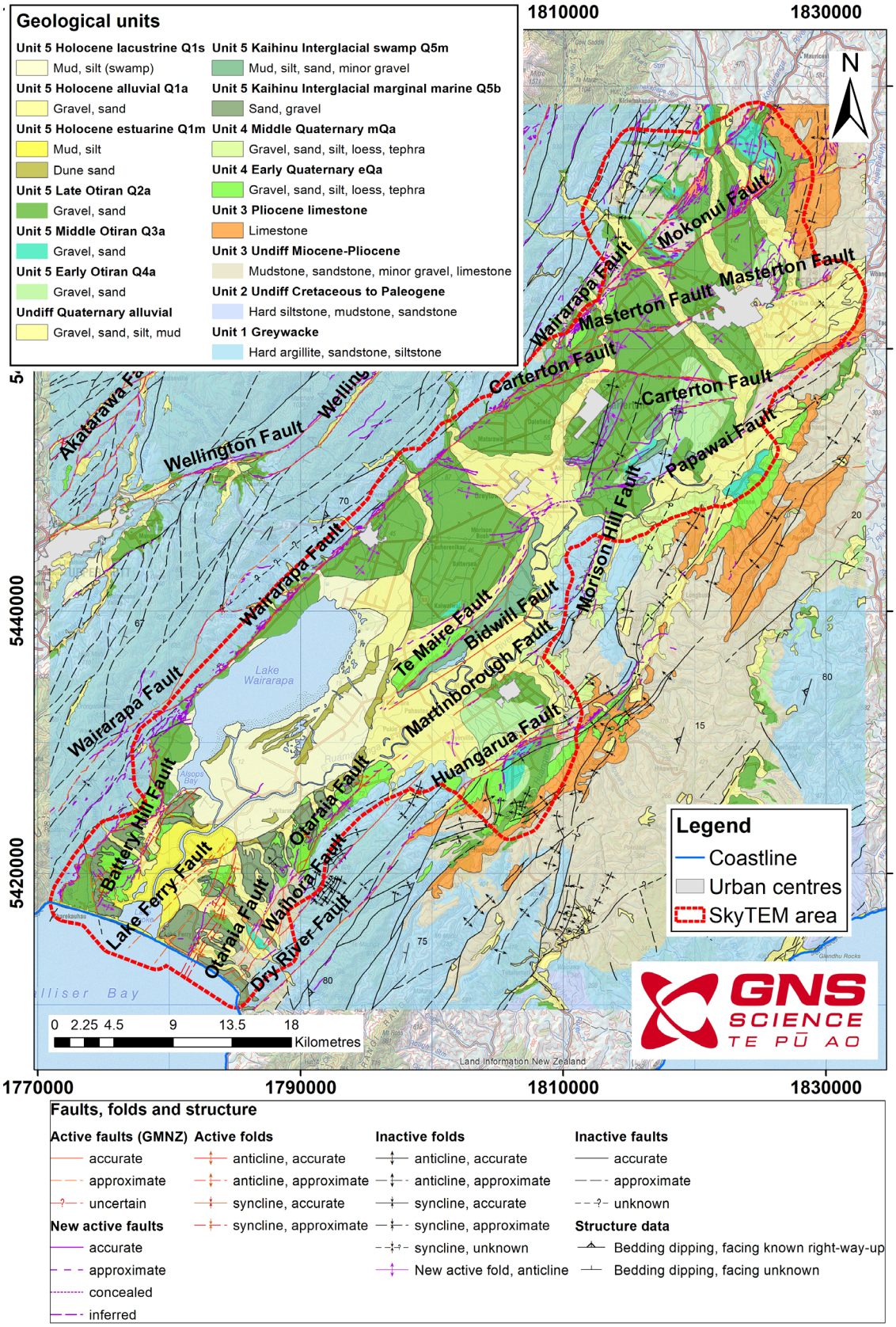

Figure 3.1 Geological map for Wairarapa with differentiated Quaternary units, with correlation to the labels and names in Figure 3.2 and Table 3.2. Updates to the geology include minor amendments to geological boundaries in the late Quaternary and the addition of the Bidwill Fault. The Papawai Fault and new folds were mapped from lidar (purple lines) (Coffey and Litchfield 2023; Morgenstern et al. 2024). Limestone from Unit 3 (orange) is differentiated.

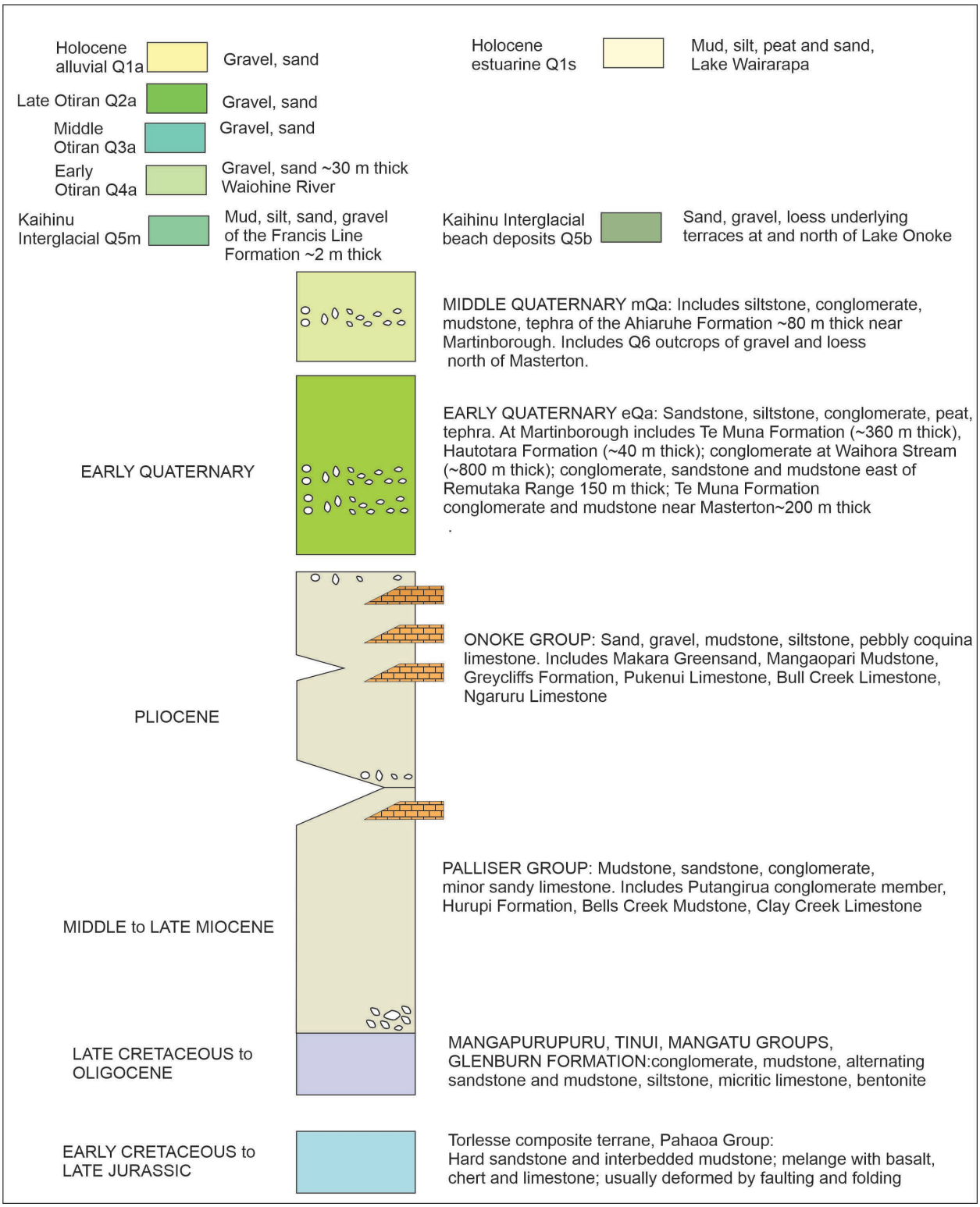

Figure 3.2 Detailed legend of the geological units in the Wairarapa area, including names of formations and thicknesses where known. Colours correspond to the map in Figure 3.1.

A limited number of seismic reflection lines have been collected in the Wairarapa Valley (Cape et al. 1990; Nicol et al. 2002; Kellett et al. 2024). These seismic lines show the structural style of deformation dominated by northwest-dipping reverse faults with anticlines on the upthrown side of faults and synclines in the downthrown side (Cape et al. 1990; Nicol et al. 2002). This structural style is summarised in a northwest–southeast cross-section from Featherston to Martinborough (Figure 3.3) (from Begg and Johnston [2000]).

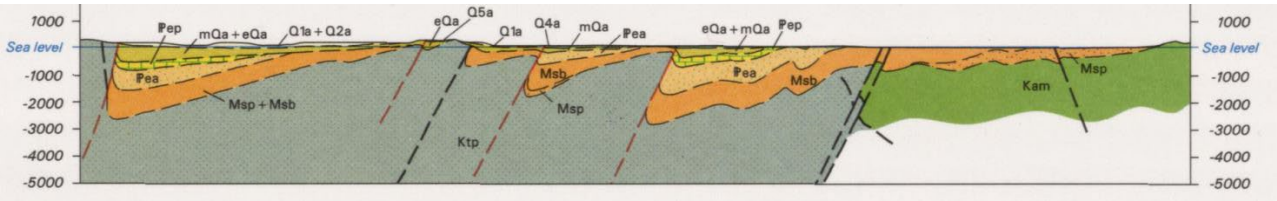

Figure 3.3 A cross-section from Featherston in the west and east to Martinborough and towards the coast (Begg and Johnston 2000). See Figure 3.7 for location. Ktp (blue-grey) and Kam (green) = Early Cretaceous to Late Jurassic; Msb, Msp (dark orange) = Miocene; Pea (light orange pink) = Pliocene; Pep (yellow) = Pliocene limestone; mQa, eQa, Q1a, Q2a, Q5a units are explained in Figure 3.2.

The locations of the main synclines or sub-basins are based on surface geology and geomorphology as shown in Figure 3.4. Within the Wairarapa Valley, smaller, active sub-basins are located near Lake Ferry, while basins just east of Carterton and Masterton are currently classed as inactive (see Figure 1.2 for locations). The synclines on the downthrown side of the faults are filled with Miocene (Msb, Msp in Figure 3.4), Pliocene (Pea) and Quaternary sediments that overlie greywacke basement (Ktp). The seismic data from Cape et al. (1990) suggest that the top of the greywacke lies at a maximum of 2.0–2.5 km depth in the vicinity of Masterton and Carterton. Begg et al. (2005) and Gyopari and McAlister (2010a, 2010b, 2010c) discuss the implications of the synclines, anticlines and faults for the regional groundwater flow.

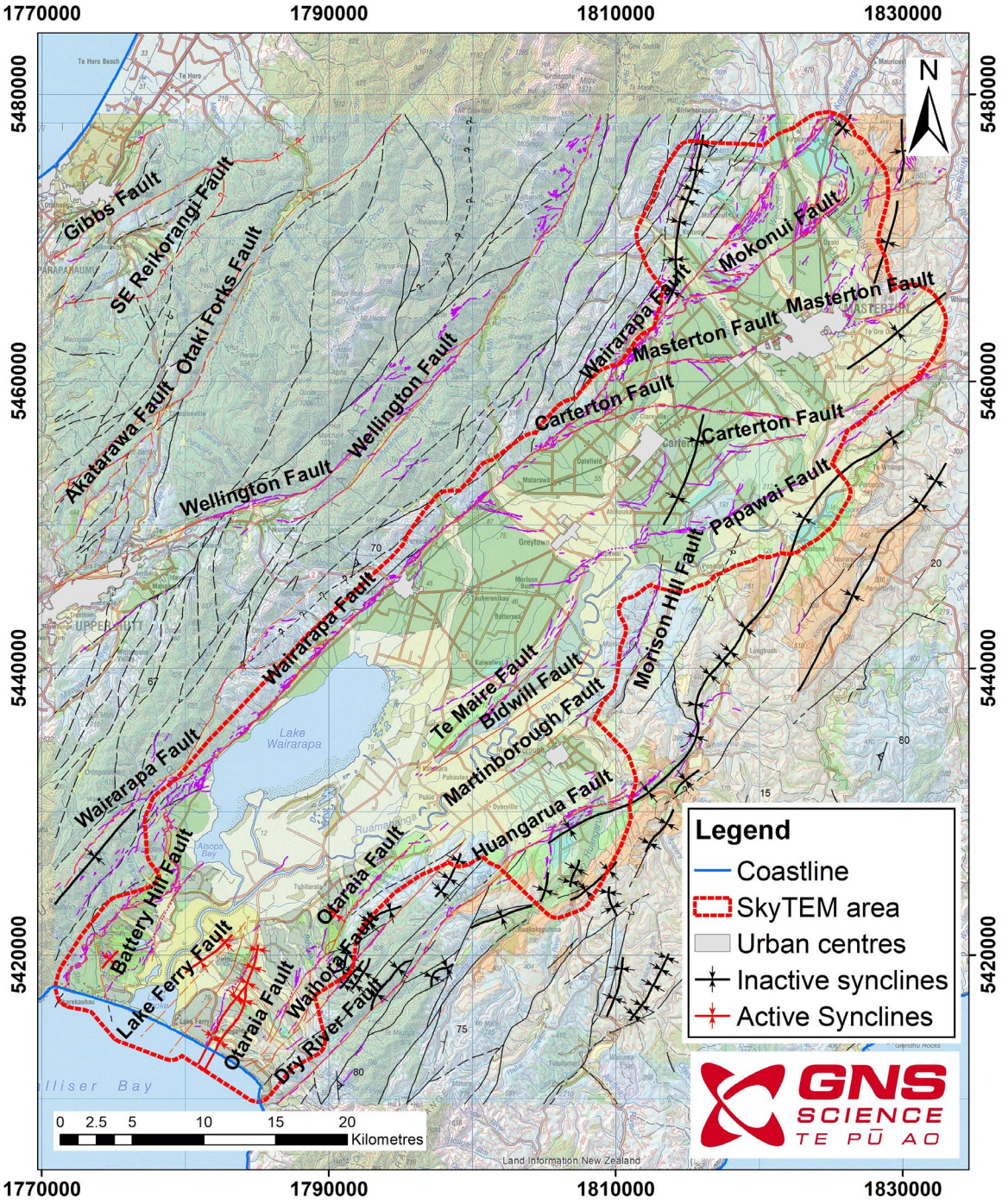

Figure 3.4 Location of synclines (sub-basins) in the Wairarapa area.

3.2.1 Geological Units

This section briefly describes the distribution of the rock units in Figure 3.1 and provides thicknesses where they are known. More detailed descriptions of the lithologies can be found in Begg et al. (2005), Begg and Johnston (2000) and Lee and Begg (2002).

The oldest rock unit of deformed sandstone and mudstone (greywacke, Unit 1) is mostly found on western and eastern margins of the Wairarapa Valley forming the Tararua and Aorangi ranges (see Figure 1.2 for locations); it is also found as uplifted fault blocks in the central part of the valley along the Te Maire, Bidwill, Papawai and Morison Bush faults (Figure 3.1 and Figure 3.4).

Unit 2 includes undifferentiated Late Cretaceous to Oligocene conglomerate, sandstone and mudstone that crop out towards the east coast, but have not been identified in surface outcrop or in the subsurface within the Wairarapa Valley (Kam [in Figure 3.3]).

Miocene and Pliocene mudstone, sandstone, siltstone and limestone (Unit 3) are mostly distributed on the eastern side of the valley. Faulted slivers lie along the Wairarapa and Mokonui faults north of Masterton. Limestone beds, up to 90 m thick, are mapped in the Masterton and Martinborough areas (see Figure 1.2 for locations). The limestone is mostly made up of coarse shell fragments (known as coquina) and are mostly soft, porous and sandy (Beu 1995). Miocene and Pliocene rocks are mapped to be up to 2 km thick in the subsurface (Figure 3.3).

Early and Middle Quaternary (Unit 4) mostly comprise gravel, sand, silt and clay with minor loess and tephra deposits; they are distributed mostly in the eastern side of the Wairarapa Valley, with some outcrop south of Lake Wairarapa near the coast. Begg et al. (2005) subdivided Unit 4 into the Te Muna (Early Quaternary) and Ahiaruhe (Middle Quaternary) formations (Table 3.2).

Table 3.2 Quaternary units as categorised in Begg et al. (2005) with codes for each unit added for Figure 3.1 and Figure 3.2.

	Relative Age	Material	Local Name	Depositional Environment	Map Name	Absolute Age (ka)
Unit 5	Holocene	Mud and silt	-	Estuarine, lacustrine	Holocene estuarine Q1s	0–7
Unit 5	Holocene	Gravel and sand	-	Alluvial	Holocene alluvial Q1a	0–10
Unit 5	Late Quaternary (Late Otiran)	Gravel and sand	Waiohine	Alluvial	Last Glaciation Q2a	10–25
Unit 5	Late Quaternary (Middle Otiran)	Gravel and sand	Ramsley	Alluvial	Q3a	25–50
Unit 5	Late Quaternary (Early Otiran)	Gravel and sand	Waipoua	Alluvial	Q4a	50–70
Unit 5	Late Quaternary (Kaihinu Interglacial)	Mud, silt, sand, minor gravel	Francis Line	Swamp, lacustrine	Q5m	70–125
Unit 5	Late Quaternary (Kaihinu Interglacial)	Sand, some gravel	Eparaima	Marginal marine	Q5b	70–125
Unit 4	Middle Quaternary (Waimea Glacial)	Gravel and sand	-	Alluvial	Q6a	125–186
Unit 4	Middle Quaternary	Gravel, sand, silt, loess, tephra	Ahiaruhe	Alluvial, swamp	mQa	186–>500
Unit 4	Early Quaternary	Gravel, sand, silt, loess, tephra	Te Muna	Alluvial, swamp	eQa	c. 500–1000

Collectively, the Te Muna and Ahiaruhe formations are more than 450 m thick in the Martinborough area (Collen and Vella 1984). Over 800 m of Early Quaternary conglomerate, sandstone and sandy siltstone unconformably overlie greywacke in the Aorangi Range just east of Lake Wairarapa (Arnot 1989). To the east of the Wharekauhau Thrust there is over 150 m of Early Quaternary conglomerate, sandstone and mudstone unconformably overlying greywacke of the Remutaka Range (see Figure 1.2 for locations) just south of Lake Wairarapa (Bloom 1951). West of Masterton, Te Muna formation conglomerate and alternating mudstone is around 200 m thick (Wells 1989). Small pockets of the Waimea Glacial (Q6) deposits crop out around the Masterton and Mokonui faults.

Holocene and Otiran (Late Quaternary) deposits are found over most of the Wairarapa Valley (Figure 3.1 and Figure 3.2). Begg et al. (2005) categorised Unit 5 into seven sub-units (Table 3.2) of gravel, estuarine/lacustrine and marginal marine deposits. Their distribution is shown in Figure 3.5 and coloured differently to Figure 3.2 to more easily locate each sub-unit. Marginal marine deposits (Q5b) of mostly gravel and sand are around 10 m thick and are found in terraces distributed to the south and southeast of Lake Wairarapa. Fine-grained lacustrine and swamp deposits of mud, silt and sand (Q5m) up to 2 m thick crop out to the north of Masterton and were deposited around the same time as Q5b. Outcrops of Early and Middle Otiran gravel and sand (Q4a, Q3a) are found at Martinborough, Carterton and in the northernmost part of the Wairarapa Valley. Late Otiran (Q2a) gravel and sand fan deposits are found north of Lake Wairarapa covering a large area of the valley floor; the fans from the Waiohine and Tauherenikau rivers (see Figure 1.2 for locations) are around 30 m thick and contain poorly sorted gravel and sand; gravel boulders are up to 1 m in size (Vella 1963). Borehole logs show the gravel also contains silt and clay. Holocene gravel and sand (Q1a) are distributed along the river and stream channels. Estuarine mud (Q1m) around Lake Wairarapa is found from borehole data to be between 20–40 m thick (Begg et al. 2005).

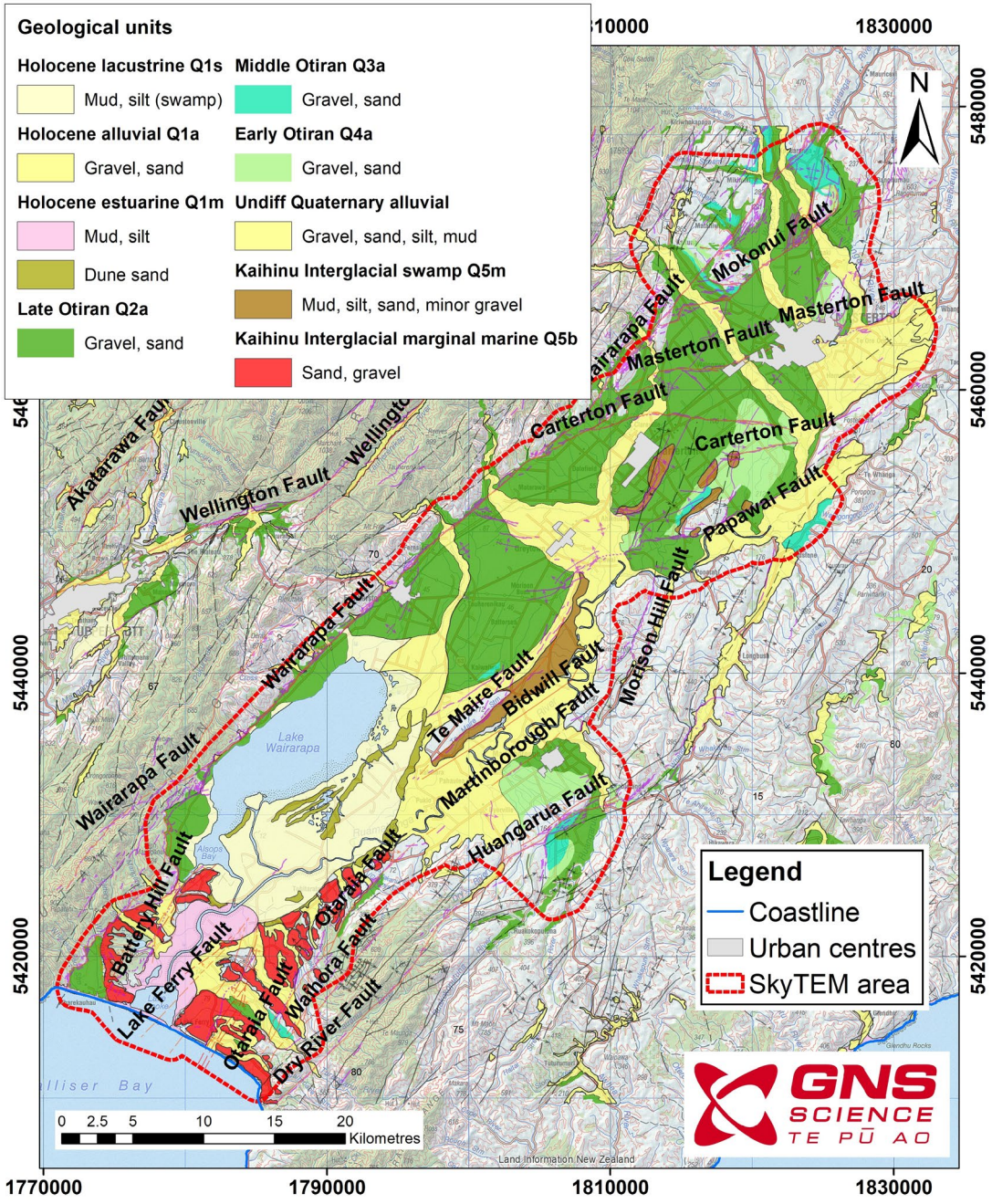

Figure 3.5 Distribution of Quaternary units.

3.3 Cross-Sections

Geological cross-sections provide interpretation of the subsurface based on the distribution, thickness and dip of the surface geology. Many cross-sections have been developed in Gyopari and McAlister (2010a, 2010b, 2010c) for the lower, middle and upper valley based on boreholes. These cross-sections were used to support the interpretation of the SkyTEM data, but only provide constraints on subsurface interpretation at shallower depths (<50 m).

Key cross-section locations from published reports are shown in Figure 3.6. The cross-section from Nicol et al. (2002) is based on a seismic reflection line and provides a constraint on the deeper parts of the SkyTEM model (Figure 3.7 and Figure 3.8). The cross-section from Cape et al. (1990) is based on both seismic reflection and gravity data. Figure 3.9 shows this cross-section alongside the SkyTEM resistivity model. The section from Begg and Johnston (2000) is shown as Figure 3.3. The locations of additional Leapfrog cross-sections (Figure 3.10 and Figure 3.11) are also shown on the map.

In the following section we discuss the cross-sections in more detail.

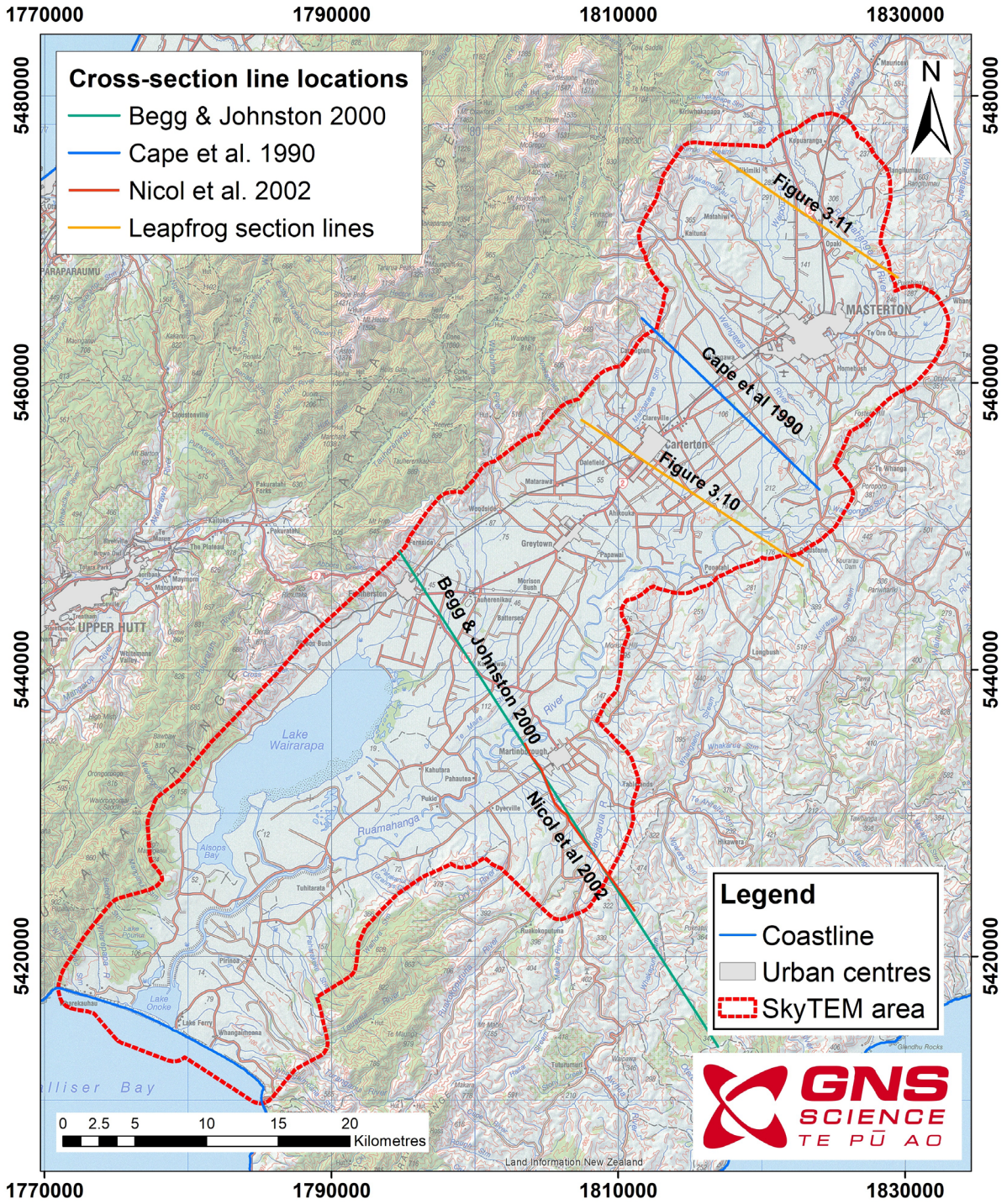

Figure 3.6 Location of key geological cross-sections used to construct the hydrogeological model and Leapfrog figures shown in Section 3.4.

3.4 Correlation of Geology with SkyTEM Data

In the Leapfrog software, the surface geology, geological cross-sections and SkyTEM data can be displayed together to visualise correlations between these datasets. In the following section we describe five cross-sections in detail to represent the variation on subsurface geology across the Wairarapa Valley and the correlation with the SkyTEM resistivity models.

A cross-section near Martinborough (see Figure 3.6 for location of the Nicol et al. 2002 section) shows Miocene and Pliocene rocks projected at depth using the dips of bedding at the surface (Figure 3.7). The section shows subsurface interpretation to 2 km depth across the Martinborough and Huangarua faults. The Martinborough and Huangarua faults are west-dipping reverse faults that create anticlines on the upthrown side and synclines on the downthrown side. A near-complete sequence of the stratigraphy is present in the syncline to the east of the Huangarua Fault, whereas it is incomplete to the east of the Martinborough Fault. Figure 3.8 shows the correlation of the SkyTEM resistivity model with the geological section. The pattern of anticlines, thrust faults and synclines is clearly seen in the resistivity model. The Ahiaruhe formation (Middle Quaternary [Figure 3.2]) and Te Muna formation (Early Quaternary [Figure 3.2]) have high resistivity while the underlying Mangaopari Mudstone (Pliocene [Figure 3.2]) has low resistivity. The Pukenui Limestone (Pliocene [Figure 3.2]) is present on the Huangarua syncline and is resistive.

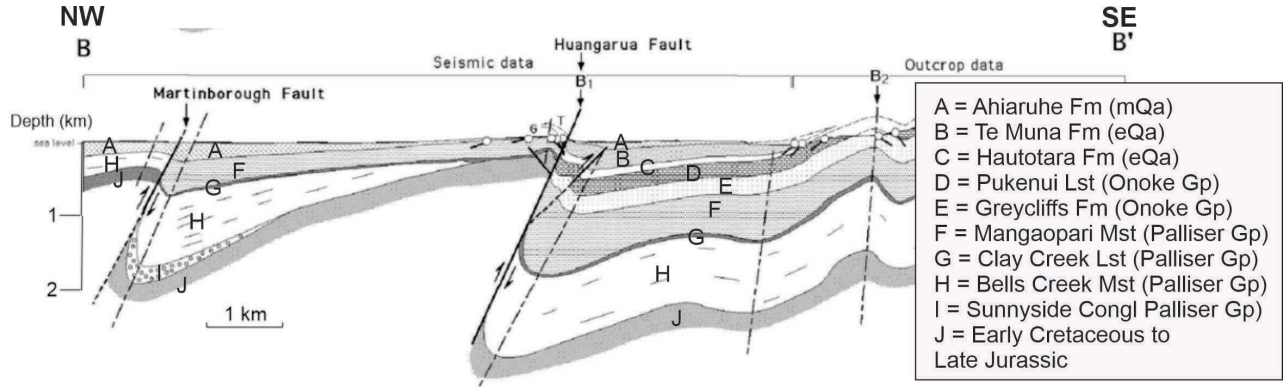

Figure 3.7 Cross-section B from Nicol et al. (2002) that runs from Martinborough in the west (B) and eastward through the Huangarua River (B'). Vertical and horizontal scale has been added. See Figure 3.6 for line location. The Martinborough and Huangarua faults dip to the northwest; the sequence of geological units is more complete on the downthrown side of the Huangarua Fault and incomplete to the east of the Martinborough Fault. Refer to Figure 3.2 legend for explanation of geological formation names.

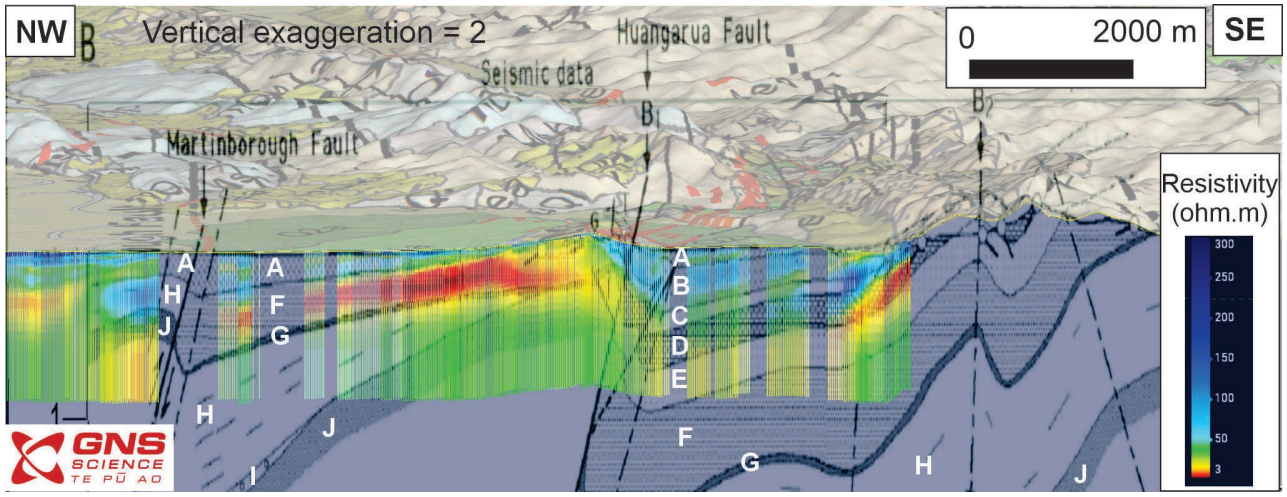

Figure 3.8 A slice view in the Leapfrog model of the Nicol et al. (2002) cross-section with the smooth SkyTEM resistivity model superimposed. The key for the units is shown in Figure 3.7. Vertical exaggeration is 2x. The view is to the north.

Cape et al. (1990) produced a regional cross-section based on the seismic reflection and gravity data across the upper valley between Carterton and Masterton. The section shows the Quaternary and Pliocene units with high confidence based on the seismic data. The Miocene and basement contacts are less well defined in the seismic data. Figure 3.9 shows the section with the SkyTEM

resistivity models superimposed. There is a general pattern that the Pliocene units have low resistivity (<10 ohm.m) and the overlying Quaternary units have high resistivity (>100 ohm.m), and the pattern of synclines and anticlines is seen in the resistivity model. However, in the centre of the cross-section the resistivity boundary lies within the Early Quaternary indicating that there are lateral changes in facies within the Early Quaternary that are being mapped by the SkyTEM resistivity.

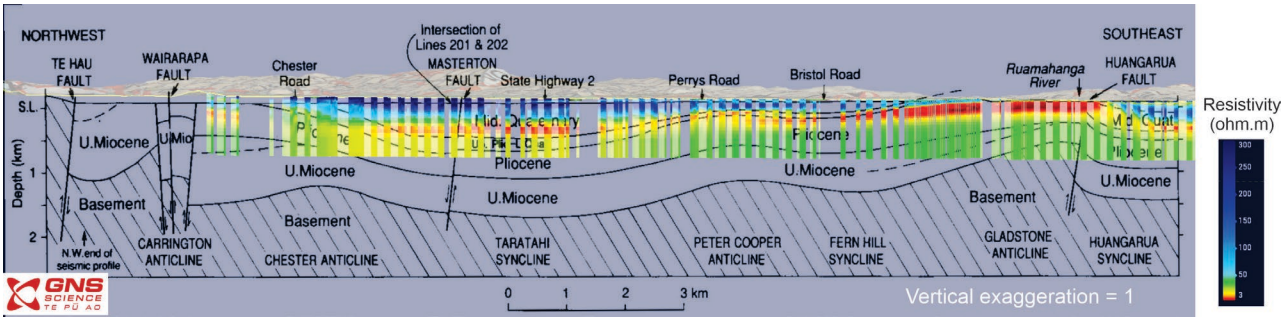

Figure 3.9 Leapfrog model view to the northeast showing the interpreted cross-section from seismic reflection and gravity data with the SkyTEM models in the foreground (Cape et al. 1990). Vertical exaggeration x1. See Figure 3.6 for cross-section location, line labelled Cape et al. (1990).

Further to the south, a cross-section located near Carterton shows that a block of greywacke (arrowed, Figure 3.10) has been uplifted by the Papawai Fault to form the core of the Tiffin anticline (Warnes 1992; Ingham 2014). The greywacke outcrops on Tiffin Hill (see Figure 1.2 for location) are interpreted to plunge to the northeast as a narrow ridge. The SkyTEM models show that the greywacke has high resistivity (>150 ohm.m) and extends under the Quaternary and Tertiary cover rocks to the west.

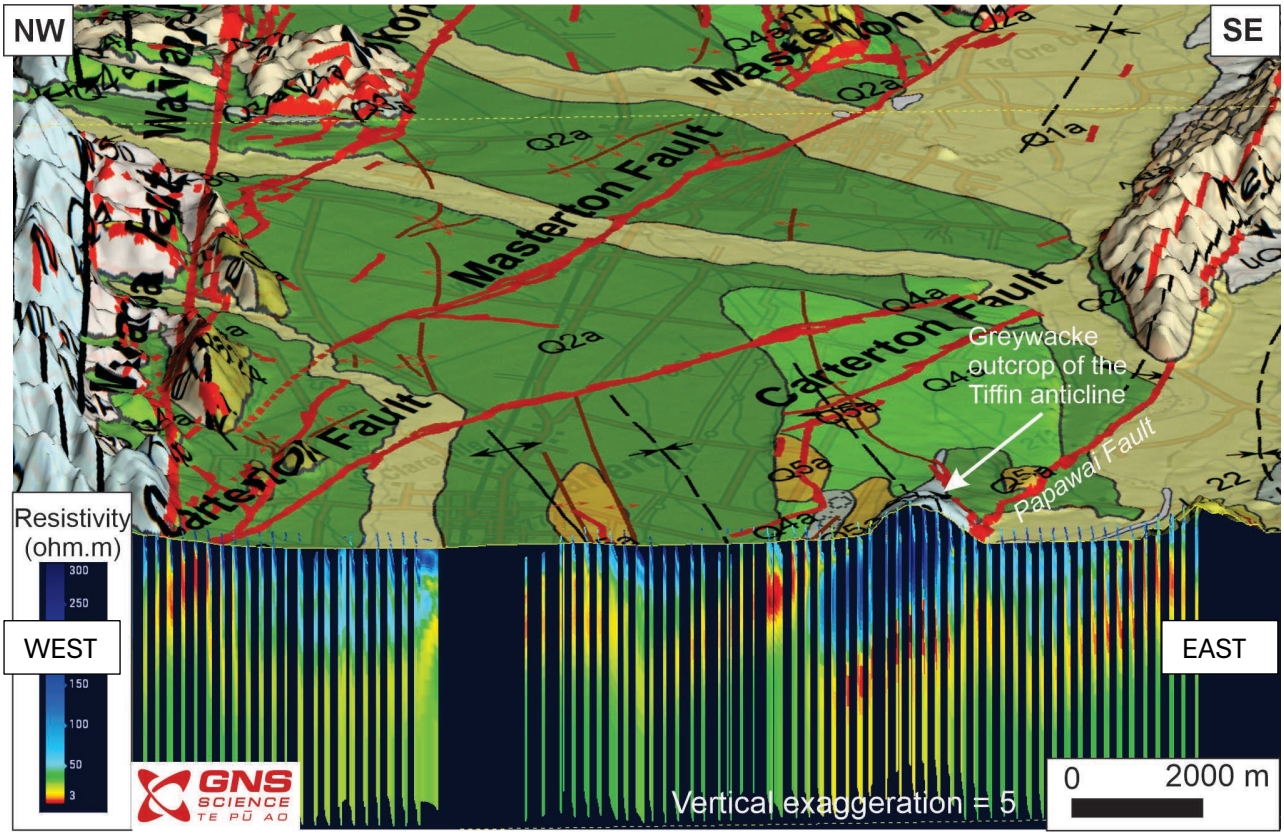

Figure 3.10 Leapfrog cross-section viewed to the northeast. A greywacke block (Unit 1) within the Tiffin anticline southeast of Carterton is uplifted by the Papawai Fault. The greywacke is shown to have high resistivity (>150 ohm.m). Vertical exaggeration is 5x. See Figure 3.6 for line location.

A cross-section north of Masterton (see Figure 3.6 for the location) shows that thick limestone beds dip to the west with the topographic surface representing the bedding plane; this surface can be projected at depth to follow the dip in the SkyTEM resistivity model (Figure 3.11). The limestone has high resistivity (>100 ohm.m) while the underlying mudstone has low resistivity (<30 ohm.m).

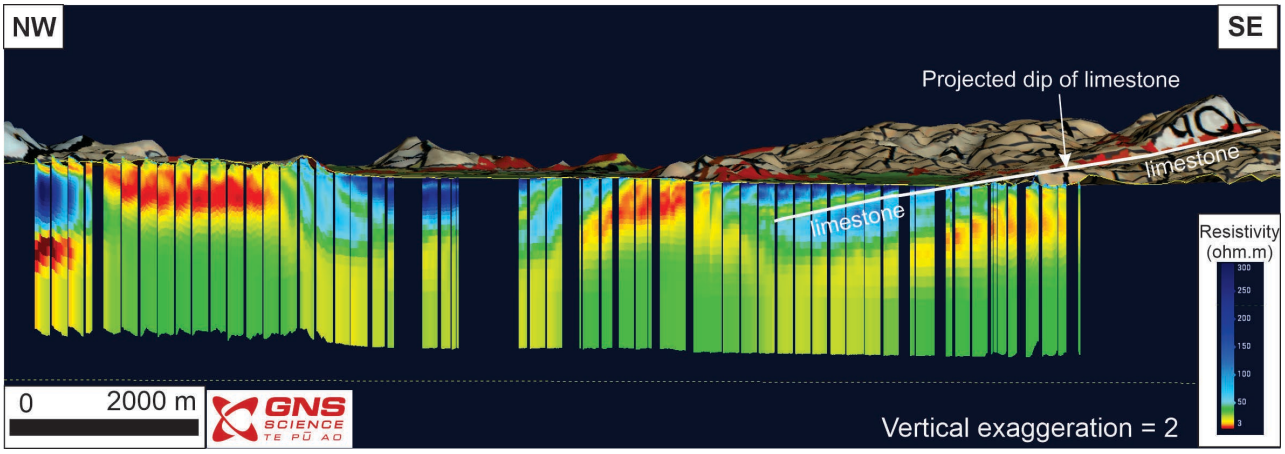

Figure 3.11 Leapfrog cross-section view of limestone at the surface dipping to the west and projected at depth. Vertical exaggeration is 2x. The view is to the north. See Figure 3.6 for line location.

3.5 Radiocarbon Ages

Many of the Holocene and Quaternary geological units have similar descriptions, e.g. alluvial gravel with sand and silt. Providing absolute ages for organic rich or shelly material within the sedimentary units allows us to make more accurate stratigraphic correlations across the Wairarapa Valley and define intervals that make up a hydrogeological model. Radiocarbon ages from cores, boreholes and surface outcrops are available primarily from the lower part of the Wairarapa Valley. Most radiocarbon dates provide an age on estuarine and shallow marine facies, and can help identify the inland extent of these facies in the last 30 ka years (Leach and Anderson 1974; Hayward et al. 2011). These deposits are likely to be fine-grained intervals and can act as confining layers in a hydrogeological model.

The age of 5.2–6.0 ka for the interval from 26 m to 35 m depth in two Pouawha boreholes (Clark et al. 2011; Begg et al. 2005) is correlated with the Holocene sea level high-stand when estuarine conditions existed around the southern end of the current Lake Wairarapa (see Figure 1.2 for the location of Pouawha). Ages older than 30 ka have been identified in two boreholes at depths of 29.5 m near Carterton and 47 m near Kahutara (Begg et al. 2005). These ages correspond to Q3a or older.

3.6 Correlation of Conceptual Geological Model with SkyTEM Interpreted Units

Combining all of the information from these regional and detailed geological studies and the previous hydrogeological interpretation into a single framework is important for making a consistent interpretation of the SkyTEM resistivity model. A layered model is the first stage of the hydrogeological model development, linking SkyTEM-derived resistivity values to the geologically mapped strata. This layered model is described as hydrogeological units as follows:

- HU-1 represents Q1a, Q2a, Q3a, Q4a (Holocene and Otiran units).
- HU-2 includes Q5a, Q5b, eQa, mQa (Early Quaternary, Middle Quaternary and Last Interglacial).
- HU-3 includes Pliocene, Miocene and potentially Late Cretaceous to Oligocene units.
- Basement includes the Mesozoic greywacke.

Section 7 describes the development of the hydrogeological units in detail.

4.0 Previous Hydrogeological Models

4.1 Regional Models

One of the key aims of the SkyTEM project is to provide a foundation for the development of numerical groundwater flow models that more accurately represent the groundwater conditions in the Wairarapa. Having more accurate models will allow better decisions to be made about groundwater allocations and assessments of the impacts of increased abstraction. Building more reliable numerical flow models requires more detailed hydrogeological models with greater confidence on the distribution of hydraulic properties. Developing a flow model is not within the scope of the current project. However, an understanding of the current status of numerical models is key to building a hydrogeological model that can meet the requirements of any new numerical model development.

Existing numerical models of the groundwater system in the Wairarapa Valley present good starting points for further development of such models. The existing numerical models are also used to support the interpretation of layers and their role as aquifers or aquitards in the current hydrogeological model development.

The regional hydrogeological unit map (White et al. 2019) has also been used to support the extrapolation of the Quaternary and Tertiary aquifers under the surficial sediments.

The current numerical groundwater flow models for the Wairarapa Valley (Johnson et al. 2019) were constructed from a series of hydrogeological models developed by Gypopari and McAlister (2010a, 2010b, 2010c) and presented in Hughes and Gyopari (2014) and Jones and Gyopari (2006). The flow models are developed from a conceptual hydrogeological model based on the geological interpretations of Begg et al. (2005). The models rely on the surface geology from Begg and Johnston (2000) and Lee and Begg (2002), and the cross-sections presented in Gyopari and McAlister (2010a, 2010b, 2010c). The models also include the Carterton and Masterton faults. The three-dimensional view of the model conceptualisation for the northern part of the valley is shown in Figure 4.1. It is primarily a hydrogeological model of the unconsolidated upper and middle Quaternary sediments with a limited depth extent (approx. 50 m). The numerical model was implemented using FEFLOW code, a finite element groundwater modelling software originally developed in 1979 by DHI-WASY (now part of the DHI Group). FEFLOW has been widely applied in previous studies to simulate groundwater flow, nitrate transport and delineate groundwater protection zones for key wells in the Wairarapa (Moore et al. 2017; Toews and Donath 2015; Toews et al. 2016).

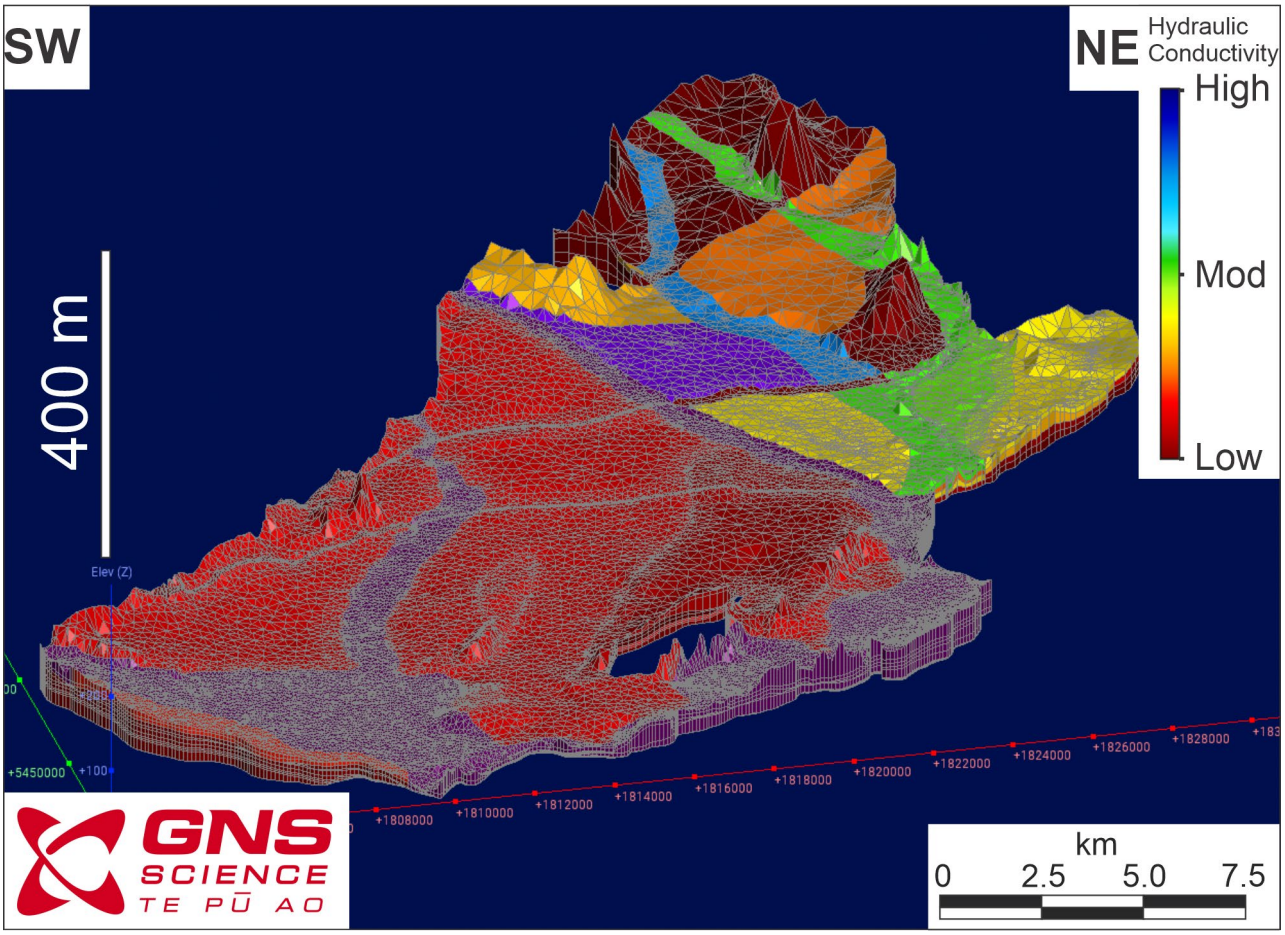

Figure 4.1 The central and northern portion of the current FEFLOW model for the Wairarapa Valley (Gyopari and McAlister [2010a, 2010b]). The model has been imported into Leapfrog. The view is to the northeast and centred on Masterton. The vertical exaggeration is 20x. The cells are coloured by the hydraulic conductivity in the x direction (Kxx). The greywacke basement cropping out at Tiffin Hill (see Figure 1.2 for the location) is seen as the hole in foreground of the model.

4.2 Local Models

In 2016, the GWRC commissioned the development of four Leapfrog hydrogeological models for the Wairarapa Valley (Figure 4.2). The numerical models were built by Kenex using the borehole lithological database. The model covering the central Wairarapa Valley is shown in Figure 4.2 and the Pirinoa model is shown in Figure 4.3. The Ruamāhanga model covers a portion of the lower valley model south of Martinborough (see Figure 4.2). The intent of the hydrogeological model construction was to develop additional numerical flow models that would complement the Gyopari and McAlister (2010a, 2010b, 2010c) models and provide more detail in areas of particular interest to GWRC. Leapfrog viewer files are available for all of the models and these provide a useful resource for comparison with the current SkyTEM work. Some grids used to construct the models are available as ASCII files and these were used for comparison with the current modelling. The following models were imported into the new Leapfrog hydrogeological model and used to guide the SkyTEM interpretation:

- Middle Wairarapa Valley model: thickness of upper and middle Quaternary was compared with SkyTEM derived units (see Figure 4.3).
- Pirinoa terraces model: complex pattern of terraces in valleys was compared with SkyTEM model for the southeastern part of the Wairarapa Valley (see Figure 4.4).

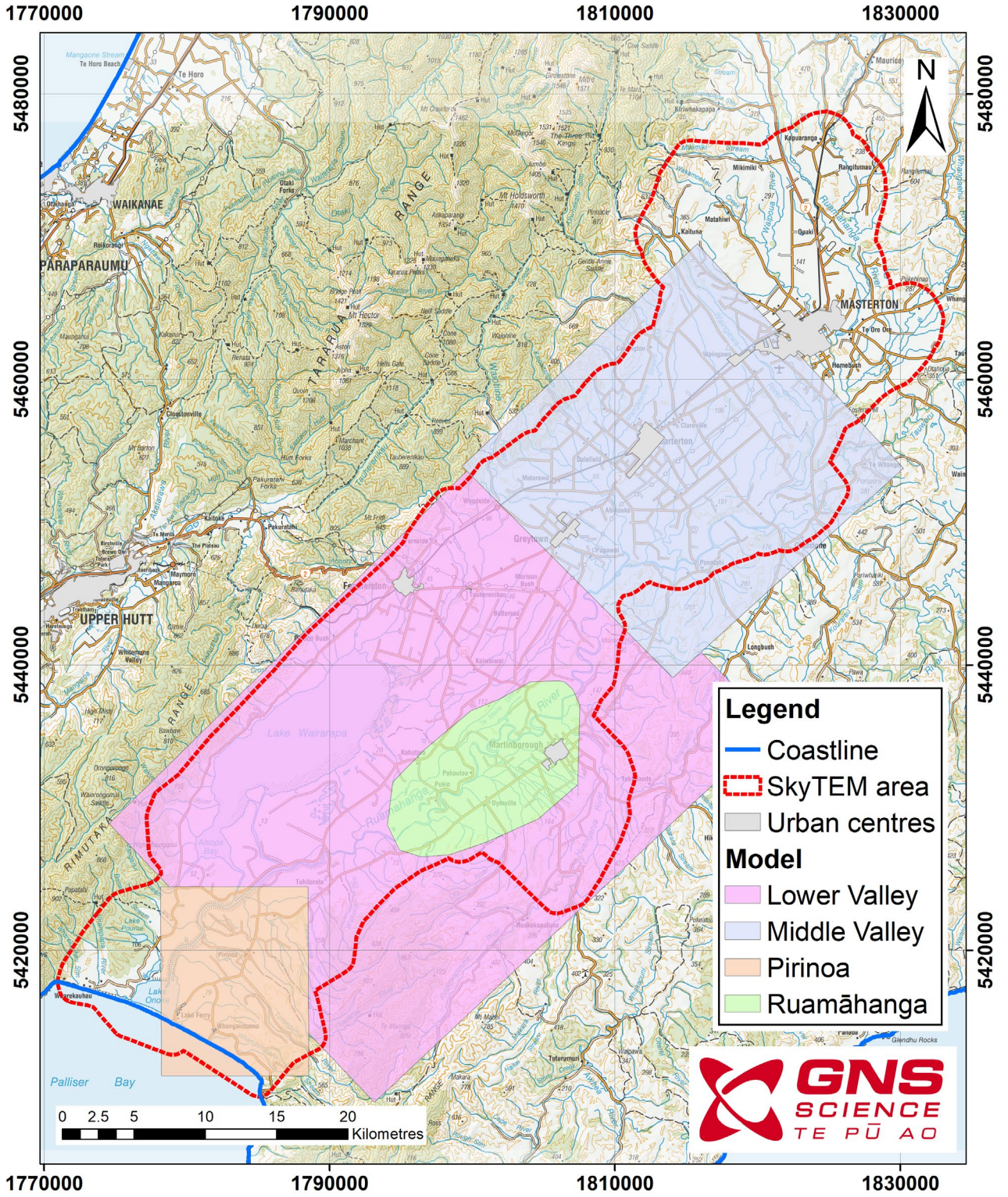

Figure 4.2 Map of the areas covered by the 2016 models constructed for Greater Wellington Regional Council by Kenex. The Ruamāhanga and Pirinoa models overlap with the Lower Valley model but are interpolated at a finer scale.

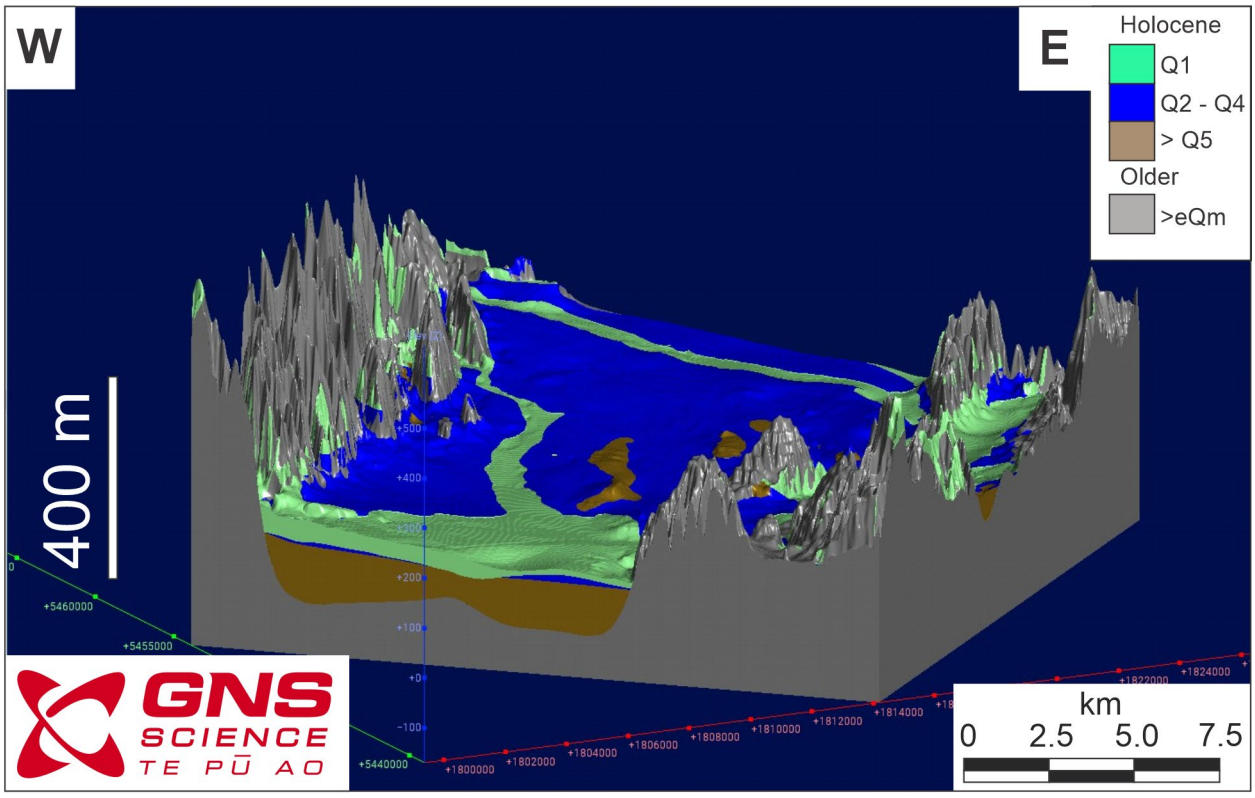

Figure 4.3 A view of the hydrogeological model constructed by Kenex in 2016 for the Middle Wairarapa Valley. Vertical exaggeration is 15x. View is to the northeast.

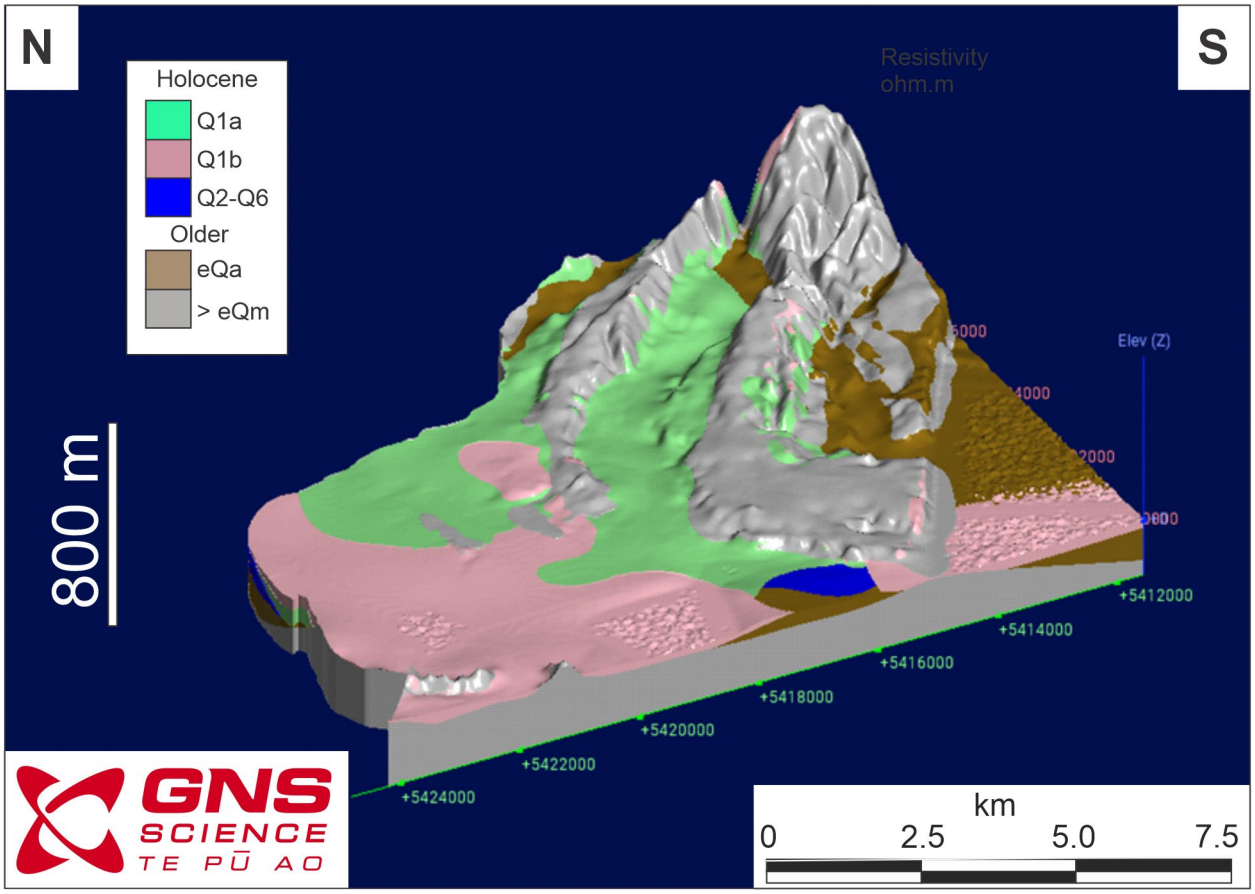

Figure 4.4 A view of the hydrogeological model constructed by Kenex in 2016 for the Pirinoa area in southern Wairarapa. The view is to the southeast centred on the village of Pirinoa. Vertical exaggeration is 5x.

5.0 Borehole Geological Data

5.1 Greater Wellington Regional Council Borehole Database

The boreholes utilised in the development of the hydrogeological model are derived from the GWRC borehole database[1] (accessed 1 July 2023). The database has been divided into three subsets (primary, secondary, third tier) based on the following criteria:

- Borehole depth: Deeper boreholes provide constraints over more of the SkyTEM model.
- Presence of detailed lithological information: Finer divisions and more detailed descriptions in the lithological log help build up a more detailed view of the variations in lithology within units.
- Proximity to SkyTEM data and supporting geophysical data: Boreholes that are within 100 m of a SkyTEM, GroundTEM or DC resistivity model point (Kellett et al. 2024) are valuable because they help bridge the gap between the resistivity model and the lithology. Interpolating more than 100 m from a borehole to the SkyTEM risks misinterpreting lateral changes in the geology.

The number of boreholes is listed below:

- Primary: 18 boreholes
- Secondary: 108 boreholes
- Third tier: 1840 boreholes

The original collection of 1953 boreholes has been supplemented by an additional 13 boreholes that became available during the current phase of the project. The 18 boreholes included in the primary subset were reviewed in detail and composite geological logs were generated to allow comparison with the SkyTEM resistivity models and ground geophysical data. In the northern part of the survey, an additional set of secondary boreholes were included in the detailed analysis to provide wider coverage across the SkyTEM survey.

The lithological data contained in the database was reviewed and re-interpreted to make a more consistent characterisation of the sediments in terms of clay, silt, sand, gravel, organic material and any shell material. The consolidated lithologies were classified as mudstone, sandstone, limestone or greywacke bedrock. A small number of borehole lithology logs (borelogs) contained references to conglomerates, breccias, volcanic rocks and undifferentiated Tertiary sediments.

Figure 5.1 shows an example of the composite log for the primary borehole BP33/0047. The lithological log shows the presence of a thick gravel dominated unit from 2 m to 35 m depth. The upper portion contains some clay. The SkyTEM model shows that the resistivity increases from 75 ohm.m to 120 ohm.m across the interval with clay. The interval from 10 to 30 m depth is massive gravel with a resistivity greater than 300 ohm.m. The second major layer in the borelog is from 35 m to 90 m depth and is dominated by clay with several gravel and sand units between 5 m and 10 m thick. There is also a component of organic material in two main horizons within the interval. The SkyTEM model responds to the clay unit and the resistivity drops to approximately 50 ohm.m. The basal section of the borehole is a 15-m-thick bed of massive gravel and the resistivity increases to over 100 ohm.m. The level of detail shown in Figure 5.1 is typical for most of the boreholes in the primary and secondary datasets.

The distribution of primary and secondary boreholes across the survey area is shown in Figure 5.2. The boreholes are presented as cylinders in the Leapfrog model illustrating the main lithology.

1 https://gwrc-open-data-11-1-gwrc.hub.arcgis.com/datasets/b52e4f95910141118fce229f33928d4c_1/explore

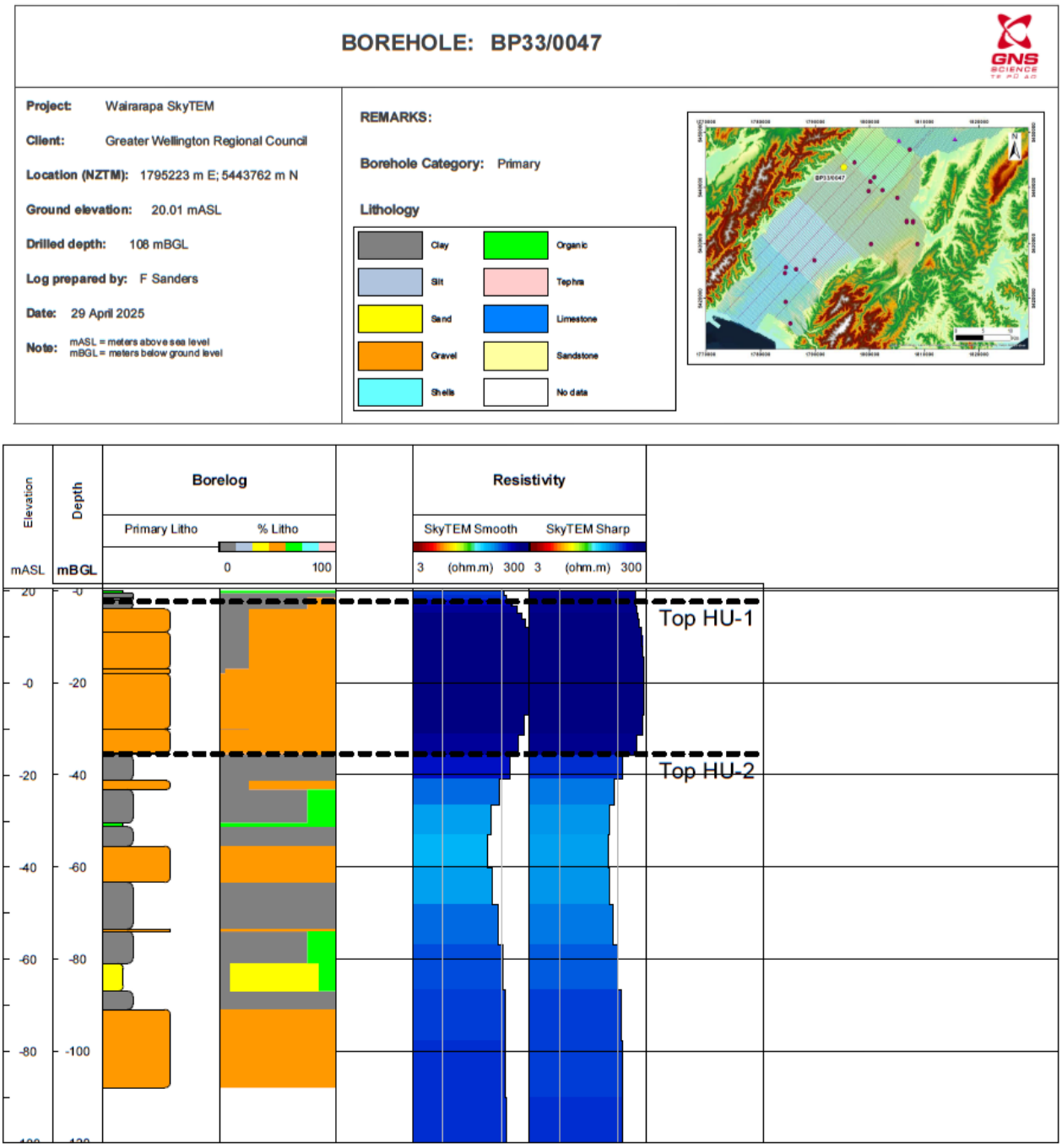

Figure 5.1 An example of a composite log for borehole BP33/0047. The tracks include the primary lithology, the percentage of different grain sizes in each depth interval, and the closest SkyTEM resistivity model presented as both the smooth and sharp model. The resistivity is shown on a logarithmic scale from 30–300 ohm.m. The tops of the interpreted hydrogeological units are shown for HU-1 and HU-2.

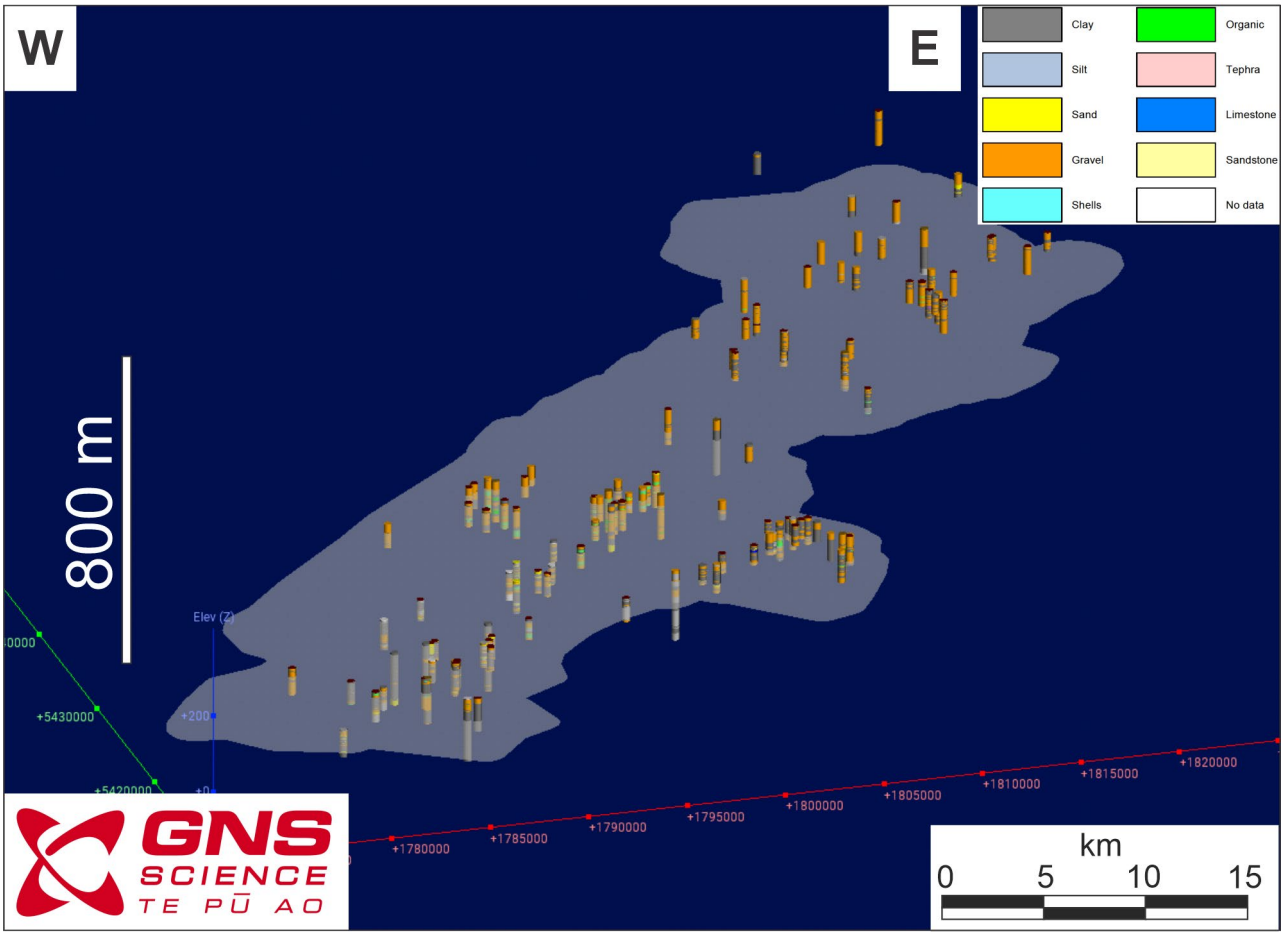

Figure 5.2 A view of the distribution of primary and secondary boreholes across the Wairarapa Valley within the Leapfrog hydrogeological model. The vertical exaggeration is 20x. The area of the SkyTEM survey is shown as the grey polygon. The view is towards the northeast. The main lithology present in each layer is coloured according to the legend.

5.2 Interpreted Cross-Sections

During a series of workshops held in collaboration with staff at GWRC, the SkyTEM resistivity models were interpreted on key cross-sections. The locations of these cross-sections were chosen to match those of some of the cross-sections presented by previous studies (Gyopari and McAlister 2010a, 2010b, 2010c) and discussed in Section 3. Some of the sections focussed on areas of interest to GWRC, including (see Figure 1.2 for the locations):

- Pirinoa in southern Wairarapa.
- Martinborough.
- The Parkvale basin east of Carterton.
- The Te Ore Ore basin east of Masterton.
- The northwestern part of the survey area north of the Waingawa River.

Figure 5.3 shows the locations of the primary and secondary boreholes used to support these interpretations. Two examples of the cross-sections are presented in this report to illustrate the correlation between the borehole lithology and the smooth SkyTEM resistivity models. Both the smooth and the sharp resistivity models are available on each composite log. The models are similar (see Figure 5.1), so, for simple presentations on a cross-section, only the smooth resistivity model is shown. The hydrogeological units (HU-1, HU-2 and HU-3) presented on the sections are discussed in more detail in Section 7. In most cases the SkyTEM resistivity model is within 100 m of the borehole.

In the case of BQ33/0037 and T26/0737, the closest SkyTEM model was 480–500 m away. Interpolating the SkyTEM model 500 m to a borehole will increase the uncertainty in the correlation between the resistivity and the lithology. However, the lateral changes are smooth, so this uncertainty is acceptable.

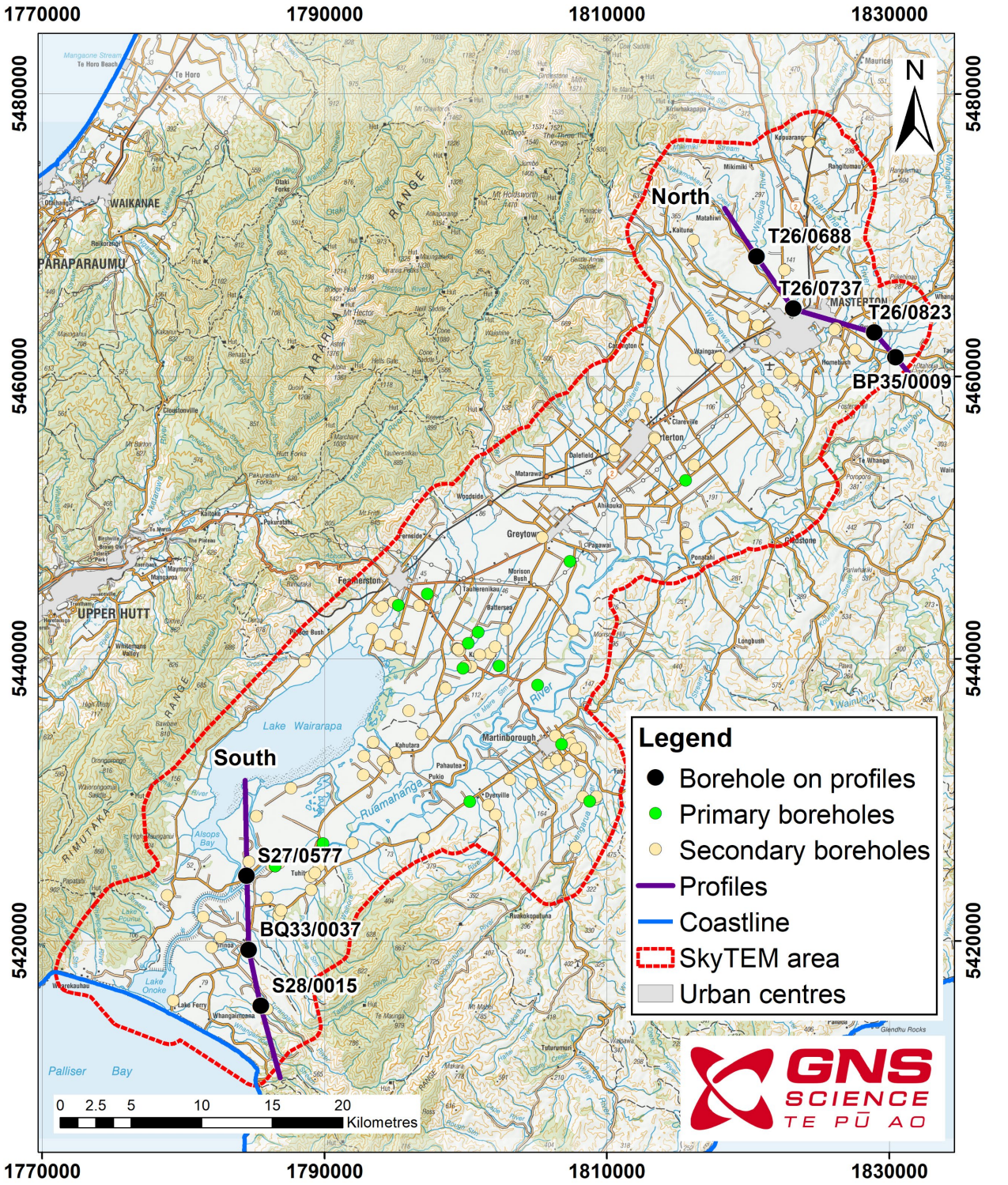

Figure 5.3 Locations of the two cross-sections constructed from detailed borelogs.

The southern cross-section (Figure 5.4) extends from S27/0577 in the centre of the southern Wairarapa Valley on the western back of the Ruamāhanga River. The section is similar to those presented in Kellett et al. (2022). The borehole is dominated by clay to a depth of 120 m and the SkyTEM resistivity model shows low resistivities to at least 200 m depth. The lowest resistivity (<5 ohm.m) is encountered at 10 m depth.

Borehole BQ33/0037 lies 5 km southeast on the terraces above the Turanganui Valley (see Figure 1.2 for location). This well shows the presence of two, thick gravel units separated by a fine-grained sequence of clay, sand and some shell material. The SkyTEM resistivity model matches the lithology variations in the top 100 m closely, with the gravel units showing high resistivity (>100 ohm.m) and the clay units have low resistivity (<30 ohm.m). Borehole S28/0015 is located in the upper reaches of the Turanganui Valley (see Figure 1.2 for location). It encountered 25 m of gravel and sand then a thick mudstone layer to the base of the borehole at 177 m depth. The SkyTEM model shows the presence of the gravel layer as a high-resistivity layer at surface (>100 ohm.m) that decreases in resistivity towards a sharp base at 25 m depth. The lower 200 m of the SkyTEM model has very low resistivity (<3 ohm.m) consistent with the Pliocene mudstone (see Section 3.4 and Figure 3.8).

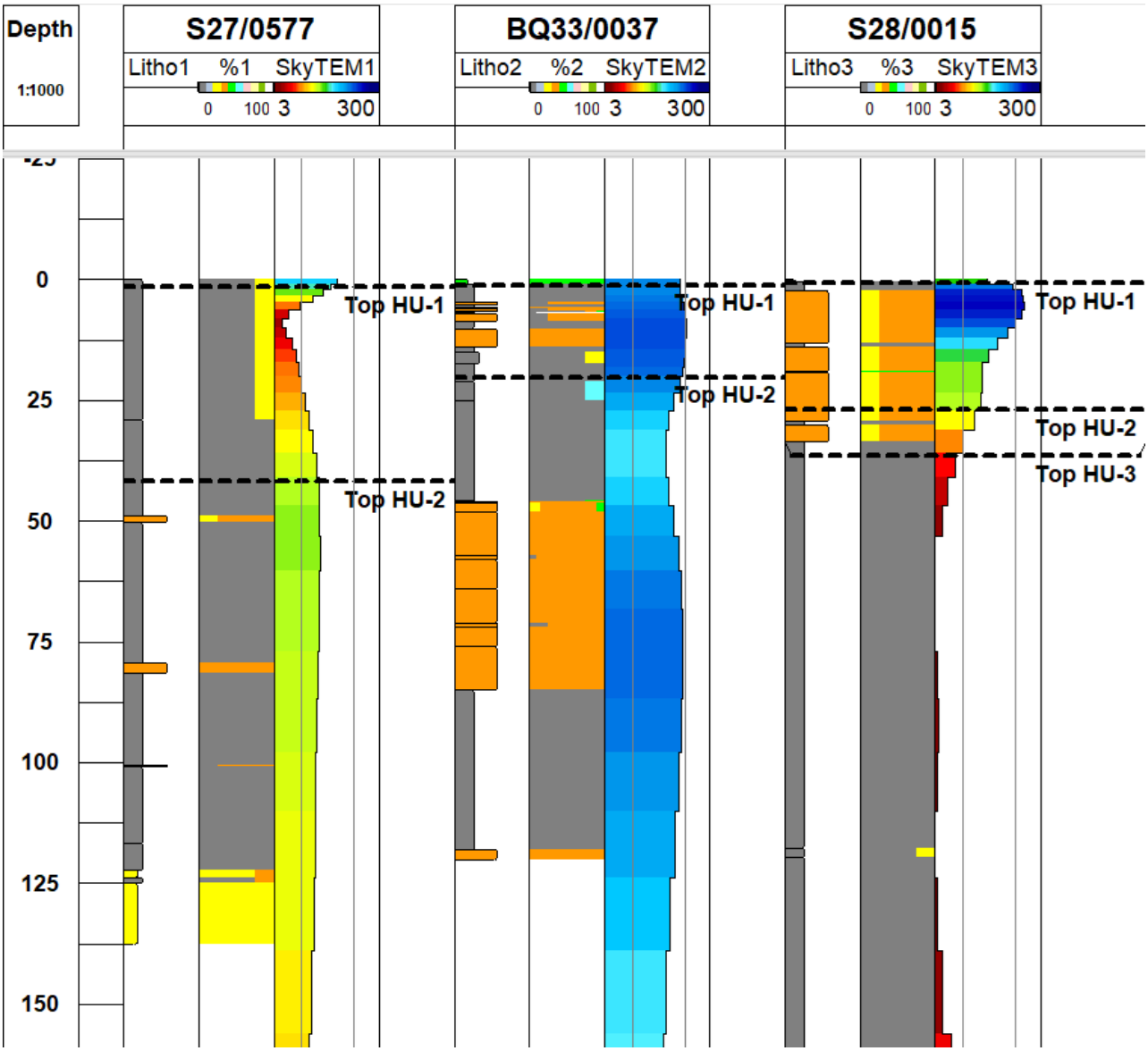

Figure 5.4 Cross-section across the southern part of the Wairarapa Valley between Lake Wairarapa and the Turanganui Valley. The location is shown in Figure 5.4 as profile South. Each borehole is presented as the primary lithology, the % of lithologies, and the SkyTEM smooth resistivity model (30–300 ohm.m on a logarithmic scale). The borelogs for the three boreholes are shown as depths below ground surface. Colours for the lithologies are as per Figure 5.1.

The northern cross-section (Figure 5.5) includes T26/0688 in the northwestern part of the survey area. The borehole has a 30-m-thick sequence of gravel at the surface. The base of the borehole is characterised by sand with clay and organic material. The SkyTEM resistivity model picks up the base

of the gravel as a sharp drop in resistivity and this is interpreted to be the base of HU-1. The base of HU-2 is not interpreted in the lithological logs. However, when mapping HU-2 across the SkyTEM profiles, the base is mapped as a decrease in resistivity (see Section 7), so at this location it is picked at a depth of 130–150 m below ground surface.

Borehole T26/0737 is located on the western edge of Masterton. The gravel layer is 50 m thick and lies directly on a thick sequence of clay. There is a slight increase in gravel content at 100 m depth. The SkyTEM resistivity model shows a gradual decrease in resistivity with depth through the gravel. The low-resistivity layer correlates closely to the clay layer. In many cases the surfaces used to correlate the hydrogeological units across the model are not clearly identified as the top or base of a resistivity layer, and surfaces are interpolated from adjacent SkyTEM models.

T26/0823 lies east of Masterton in the centre of the Te Ore Ore basin (see Figure 1.2 for the locations). The borelog contains two gravel units separated by a clay layer. The SkyTEM resistivity is significantly lower than at the previous two sites, but the base of each gravel layer does coincide with a drop in resistivity. This drop in overall resistivity could be related to the clay content of the gravel units or an increase in groundwater salinity (see Section 6). The base of HU-2 is interpreted to be close to the base of the well on the basis of adjacent borelogs and the subtle change in resistivity.

The eastern end of the profile is marked by borehole BP35/0009. The borehole is located on a slope on the eastern edge of the Te Ore Ore basin. A limestone layer was encountered at 50 m depth. The closest SkyTEM sounding approximately 300 m to the west shows a low-resistivity layer in the top 50 m with an increase in resistivity matching the top of the limestone. This high-resistivity layer is approximately 100 m thick. The basal section of the SkyTEM model has a lower resistivity consistent with mudstones that are mapped in outcrop to the east.

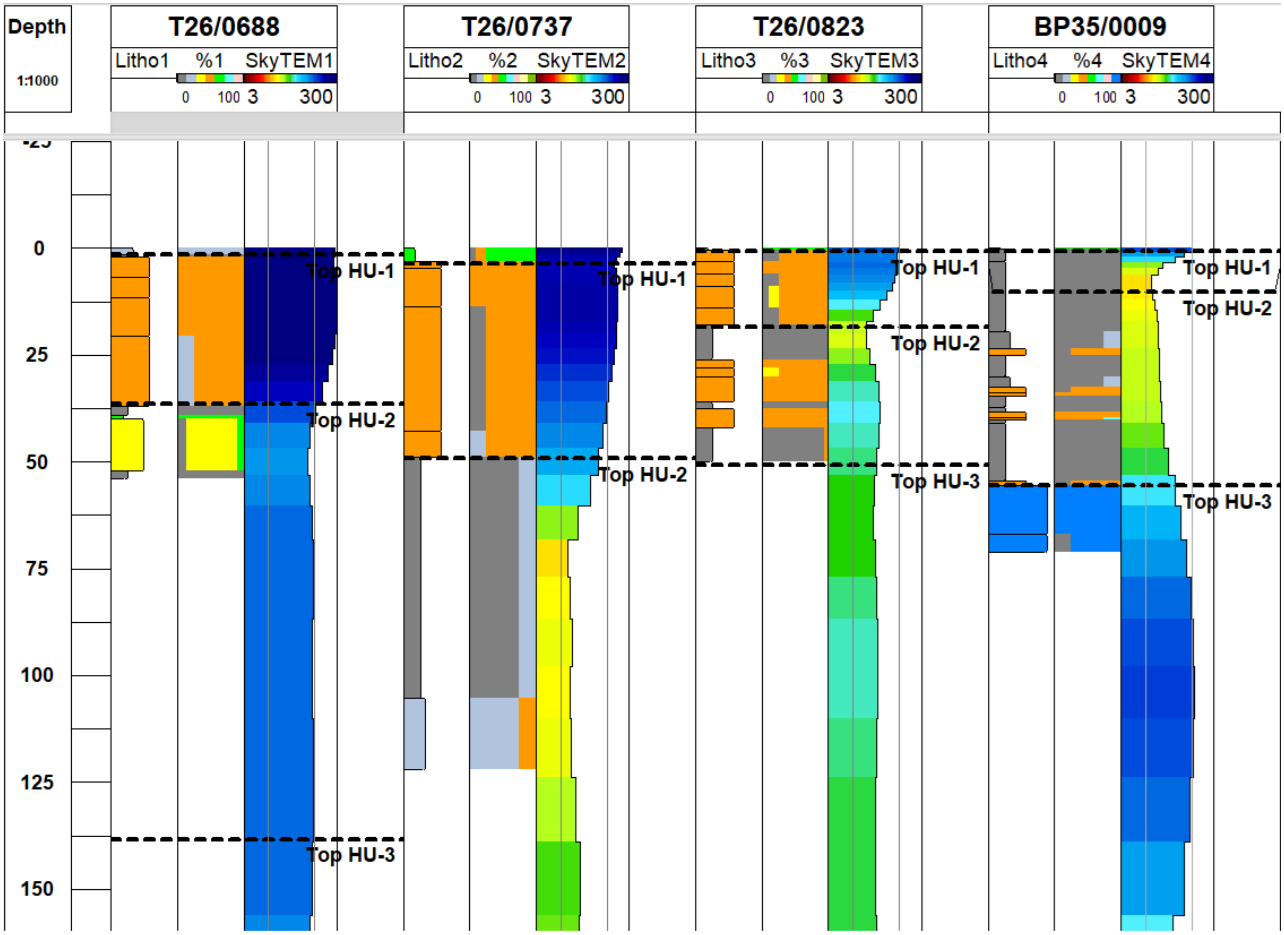

Figure 5.5 Cross-section across the northern part of the Wairarapa Valley in the vicinity of Masterton and the Te Ore Ore basin. The location is shown in Figure 5.4 as profile north. Each borehole is presented as the primary lithology, the % of lithologies and the SkyTEM smooth resistivity model (30–300 ohm.m on a logarithmic scale). The borelogs for the four boreholes are shown as depths below ground surface. Colours for the lithologies are as per Figure 5.1.

Both of these cross-sections illustrate the strong relationship between the resistivity and the lithologies at each borehole when the layers are resolvable in the SkyTEM. They also demonstrate that a hydrogeological unit used to interpret the SkyTEM models (HU-1, HU-2 and HU-3) can be composed of sedimentary facies that range in resistivity from high (gravel) to low (clay). In some cases the hydrogeological unit contains thin intervals of both gravel and clay, and the resistivity of the interval is an average of the two (see Figure 5.4 [BQ33/0037] and Figure 5.5 [T26/0823]).

6.0 Relationships Between SkyTEM Resistivity and Aquifer Potential

6.1 General

SkyTEM is a time-domain, airborne electromagnetic (AEM) system widely used in hydrogeological investigations. It provides high-resolution, three-dimensional resistivity models that can be interpreted to infer geological and hydrogeological formations, identify aquifer boundaries and assess groundwater resource potential (Auken et al. 2017; Knight et al. 2018). The method measures the subsurface electrical resistivity, which helps to characterise geological properties, such as porosity, saturation and lithology. Electrical resistivity varies widely with geological materials and fluid content and quality, making it an indirect but powerful tool for three-dimensional aquifer mapping, especially when combined with borehole lithological logs, geological maps and hydrogeological data, such as groundwater quality, hydraulic conductivity and transmissivity of the target geological materials that host the aquifer.

6.2 SkyTEM Interpretation Method

The resistivity of geological materials is broadly indicative of their aquifer potential.

- Clay-rich geological materials typically exhibit low resistivity due to fine grain size and high surface area, which promotes cation exchange and water retention. From an aquifer potential point of view, clay layers often act as confining units with poor aquifer potential properties due to very low hydraulic conductivity.
- Sand exhibits a moderate resistivity range of 30–100 ohm.m, depending on grain sorting and water content. Clean saturated sands with a considerable thickness are good aquifers due to relatively high hydraulic conductivity and transmissivity as compared with clay-rich materials.
- Gravel generally shows the highest resistivity of all unconsolidated deposits, especially when it is unsaturated. Thick, saturated gravels are typically the best aquifers due to their coarse texture and very high hydraulic conductivity and transmissivity.
- Bedrock aquifers are usually characterised by highly variable resistivity. Fractured and weathered bedrock units like limestone and sandstone usually store and transmit economic amounts of groundwater to wells. Massive crystalline and metamorphic bedrocks (including greywacke) are often resistive and are characterised by very low aquifer potential, unless fractured.

In addition to the lithological controls on aquifer potential, groundwater quality plays a crucial role in interpreting SkyTEM data. Saline groundwater significantly lowers the bulk resistivity, making a sandy or gravelly aquifer appear similar to a clay-rich unit. This influence of salinity is particularly relevant in coastal or low-lying regions like the southern Wairarapa Valley, where saline intrusion or brackish groundwater conditions might exist. Therefore, simultaneous evaluation of groundwater electrical conductivity (EC), geology and well lithological logs was found essential in interpreting the SkyTEM resistivity in the Wairarapa Valley.

In the present hydrogeological model development, the approach used to translate the electrical resistivity, in the SkyTEM resistivity model, to a set of aquifer characteristics followed the criteria listed above. The approach is adapted from the methods described by Rawlinson et al. (2024), Sahoo et al. (2023), Rawlinson (2023) and Minsley et al. (2021).

The main steps followed in the interpretation of the SkyTEM data involves:

1. Facies classification: Resistivity values are divided into discrete classes using logarithmic scaling to distinguish between conductive and resistive units both in the consolidated and unconsolidated deposits. These classes are referred to as resistivity facies.

2. Correlation with geology: Surface geological units from QMAP and borehole lithological units from logs are compared with resistivity facies to refine the interpretations.
3. Assessment of water quality: EC measurements are collected from a set of monitoring wells throughout the valley to identify regions of saline influence.
4. Integrated interpretation: All data sources (SkyTEM, borehole lithological logs, geological maps and cross-sections, groundwater quality and other available groundwater information) are jointly interpreted to build the final hydrogeological model and aquifer potential of the whole Wairarapa Valley.

6.3 Resistivity Facies Classification

Resistivity values from the SkyTEM data are transformed into discrete facies using a logarithmic scale to better capture geological variability. These facies are defined across a range from 5.6 to 501 ohm.m divided into 15 classes ($\log_{10}$(resistivity) = 0.15 per division). This broad range of resistivity covers lithologies from clay-rich unconsolidated sediments to silt, sand and gravel with moderate to high resistivity and includes indurated greywacke basement with very low aquifer potential. The logarithmic scaling suits electrical resistivity values derived from AEM systems because the measurement has the same sensitivity to changes between 5 and 8 ohm.m, as between 355 and 500 ohm.m.

In a general sense the classification captures a continuum of geological materials following Palacky (1987):

- Very low resistivity (<5 ohm.m): clay-rich materials, saline aquifers and highly saturated fine-grained sediments.
- Low to moderate resistivity (5 to 100 ohm.m): silts and fine to medium sand dominated unconsolidated deposits.
- High resistivity (100 to 300 ohm.m): saturated, gravel-rich, coarse-grained unconsolidated sediments, including coarse-grained sand, pure gravels and consolidated aquifers like fractured sandstone and limestone.
- Very high resistivity (>300 ohm.m): unsaturated gravels and crystalline or unfractured basement rocks with very low hydraulic conductivity.

6.4 QMAP Outcrop Versus Shallow SkyTEM Resistivity

The next phase of the interpretation focused on analysing spatial variations in the shallow resistivity from the SkyTEM models compared with the outcropping geological units. The analysis area was constrained to the spatial extent of the SkyTEM data and was intersected with the 1:250,000 QMAP geological data set (Heron 2023). To represent the surficial hydrogeological framework the resistivity of the top 4 m of the SkyTEM model was computed by averaging the top four layers of each smooth SkyTEM resistivity model (Figure 6.1). A depth of 4 m was chosen to be representative of the surface geology and typically encompasses regions above and below the water table. From a AEM perspective the resistivity of the top 4 m is well constrained. From a geological perspective, the upper 4 m is sufficiently deep to avoid any soil or regolith response and provide valid resistivity measurements for the Holocene, Pleistocene and outcropping consolidated Tertiary formations. The older Mesozoic greywackes are likely highly weathered, so may not yield the resistivity of fresh basement.

A GIS-based geostatistical approach was then used to calculate the statistics (including the number of points, average, median and standard deviation) of resistivity measurements within each geological unit. Polygons were rejected if they contained less than 10 resistivity measurements. Figure 6.2 shows the map of the median resistivity in each QMAP unit. The median was chosen as the main parameter to analyse as it was less biased by large variations in resistivity within individual geological units.

Comparing Figure 6.2 with the surficial geology shown in Figure 3.1 indicates that there are some significant trends that are helpful in determining the relationship between bulk resistivity and lithology.

The area offshore and extending to Lake Onoke (see Figure 1.2 for location) has a consistently low resistivity of <5 ohm.m, consistent with the high salinity. The lower reaches of the Ruamāhanga River as far as the southern end of Lake Wairarapa (see Figure 1.2 for locations) also show low-resistivity zones, likely reflecting combinations of fine-grained floodplain deposits, high moisture content and possible salinity influence from shallow groundwater-surface water interactions.

In contrast, the Q2 gravel fans (see Table 3.2 and Figure 3.5) on the southwestern side of the valley and the Tauherenikau fan between Featherston and Carterton (see Figure 1.2 for locations) have the highest resistivity (>300 ohm.m). This deposit consists predominantly of coarse-grained, well-drained gravels, which are often unsaturated in the upper layers. Such materials typically function as high-transmissivity, unconfined aquifers offering substantial groundwater storage and flow capacity.

The Ruamāhanga River valley along the eastern edge of the central part of the valley and around Martinborough displays lower resistivities than the western and northern part of the basin (see Figure 1.2 for locations). This response may reflect finer sediment textures, higher water saturation or chemical factors, such as groundwater salinity or mineralisation.

The Q2 and Q3 terraces are more resistive that the young Q1 alluvial channels, implying coarser grain sizes and better drainage. However, saturation levels were not explicitly accounted for in this part of the analysis. Since pore water saturation significantly affects resistivity, further work should incorporate saturation models or employ hydrological simulation to quantify the role of partial saturation in the Holocene and Pleistocene units on the elevated terraces.

Figure 6.3 shows a box and whisker plot of the median resistivity for each of the main geological units computed by combining all polygons with the same age and rock type. The large scatter shown by the extremes of the whiskers indicates that each QMAP unit contains a large range of resistivity values. However, when viewed together with Figure 6.2, the following trends are present in the data based on the upper and lower quartiles or the inter-quartile range:

1. Saline water is <5 ohm.m and freshwater is between 25 and 62 ohm.m.
2. Q2 gravel is the most resistive surficial deposit (median = 70–180 ohm.m).
3. Q1 gravel is slightly less resistive (median = 35–15 ohm.m).
4. Q3–Q8 gravel units are difficult to distinguish, having median resistivities between 35 and 135 ohm.m.
5. The older mQ gravel has the narrowest range in resistivity (median = 40–55 ohm.m).
6. The Pliocene and Miocene units are difficult to separate based on the resistivity, but the map shows the units around the edges of the basin have medians between 21 and 60 ohm.m.
7. The exposed Mesozoic greywacke basement has a large range of median resistivities but is still slightly more resistive than the Q2 gravel.

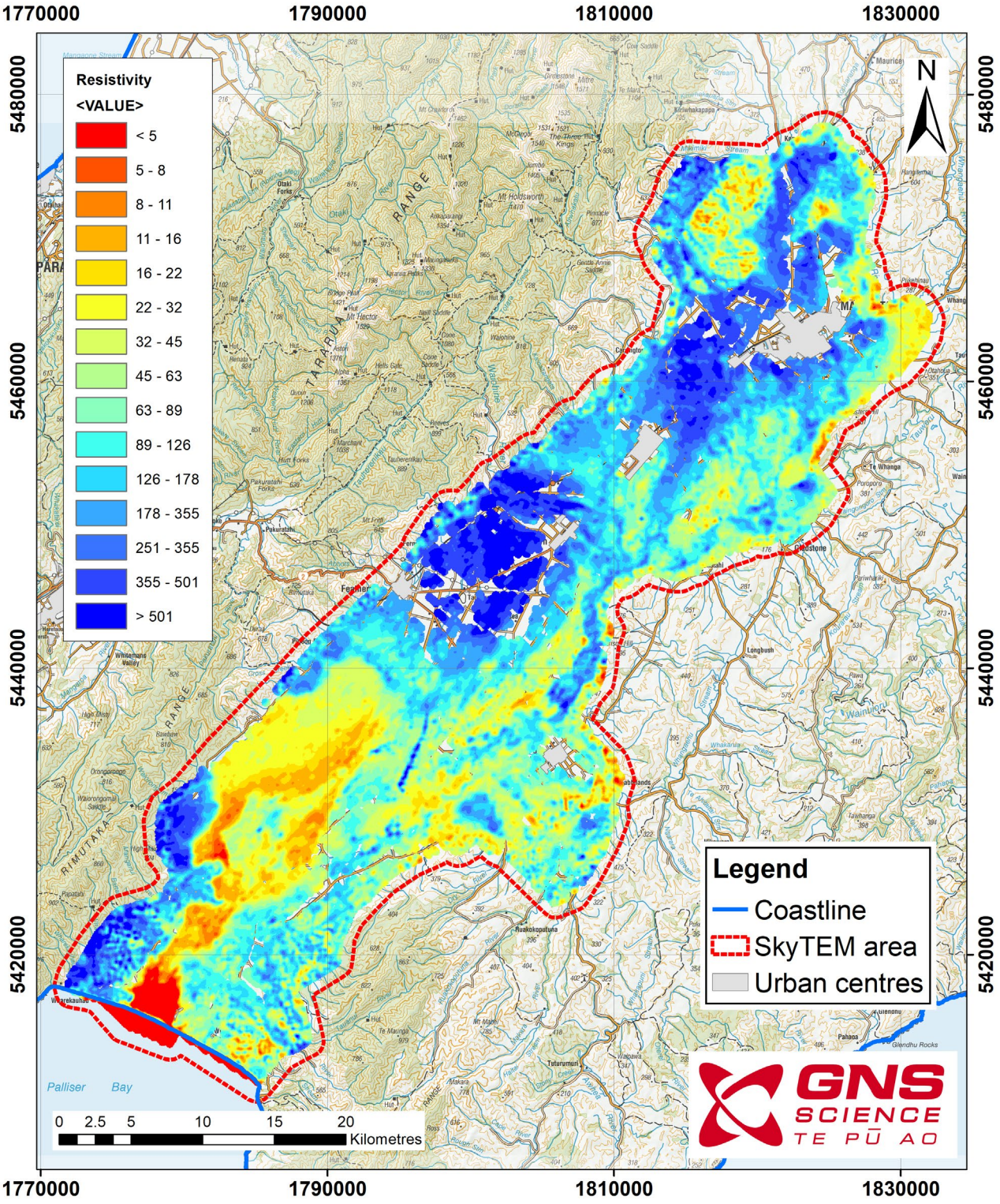

Figure 6.1 The resistivity of the top 4 m of the SkyTEM smooth model. The map shows the resistivity values classified into 15 facies on a logarithmic scale from 5 to 500 ohm.m.

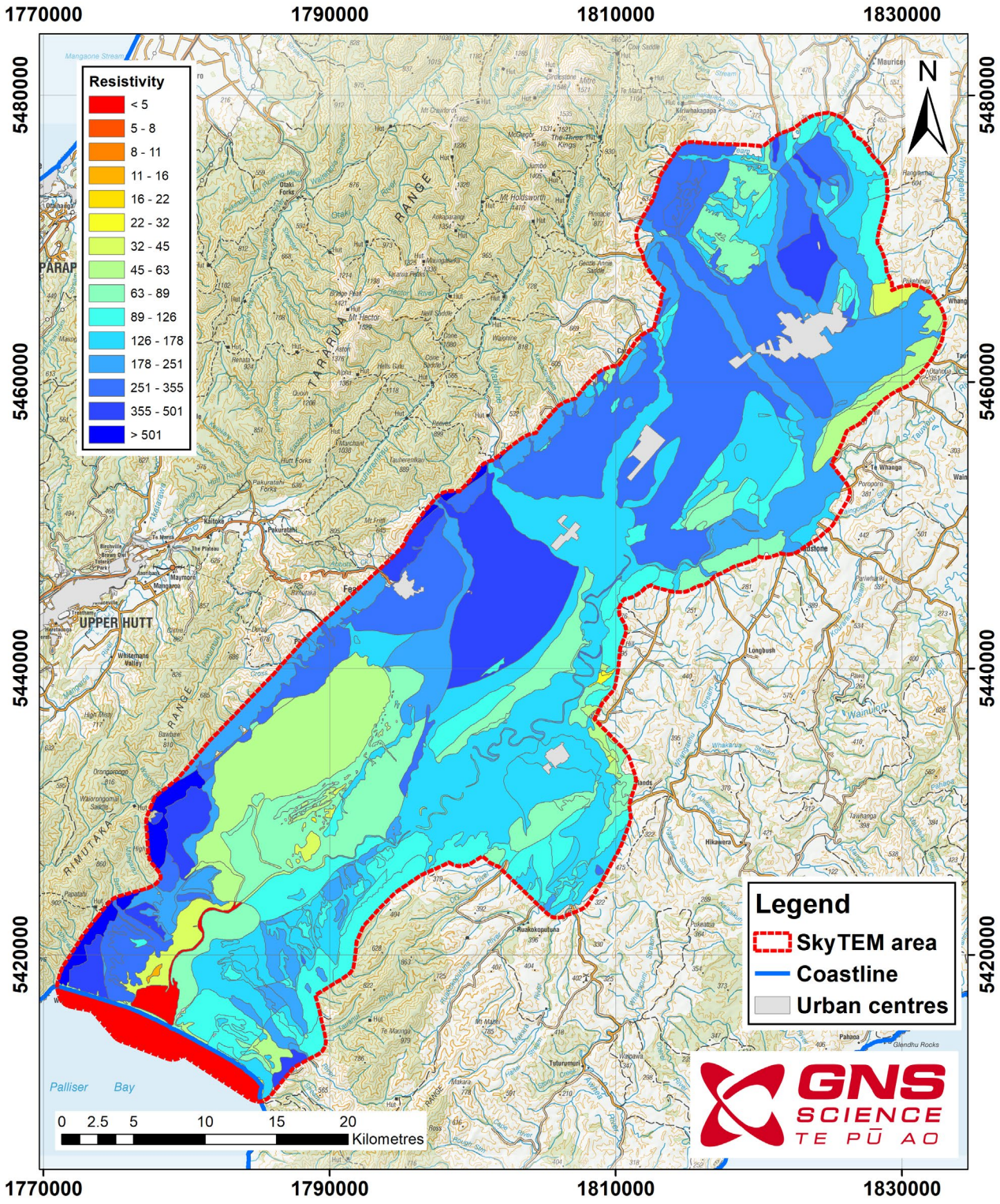

Figure 6.2 The median resistivity of the top 4 m of the SkyTEM smooth model is calculated for each QMAP polygon. The map shows the resistivity values classified into 15 facies on a logarithmic scale from 5 to 500 ohm.m.

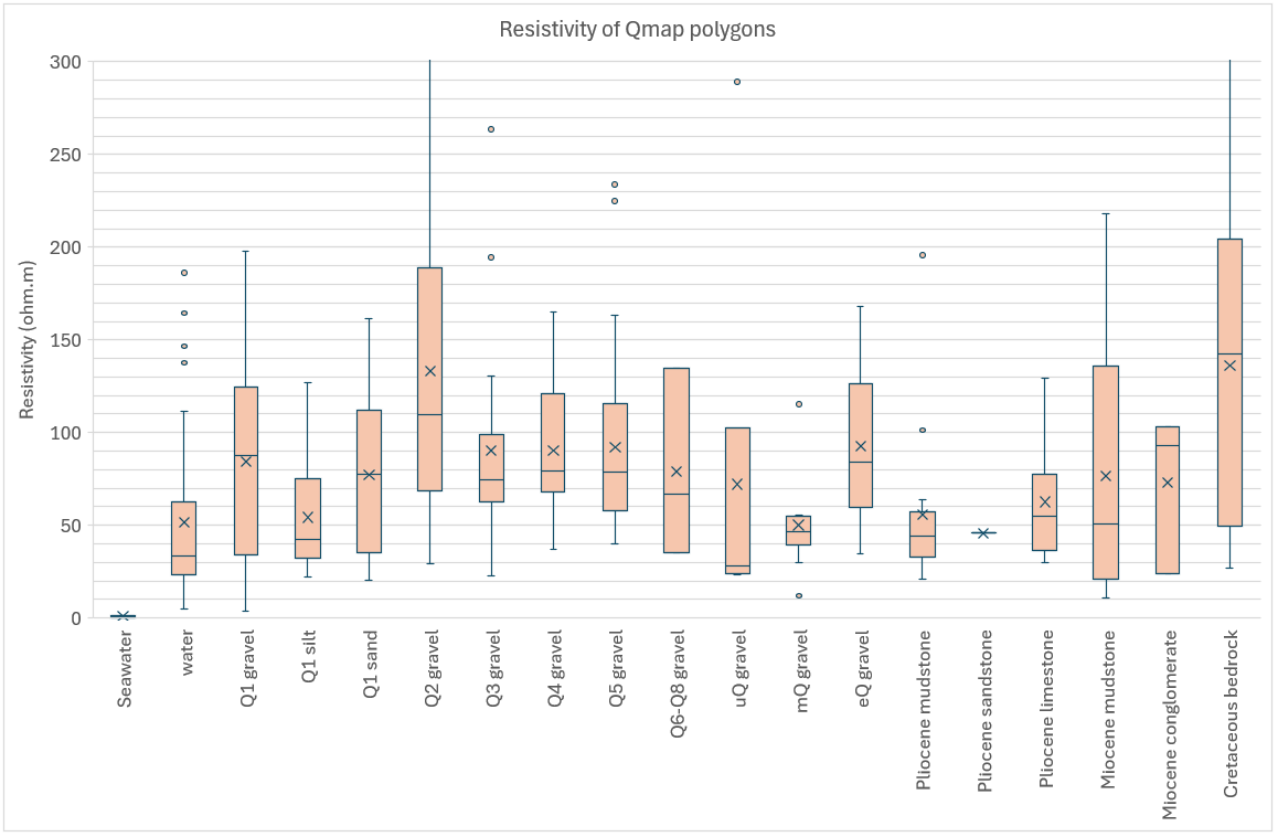

Figure 6.3 The median resistivity of the top 4 m of the SkyTEM smooth model is calculated for each QMAP unit. The units have been divided into surface water, Quaternary surficial units Q1 to Q5 (and some Q6–Q8), exposed upper (uQ), middle (mQ) and early (eQ) Quaternary units, exposed Pliocene and Miocene consolidated sediments, and Mesozoic greywacke bedrock. The box and whisker plot presents the median and quartile values as a box, and the spread of the data as whiskers. The average is presented as the X in each box. In this case it is the average of the median values for the set of QMAP polygons in each category. The outliers are plotted as individual points.

6.5 Borehole Lithology Versus SkyTEM Resistivity

To evaluate the relationship between electrical resistivity and subsurface lithology at greater depths particularly within the Holocene, Quaternary and Tertiary units, an integrated analysis was conducted using borehole lithological logs in conjunction with SkyTEM resistivity data. A total of 1474 boreholes from all three categories of bore (see Section 5) were included in the study, each located within 300 m radius of a corresponding SkyTEM model point. This approach enabled a spatially coherent correlation between borehole recorded lithology and geophysical signatures, thereby enhancing the interpretation of hydrogeological units and aquifer potential. The dataset is predominantly composed of shallow wells, which are mainly screened within unconsolidated alluvial sediments typical of the Holocene depositional environment:

- 79% of the boreholes sampled geological materials at depths <25 m.
- 15% of the borehole data fell between 26 and 50 m depth, intersecting some deeper parts of the Quaternary aquifer system.
- 6% extended below 51 m depth, partially assessing early to middle Quaternary deposits.

Statistical analysis was conducted using all available resistivity data from the SkyTEM smooth models, extracted at borehole locations and categorised by dominant lithology. The range in resistivity for the units encountered in the boreholes is shown in Figure 6.4. This analysis differs from the analysis of the surficial geological layer because all data were available for the calculations of the statistics. The box and whisker plots include the average and median of the distributions. The following trends are observed based on the average and the upper and lower quartiles:

1. Soils and surficial layers exhibit a broad resistivity range (80–215 ohm.m), reflecting heterogeneity in grain size, moisture content, and degree of compaction. These units may include both unsaturated and partially saturated intervals.
2. Clay-rich formations characterised by high cation exchange capacity and low hydraulic conductivity showed consistently low resistivities (50–80 ohm.m). These layers typically function as aquitards or confining units impeding vertical and lateral groundwater movement.
3. Silts and fine sands displayed intermediate resistivities (85–110 ohm.m), indicating relatively low to moderate effective porosity and hydraulic conductivity, compared with gravel. These layers often act as leaky confining layers or marginal aquifers.
4. Gravel dominated lithologies exhibited the highest average resistivities (>130 ohm.m). This category of primary lithology is broken down into a range of sub-classes. The gravel and silt combination class had an upper quartile resistivity of 235 ohm.m, suggesting well-drained, dominantly coarse-textured sediments that are typically associated with high yield, unconfined aquifers.
5. Consolidated Miocene and Pliocene sediments, likely consisting of compacted sands, silts and calcareous rocks had lower average resistivity values (55 ohm.m). The drop in resistivity could be due to salinity of the pore fluids or weathering of some components of the matrix to clay minerals. The consolidated units were under-represented in the sample due to the lack of deep wells.
6. Cretaceous greywacke basement units, although under-represented in the dataset, showed average resistivities of 80 ohm.m. These rocks generally act as hydraulic basement with limited water storage capacity, unless secondary porosity features, such as faults or weathered zones, increase permeability.

In summary, this part of the analysis emphasises the utility of resistivity data in distinguishing aquifer versus aquitard zones, particularly when integrated with borehole lithological logs and stratigraphic information.

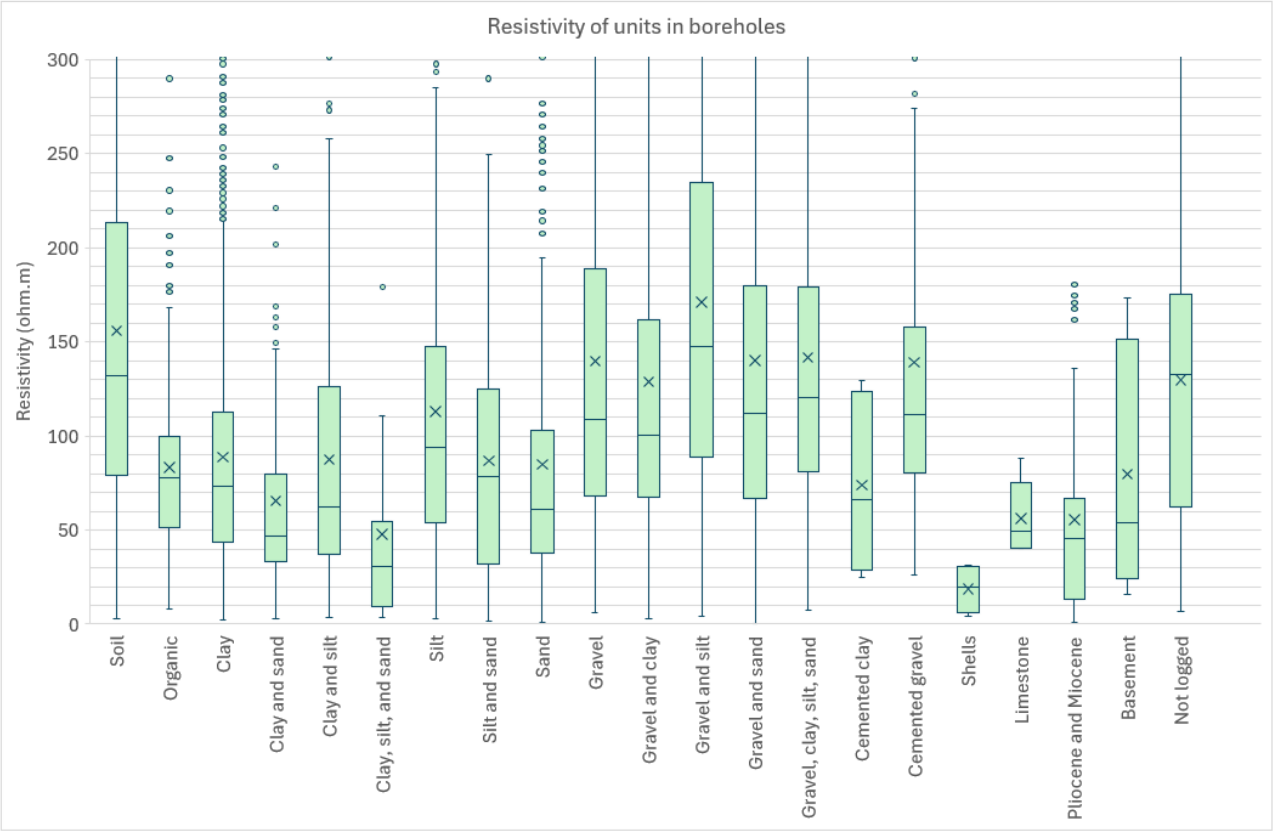

Figure 6.4 The resistivity of the geological units mapped in 1474 boreholes from the Greater Wellington Regional Council database. The resistivity is extracted from the SkyTEM model closest to the bore within a radius of 300 m. The units are categorised by their primary lithological description. The box and whisker plot presents the median and quartile values as a box, and the spread of the data as the whisker. The average is presented as the X in each box. In this case it is the true average of all samples for that class of lithology. Outliers are plotted as individual points.

6.6 Groundwater Quality

Groundwater quality, specifically the ionic composition and salinity of pore water, has a profound influence on the bulk resistivity measured by AEM methods such as SkyTEM. In porous and permeable lithologies, such as sand and gravels, the resistivity is governed not only by grain structure and saturation but also by the electrical conductivity of the groundwater filling the pore spaces. Thus, data on the chemistry of the groundwater are important in the interpretation of bulk resistivity, especially in the highly permeable and porous lithologies. High levels of total dissolved solids (TDS in ppm) and elevated chlorides can reduce the resistivity of the groundwater and, in turn, reduce the bulk resistivity of the geological unit. To quantify this relationship, a set of 74 monitoring wells across the valley were identified that had field or laboratory electrical conductivity (EC in µS/cm) measurements available for analysis (Figure 6.5). The data are measured at regular intervals as part of the GWRC monitoring programmes. The data obtained from the GWRC water quality database[2] were taken close to the timing of the SkyTEM survey (February to March 2023) to reduce any temporal bias in the groundwater quality data caused by groundwater quality changes with time.

2 Environmental Data Dashboard | Greater Wellington Regional Council — GWRC | Te Pane Matua Taiao

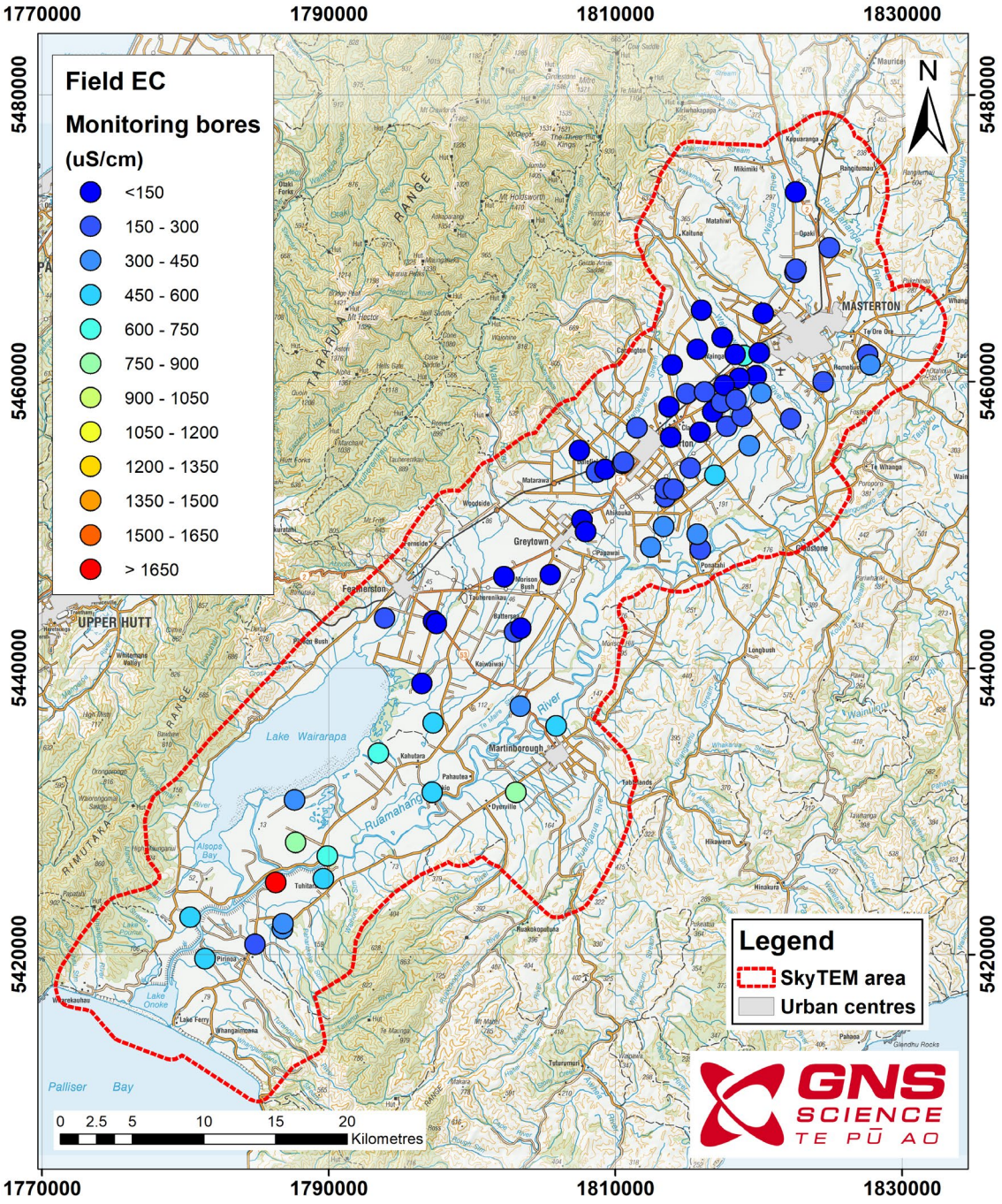

Figure 6.5 Location of the monitoring bores with groundwater conductivity measurements. The field EC values are plotted in μS/cm.

The key findings of the analysis of the groundwater chemistry are:

- A clear spatial gradient of increasing conductivity was observed from north to south. One of the monitoring bores adjacent the Ruamāhanga River shows significantly elevated conductivity (>1500 μS/cm) that reflects either natural salinisation, evaporative concentration or mixing with deeper and more mineralised waters.
- The values in the western half of the Wairarapa Valley are slightly lower than those along the eastern side of the valley.
- In the eastern part of the Wairarapa Valley the groundwater tends to exhibit slightly higher salinity levels than the western side, possibly due to longer groundwater flow paths, rock-water interaction or localised discharge and recharge dynamics.

More detailed studies of the groundwater chemistry (O'Dea et al. 1980; Morgenstern 2005; Daughney et al. 2009; Van de Raaij 2024) indicate that local variations in EC might be more significant than the regional trend observed in Figure 6.5.

The electrical conductivity was converted to a resistivity in ohm.m for direct comparison with the SkyTEM models. Figure 6.6 shows the resistivity plotted against the depth of the screened interval in the well. There is a general trend of the resistivity of the groundwater decreasing with depth, but there is significant scatter. The graph may be showing a bias due to shallower wells being prevalent in areas with groundwater that has a higher resistivity, and deeper wells being more common in areas in the southern part of the valley where the salinity is slightly elevated. In summary, a general trend of decreasing resistivity with depth was evident, aligning with understanding that deeper aquifers are more likely to contain older and more mineralised water.

The range in resistivity is 6 ohm.m to 122 ohm.m (1658 to 82 μS/cm).

From a hydrogeological perspective, groundwater resistivity <30 ohm.m may mask lithological contrasts, especially in units composed of silts and fine sands, due to overriding influence of electrolyte condition. Conversely, freshwater aquifers with resistivity >50 ohm.m are more easily distinguishable from adjacent aquitards, improving the accuracy of aquifer boundary delineation. Thus, correct interpretation of SkyTEM resistivity data must incorporate groundwater chemistry, particularly in areas affected by saline intrusion, geogenic contamination or deep connate water migration. In the Wairarapa Valley, such integration is vital for constructing a robust hydrogeological model, informing water resource assessment and sustainable groundwater management.

Figure 6.6 A plot of field measured electrical properties of the groundwater (in ohm.m) versus depth of the aquifer based on the reported screened interval.

7.0 Hydrogeological Interpretation and Aquifer Potential

Within the scope of the current project, the hydrogeological interpretation of the resistivity models is the process of translating resistivity values (typically represented by the unit ohm.m) to a measure of aquifer potential. Aquifer potential is a measure of the likelihood that a particular point in the model (x, y, z) contains aquifer-bearing material. The description is qualitative and is represented on a gradational scale from very low to highest. There is an equivalent numerical code that also differentiates the aquifer potential based on the expectation that the geological unit is unconsolidated or consolidated. It is outside the scope of the current study to calibrate the aquifer potential against any specific aquifer properties from groundwater bores.

The process of deriving the aquifer potential volume involves two main steps, including (1) development of a hydrogeological framework and (2) translation of resistivity and hydrogeological framework into the aquifer potential.

7.1 Hydrogeological Framework

The numerical values present in a resistivity model are a function of complex relationships between porosity, permeability, grain size and sorting, mineralogical content, such as clay, and fluid properties. There are no unique mathematical equations established that directly link lithological units with resistivity values. Wide ranges of resistivity values have been empirically correlated to various unconsolidated and consolidated lithologies (Rawlinson 2013). These values will be locale-specific and may be spatially variable within an area due to subtle geological variations (e.g. different facies or depositional processes). Therefore, in this study, to understand the spatial variability of resistivity in the study area, we have developed a hydrogeological framework that divided the stratigraphy into three hydrogeological units (HU-1, HU-2, HU-3) and a basement unit (Figure 7.1). The approach of defining a series of hydrogeological units across the SkyTEM area follows from the methodology developed in Sahoo et al. (2023).

As described in Section 3 (Conceptual Geological Model) the Quaternary units in the study are mainly unconsolidated (Begg et al. 2005). The SkyTEM resistivity model shows that there are well-defined lateral and vertical variations in resistivity within the Quaternary section. Further analysis shown in Sections 3, 5 and 6 show that there are strong correlations between resistivity and lithology, but also that facies variations within one Quaternary interval may be large. In order to accommodate this complex geological setting, the Quaternary portion of the model has been divided into two hydrogeological units (HU-1 and HU-2). In comparison with the geological framework as described in Section 3, HU-1 corresponds to upper parts of the Begg et al. (2005) Unit 5 (Q1–Q4), while HU-2 corresponds to the lower parts of the Begg et al. (2005) Unit 5 and the entire Unit 4.

The geological units underlying the Quaternary are mainly consolidated rocks of Pliocene and Miocene (Unit 3 of Begg et al. [2005], as described in Section 3). In some areas of the Wairarapa Valley, Quaternary units unconformably overlie the Mesozoic greywacke basement rocks (Unit 1 of Begg et al. [2005] in Section 3). In the current model, HU-3 represents the geological formations below the Quaternary and above the Mesozoic greywacke basement. Rocks below HU-3 have been considered as the basement unit.

The boundaries of these hydrogeological units (DEM, H1, H2, basement top), including the resistivity character used to separate them and the geological contacts seen in the borehole logs, are described in detail in Section 7.3. These boundaries are presented as grids and can be imported into any software to represent the thickness of each of the hydrogeological units or their structure.

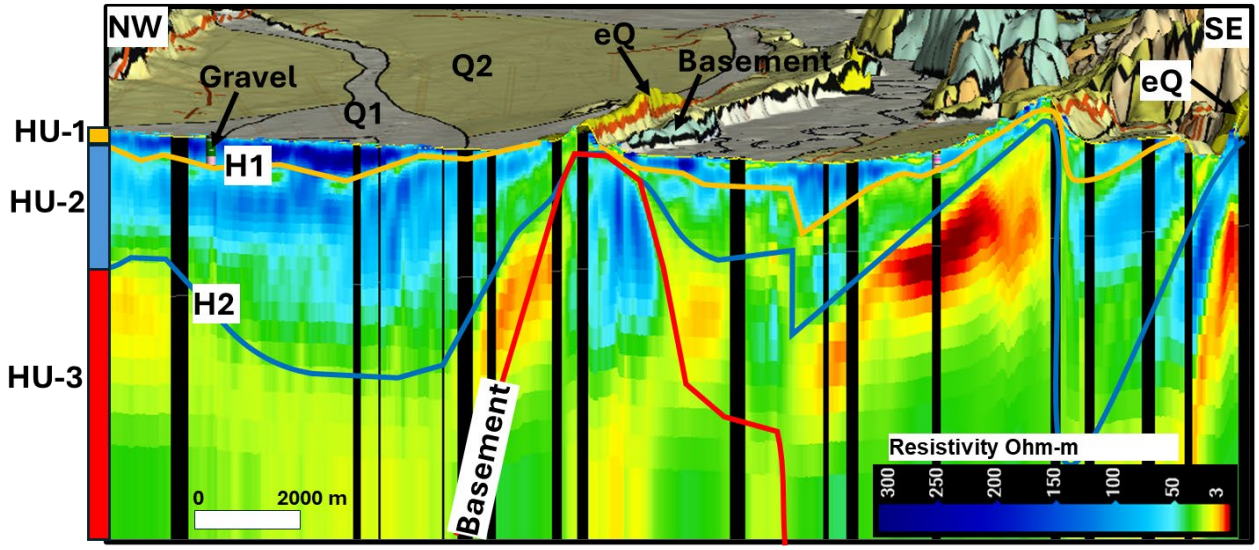

Figure 7.1 A northwest–southeast-trending resistivity profile showing the interpreted hydrogeological units (HU-1, HU-2 and HU-3) and the bounding surfaces (H1, H2 and basement). The surface geology, faults (red lines on the surface geology map), structural pattern and the borehole information have been analysed along with the SkyTEM resistivity to interpret the bounding surfaces. The section is equivalent to the Begg and Johnson (2000) and Nicol et al. (2002) sections in Figure 3.6

7.2 Delineation of Hydrogeological Boundaries and Creation of Grids

During the development of the hydrogeological framework, the SkyTEM resistivity models and supporting data (e.g. boreholes, surface geology, DEM, geological cross-sections, seismic data and gravity models) were integrated and visualised together in Leapfrog. The hydrogeological understanding of the Wairarapa Valley was accomplished by combining cross-section profiles and map-view slices with the conceptual geological model and detailed borehole interpretation.

7.2.1 Resistivity Model Interpretation

The SkyTEM smooth resistivity model was primarily used for mapping the boundaries between hydrogeological units as it provides finer detail of lateral changes in resistivity due to lithological changes, compared with the SkyTEM sharp resistivity model. The sharp resistivity model was used as a supporting reference and to assist with mapping vertical hydrogeological boundaries with reduced uncertainty, particularly in areas of more subtle resistivity variations and complex structure.

In structurally complex areas (e.g. close to bedrock highs and in narrow valleys) and in areas where resistivity data have a shallow DOI (see Section 2.1) or where data are missing due to cultural noise, the surface geology, borehole lithology and the DEM data provide regional topographic and structural information to enable boundary delineation.

Hydrogeological boundaries were interpreted and mapped by considering the following features:

- The sharp changes in the resistivity with depth along the SkyTEM profiles.
- Lateral continuity of the resistivity values.
- Major changes in lithology in boreholes on the SkyTEM profiles.
- Mapped faults and surface geology.

Fixed resistivity cut-off values derived from statistical analysis of borehole lithology and resistivity (Section 6) were used to provide a guide for interpretation of layers and ensure that layers were interpreted consistently across the Ruamāhanga Catchment.

The top of the hydrogeological model is provided by a 100 m DEM re-sampled from a 10 m DEM (LINZ 2011). The hydrogeological model was extended to a depth of 500 m below sea level to ensure it covered the DOI of the SkyTEM data and likely hydrogeological basement.

7.2.2 Greywacke Basement Modelling

As described in the conceptual geology model (Section 3), the greywacke basement outcrops in the Remutaka and Tararua ranges in the west, the Aorangi Range in the east and several up-lifted blocks in the centre of the basin (Tiffin Hill and Te Maire Ridge). At the edges of the survey and over the basement highs, the SkyTEM resistivity model produces a good image of the top of the greywacke layer. However, under the majority of the SkyTEM survey the depth to basement is well below the DOI and is thus unknown.

The interpretation of the basement boundary was guided by a regional scale 3D basement depth inversion of the gravity data using the VPMG (Vertical Prism Magnetic/Gravity) software (Fullagar et al. 2000). The gravity data were compiled from the GNS database (Stagpoole et al. 2022) and additional data from GNS and university research projects (Cape 1989; Bowler 1998; McClymont 2000; Henderson 1999) and petroleum industry data from Holdgate (1999a, 1999b). The work is an update on the model published by Hicks and Woodward (1978). This inversion represents sediments and basement as vertical cuboid prisms with a predefined density contrast within the prisms, leaving the property to be inverted as basement depth. For the inversion used in this project we used 1 km x 1 km prisms with a density contrast of -0.33 Mg/m^3 relative to the basement unit, and constrained areas of basement outcrop to have zero thickness. A density contrast of -0.33 Mgm^{-3} was derived based on a mean porosity of 20% within the sedimentary sequence, and grain density of 2.65 Mgm^{-3}, compared with a basement density of 2.65 Mgm^{-3} with zero porosity. This simplified approach is justified given that the basement depth inversions are intended to provide a regional scale view of the basement, and there is little data to constrain actual porosity or density.

Where no clear evidence of basement depth was available from the SkyTEM data, outcrop geology or other geophysical data (Kellett et al. 2024), the gravity inversion derived basement depth was used.

7.2.3 Constructing Surfaces

We used Leapfrog software to interpret the hydrogeological unit boundaries. Some of the key steps used are below.

- Seed points (manually placed interpretation points) were interpreted in the cross-sections where sharp resistivity contrasts were observed (Figure 7.1).
- Seed points were gridded using a kriging algorithm (ordinary kriging, surface resolution = 100 m, linear interpolant) to generate surfaces.
- These surfaces (H1, H2 and basement) were reviewed, and additional seed points were added where needed to ensure boundary consistency with information such as structural geology, surface geology and borehole lithology.
- The three gridded surfaces were exported from Leapfrog, re-sampled to 100 m grids and extended over the entire Ruamāhanga Catchment.
- A 3D geological model was constructed in Leapfrog using the stratigraphic order with basement surface at the bottom and H2 and H1 in ascending order. The upper surface is formed by the DEM. This simple model allows units HU-1, HU-2 and HU-3 to pinch out against older units.

7.3 Hydrogeological Units

7.3.1 HU-1

The HU-1 is the uppermost hydrogeological unit representing the distribution of the Holocene and Upper Pleistocene (mainly Q1–Q4) deposits in the river valleys and on the uplifted terraces across the valley. The interval HU-1 is bounded by the DEM and H1 surfaces. In most of the areas north of Lake Wairarapa (see Figure 1.2 for locations) and areas close to the western and eastern margins in the Wairarapa Valley, this unit is gravel dominated with moderate to high resistivity character >150 ohm.m (Figure 7.2). In these areas, the base of this unit (H1 surface) was interpreted vertically at the abrupt change in the uppermost high-resistivity unit. The lateral continuity of HU-1 is mapped following the same resistivity contrast along the SkyTEM profiles (Figure 7.2).

In some of the thick fan deposits in the Tauherenikau and Waiohine area, and in the southwest corner of Lake Wairarapa (see Figure 1.2 for location) the resistivity characteristics of the underlying unit (HU-2) is similar to HU-1. In order to separate HU-1 and HU-2, the surface H1 is extended through the thick, high-resistivity zone at a constant resistivity of 200 ohm.m, and borehole lithology and surface geology were used to define the surface. Similarly, it was also difficult to map H1 in areas where the uppermost high-resistivity unit is very thin and lateral continuity is poor. In these areas, the structural patten of the underlying layer and surface geology were used as a guide to map H1.

In the Lake Wairarapa and Lake Ferry areas (see Figure 1.2 for locations), HU-1 gradually transitions into fine-grained sediments and is characterised by resistivity values less than 30 ohm.m (Figure 7.2a). In these areas, the H1 surface was interpreted at the base of the uppermost low-resistivity units. As described in the conceptual geological model (Section 3), the gravel-dominated river deposits (Q1) transition into clay-dominated swamp and lake deposits as we go from the fans towards the east and to Lake Wairarapa.

In this study we assume that this uppermost abrupt vertical change in resistivity profiles coincides with an equivalent horizon to the base of Q4. However, there is uncertainty in this interpretation due to limited age control on sediments in the subsurface.

As observed in previous studies (Rawlinson et al. 2024; Sahoo et al. 2023) and described in detail in Section 6, the unconsolidated Quaternary units show clear relationships between lithology and resistivity, with silt and clay dominated lithologies (which typically act as confining layers and aquitards) exhibiting low-resistivity values, whereas the gravel- and sand-dominated lithologies (which comprise the main aquifer materials) display high-resistivity values.

Figure 7.3 presents a thickness map of this unit. The HU-1 is thickest in a northeast-trending corridor along the Wairarapa Valley. In general, the thickness of this unit ranges from 5 to 75 m along this corridor.

7.3.2 HU-2

The second hydrogeological unit, (HU-2) includes older Quaternary deposits (Q5 to eQ – see Section 3 for details). It is bounded by the H1 and H2 surfaces. The H2 surface was interpreted using the SkyTEM resistivity but with a stronger influence from the boreholes, the surface geology and the structural pattern (from geological cross-sections seen in Section 3).

In the majority of the regions, except areas close to basement highs in the central and eastern areas, H2 has been mapped as the base of a high-resistivity package (Figure 7.2). We have used a resistivity cut-off of >30 ohm.m to provide guidance for this interpretation. The central and eastern areas (Te Maire Ridge and Parkvale as shown in Figure 1.2) are structurally complex with the presence of a series of northeast-trending faults (Figure 3.1) and grabens. Along the structural highs, the older Quaternary units are subject to erosion and non-deposition. Therefore, it is difficult to map H2 in these areas based

on SkyTEM resistivity models alone. A combination of the SkyTEM resistivity, the structural pattern seen in the underlying Tertiary bedrock and surface geology was used to map H2 in this area.

Seismic data, geological cross-sections (Nicol et al. 2002) and surface geology suggest that the Tertiary units have steeply dipping strata (Figure 3.7, Figure 3.11) and the Quaternary is deposited on an angular unconformity (Figure 3.7). The H2 surface has been interpreted along this unconformity at the top of these steeply dipping older units (Figure 7.2). Along the eastern margin of the Wairarapa Valley, H2 represents the top of the Pliocene and Miocene strata. In the southern part of the Wairarapa, H2 may lie at the top of some more consolidated early Quaternary units (see Section 3).

As shown in the HU-2 thickness map (Figure 7.4), HU-2 is present in most of the areas along the Wairarapa Valley and ranges in thickness from 0 to ~550 m. In general, HU-2 shows a greater sediment thickness (up to ~550 m) compared with HU-1 (up to ~70 m).

There are four small depocentres associated with the synclines and thrust structures along the eastern side of the valley and in the southwest.

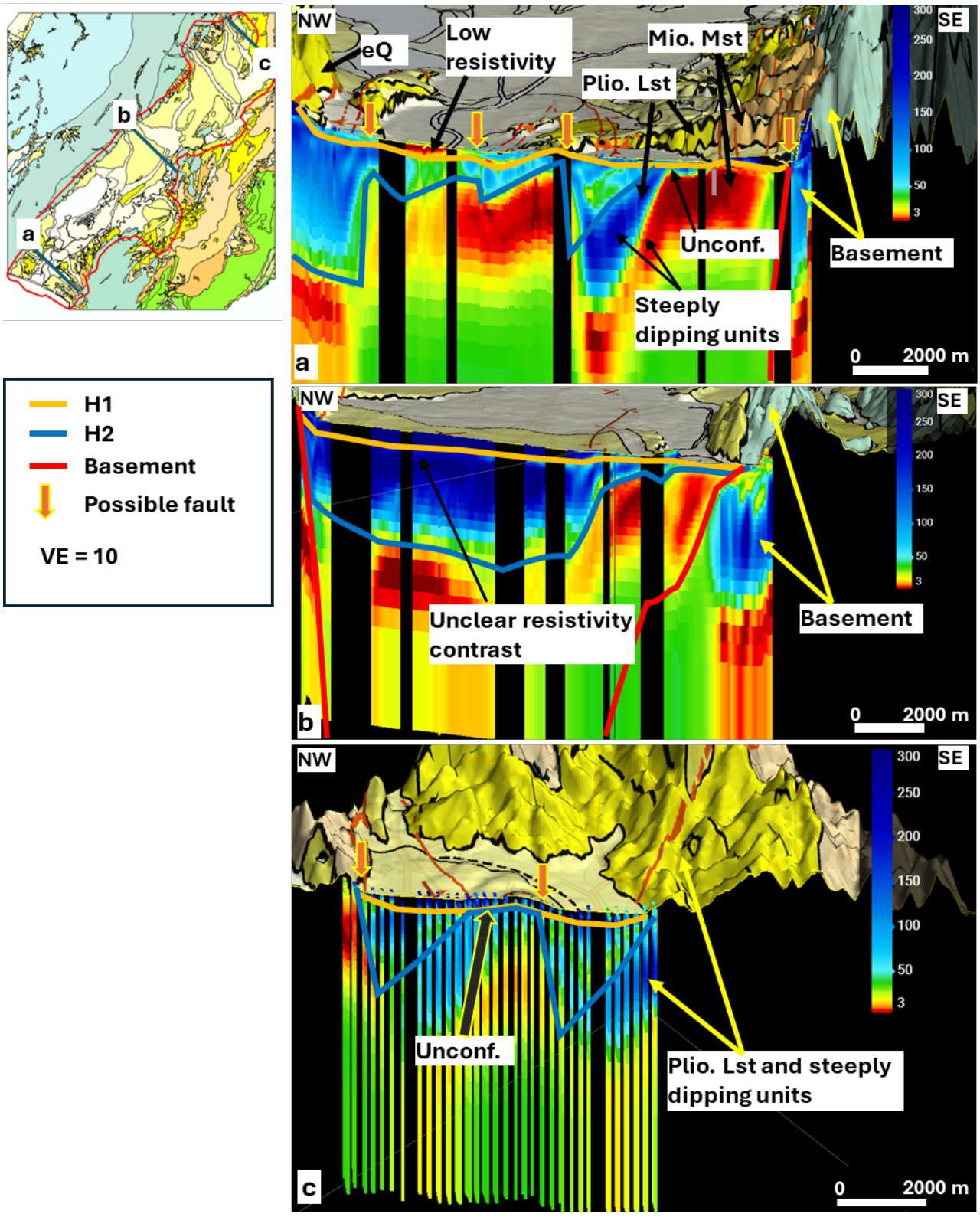

Figure 7.2 Examples of northwest–southeast-oriented cross-section profiles showing SkyTEM resistivity, surface geology, interpreted hydrogeological boundaries and key structural features. The location of these profiles is shown in the inset basemap. VE= Vertical exaggeration.

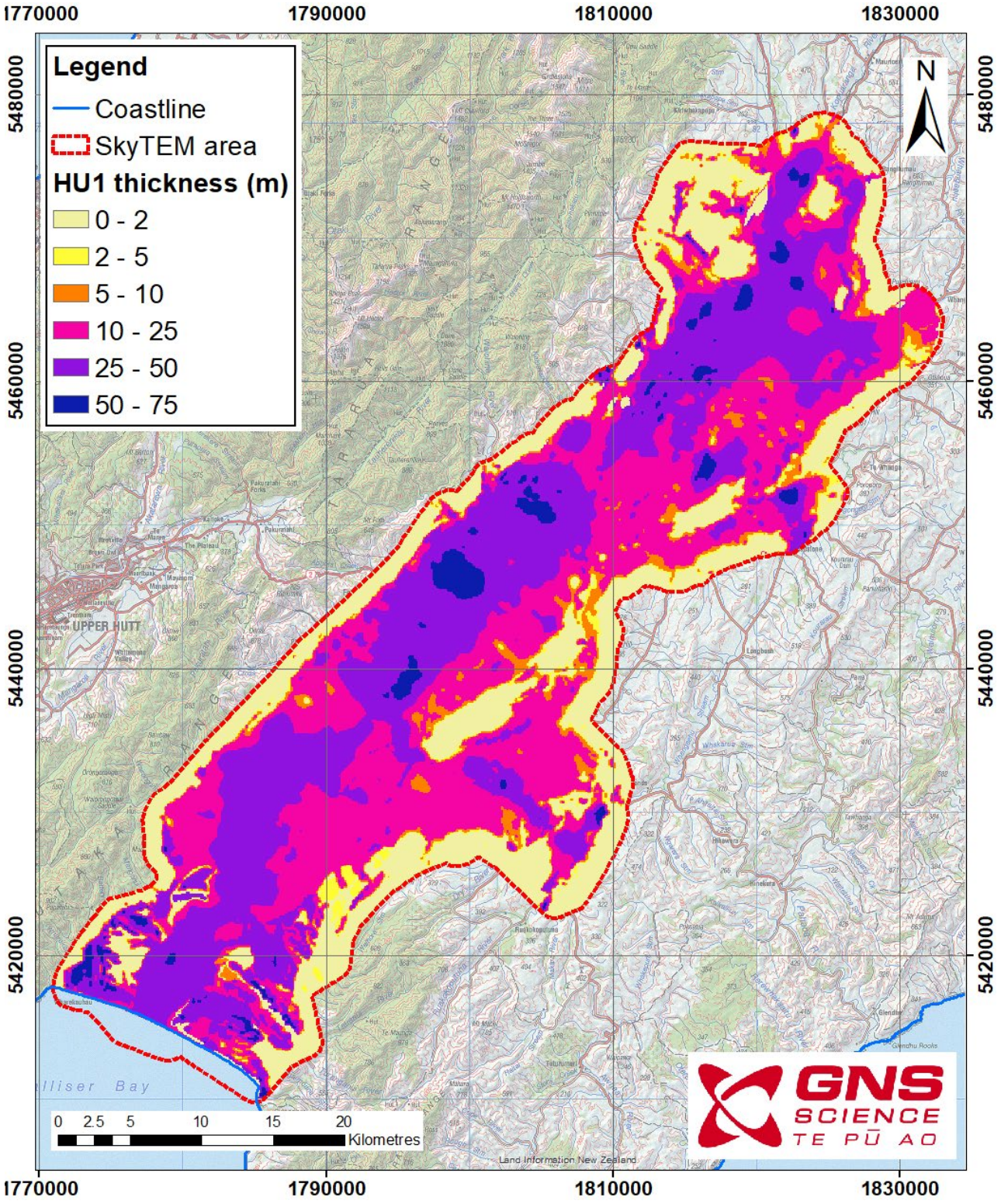

Figure 7.3 Interpreted thickness map of the hydrogeological unit HU-1.

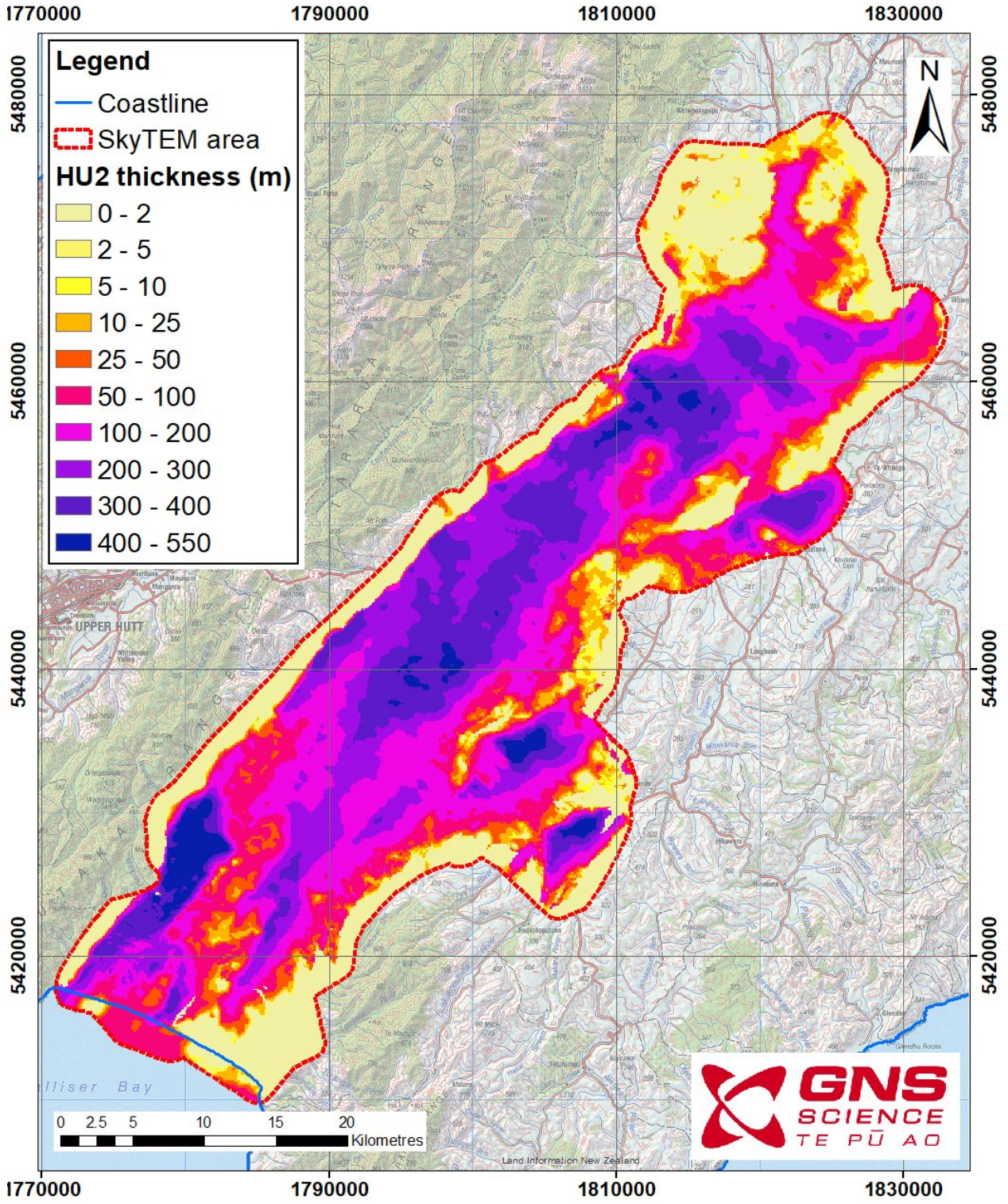

Figure 7.4 Interpreted thickness map of the hydrogeological unit HU-2. Thicknesses greater than 300 m are derived from the interpretation of the gravity and seismic data.

7.3.3 HU-3

HU-3 is the lowermost hydrogeological unit and is bounded by H2 and the basement surface. The construction of the basement surface is described in detail in Section 7.2.2.

The strata in HU-3 are likely composed of more consolidated sediments, primarily deposited during the Pliocene and Miocene periods (e.g. Onoke Group and Palliser Group [Figure 3.2]), including sandstone, mudstone and limestone. The low-resistivity units in the consolidated sedimentary

sequence (Pliocene and Miocene) mainly represent fine-grained dominated mudstone and siltstone and are considered as aquitards in this study. The high-resistivity values in the consolidated part represents a broad range of lithologies ranging from medium- to coarse-grained sandstones, conglomerate and limestone (e.g. Onoke Group and Palliser Group [Figure 3.2]). Although there is limited borehole information from the study area, examples from the Hawke's Bay area (Rawlinson et al. 2024) and global research (Lewis et al. 2006; Woessner and Poeter 2020) show these units can be potential aquifers, especially when faulted and fractured.

7.3.4 Basement Unit

This unit includes the strata below the basement surface. The greywacke exposed in the footwall of the Wairarapa Fault (Tararua Range), the eastern hills (Aorangi Range) and in faulted blocks, such as the Tiffin Anticline in the centre of the basin (see Figure 1.2 for location), consists of indurated sandstone and breccia (Torlesse composite terrane and Pahaoa Group). As described in Sections 3 and 6, these low-grade metasediments have low porosity and low permeability (Mielke et al. 2016). Based on the rock properties, the groundwater potential is considered to be low. However, in certain areas, particularly when the unit is intersected by major faults and situated in low-lying valleys, it may possess limited aquifer potential, due to fracturing of greywacke rocks. Confirming this would require ground-truthing through detail hydrogeological mapping, geophysical surveys or other subsurface exploration techniques.

7.4 Aquifer Potential Model

An Aquifer Potential (AP) model was developed using both hydrogeological unit classification and SkyTEM resistivity (Table 7.1). The model provides a qualitative assessment of the likelihood that each model cell contains aquifer-bearing material. The AP classes were defined by applying specific rules within the major hydrogeological units to determine how each resistivity facies class corresponds to aquifer potential. The thresholds used for the classification were based on a combination of the following:

- Resistivity values of QMAP units (see Section 6).
- Resistivity values of primary lithologies in boreholes (see Section 6).
- Published examples of the resistivity of aquifers and aquitards in similar lithologies.
- The combined experience of the interpretation team.

As described throughout this report, the most likely lithologies to host aquifers are coarse-grained gravel beds within the hydrogeological units HU-1 and HU-2. The next most likely aquifer units are sandy layers in the same intervals. With increasing silt and clay content, the AP will drop. Lithologies within the consolidated section (HU-3) most likely to contain aquifers are the limestone and sandstone beds. The siltstones and mudstones will have lower AP values. Additionally, anomalously high resistivity (>354 ohm.m) in the consolidated units may suggest that water content is very low and thus the AP values decrease.

The numeric value of AP listed in Table 7.1 is designed to provide a simple parameter that can be displayed in a 3D model. The number does not necessarily indicate relative potential between the consolidated and unconsolidated sequence. The AP can be considered separately between the consolidated and unconsolidated sequences. However, for visualisation purposes, it was useful to have the numbers broadly increasing from low to high potential.

In the basement sequence (HU-4), groundwater potential was assumed to be very low everywhere independent of resistivity. This approach assumes that greywacke has low porosity and low permeability.

In the consolidated sequence (HU-3), three aquifer potential classifications were used (low, medium, high), since this unit generally showed less variability in resistivity compared with the overlying unconsolidated units. Regions with resistivity between 63 and 354 ohm.m were interpreted to be likely to contain porous sandstones, and limestones with high aquifer potential. Regions with low or very high resistivity (<32 or >501 ohm.m, respectively) were considered to have low potential. This assessment is subjective but assumes that very low resistivities are more likely to contain mudstone units with low permeability, while very high resistivities within the consolidated sequence are more likely to contain compacted sandstones, conglomerate or limestones with low porosity (and hence low water content). The medium AP values were attributed to regions with resistivities between 32 and 63 ohm.m, which are likely to be siltstones with higher clay content. A second medium classification is given for high resistivities between 354 and 501 ohm.m, where we consider the porosity is likely to be too low to be an aquifer. There are very few boreholes that penetrate the consolidated units, so the thresholds were picked based on the correlation between the SkyTEM and cross-sections on seismic lines (Nicol et al. 2002; Cape et al. 1990) or close to outcrop (see Section 3 and Section 6).

The unconsolidated sequence (HU-1 and HU-2) showed more resistivity and lithological variations than HU-3. Therefore, we considered that five aquifer potential classifications are justified. Regions with resistivity >178 ohm.m were considered to have the highest aquifer potential. Zones of high resistivity between 178 and 500 ohm.m are seen in the top 100 m and correspond closely to thick Quaternary gravel sections (See Section 5 and Section 6). A portion of these high-resistivity zones could be unsaturated. A comparison of the AP with water table levels is essential when using this model. Regions with resistivity between 63 and 178 ohm.m were considered to have high aquifer potential. Like the consolidated sequence, regions with resistivity between 32 and 63 ohm.m were considered to have medium aquifer potential. The regions with resistivity <32 ohm.m were assigned low potential, with an additional category of very low aquifer potential in the unconsolidated sequence for resistivities <16 ohm.m.

Table 7.1 Resistivity thresholds used to determine the Aquifer Potential. Colours in the Aquifer Potential Classification column reflect the colours used in the JavaScript Map Server (Section 7.6).

		Lower Resistivity (ohm.m)	Upper Resistivity (ohm.m)	Aquifer Potential Number	Aquifer Potential Classification
	Basement greywacke	<5.6	>501	1	**Very Low**
Consolidated	**Mudstone**	<5.6	32	2	**Low**
HU-3	**Siltstone**	32	63	5	**Medium**
Miocene	**Sandstone and limestone**	63	354	8	**High**
Pliocene	**Low porosity sandstone**	354	501	5	**Medium**
E Pleistocene	**Very low porosity sandstone**	>501	-	2	**Low**
Unconsolidated	**Clay**	<5.6	16	3	**Very Low**
HU-1 and HU-2	**Clay to silt**	16	32	4	**Low**
Quaternary	**Silt to sand**	32	63	6	**Medium**
Holocene	**Sand to fine gravel**	63	178	7	**High**
	Coarse gravel	178	>501	9	**Highest**

7.5 Uncertainty in Interpretation

Some areas of the model were mapped with greater certainty than others, depending on the resistivity characteristics and the availability of supporting geoscience data to calibrate the interpretations.

Uncertainty can be considered from three main sources:

- Distance of a point from any borehole or geophysical measurement.
- Increase in uncertainty with depth due to the decrease in resolution of the SkyTEM models and lack of deep boreholes.
- Ambiguity in the relationship between resistivity, lithology and aquifer potential.

The SkyTEM coverage is extensive, but there are still areas with poor coverage. Urban areas were not surveyed due to flying restrictions. Powerlines, highways and railway tracks produced significant gaps in the survey due to electrical interference (Kellett et al. 2024). The distribution of boreholes is also uneven, with large areas having no deep borelogs to provide calibration points.

The SkyTEM inversion is well constrained at the surface and increases in uncertainty with depth. The thickness of the model layers increases with depth, so thin aquifers or aquitards can be missed in the modelling. The surficial layers (0–4 m) are affected by changes in the helicopter terrain clearance (e.g. shelter belts and tree coverage) and are also subject to anomalous readings due to weathering or water table depth.

The lack of a resistivity contrasts between different geological units, such as Holocene gravel, mid-early Quaternary gravels and limestone, makes differentiating these zones a challenge. There will be uncertainty associated with the mapping of the surfaces (H1, H2) and the hydrogeological units (HU-1, HU-2 and HU-3). The thickness of HU-1 and HU-2 in some areas, particularly in the southwestern part of the valley and beneath Lake Wairarapa (see Figure 7.3 and Figure 7.4), are poorly constrained.

In areas where the geological units are exposed at the surface, the dips on the contacts allow the layers to be extrapolated to depth. The SkyTEM models that can be traced from the outcrop to the interval at depth provided more certainty on the interpretation. The eastern side of the Ruamāhanga Catchment can be interpreted with high confidence.

Likewise, regions with other geoscience data present, such as the SAHKE MT line (Heise et al. 2013), seismic reflection lines (Nicol et al. 2002; Cape et al. 1990) and deep boreholes, have lower uncertainty in the basement surface interpretation.

A semi-quantitative approach to estimating uncertainty could be undertaken by developing a common risk map that combines the individual uncertainties for different depth extents, however, this is beyond the scope of the present study.

7.6 JavaScript Map Server

GNS has developed a web mapping application that can deliver 2D and 3D geoscience information (JavaScript [JS] Map Server). Originally developed for sedimentary basin studies, it has been adapted to regional tectonics and local aquifer mapping projects. See the following links:

- E Tūhura – Explore Zealandia https://data.gns.cri.nz/tez/index.html
- HBRC 3DAMP https://storymaps.arcgis.com/stories/7455b027ae0540d8a3457de98635ac84

The model was exported from the Leapfrog software in CSV format, which contains points every 50 m horizontally, and increasing from 4 m vertical resolution near the surface to 20 m resolution at depths of 300–500 m below ground level. Each point contains an estimate of resistivity, hydrological unit and aquifer potential. The JS Map Server then interrogates the CSV resistivity model to display the data.

The interface for the mapping tool is shown in Figure 7.5 and Figure 7.6. The tool enables a single point to be interrogated, producing a pseudo-borehole, which contains, from left to right, AP, the nearest smooth SkyTEM resistivity model and hydrogeological unit classification. A cross-section tool allows the user to slice through the model and see the lateral and vertical distribution of aquifer potential, resistivity and hydrogeological unit. The data are interpolated from the CSV file onto the section using nearest neighbour interpolation for AP and hydrogeological unit, and Barnes Surface interpolation for the resistivity values (Barnes 1964).

In addition to the AP model, several maps are presented in the JS Map Server. Selected depth slices in the resistivity model can be viewed, that is, modelled resistivity at a constant depth range below the ground surface. All of the individual depth slices have been provided as part of the resistivity model (Kellett et al. 2024). Also available for display is the interpreted thickness of the Holocene and Upper Pleistocene (i.e. the top unit in the section display, HU-1) and total Quaternary thickness (top two units, HU-1 and HU-2).

The locations of the primary, secondary and third tier boreholes are shown in the JS Map Server. The basic information about each borehole is available by querying the location. For the primary boreholes (Section 5) and a subset of secondary boreholes, the composite geological log (Figure 5.1) is also available as a query. The composite log shows the smooth and sharp resistivity model.

Surface geology, pulled from GNS's 1:250 000 geological map database, can be displayed, as well as topography (shaded relief and colour contoured elevation) derived from the LiDAR data (LINZ 2011). The JS Map Server dynamically links to websites that host much of the raw data and some datasets can be downloaded directly for a local GIS project. However, this JS Map Server is not intended to replace existing delivery mechanisms for this data and users are encouraged to go directly to the source of the data. The borehole logs and the water quality data are available from the GWRC portal:

- https://gwrc-open-data-11-1-gwrc.hub.arcgis.com/datasets/b52e4f95910141118fce229f33928d4c_1/explore
- https://graphs.gw.govt.nz/envmon?view=map

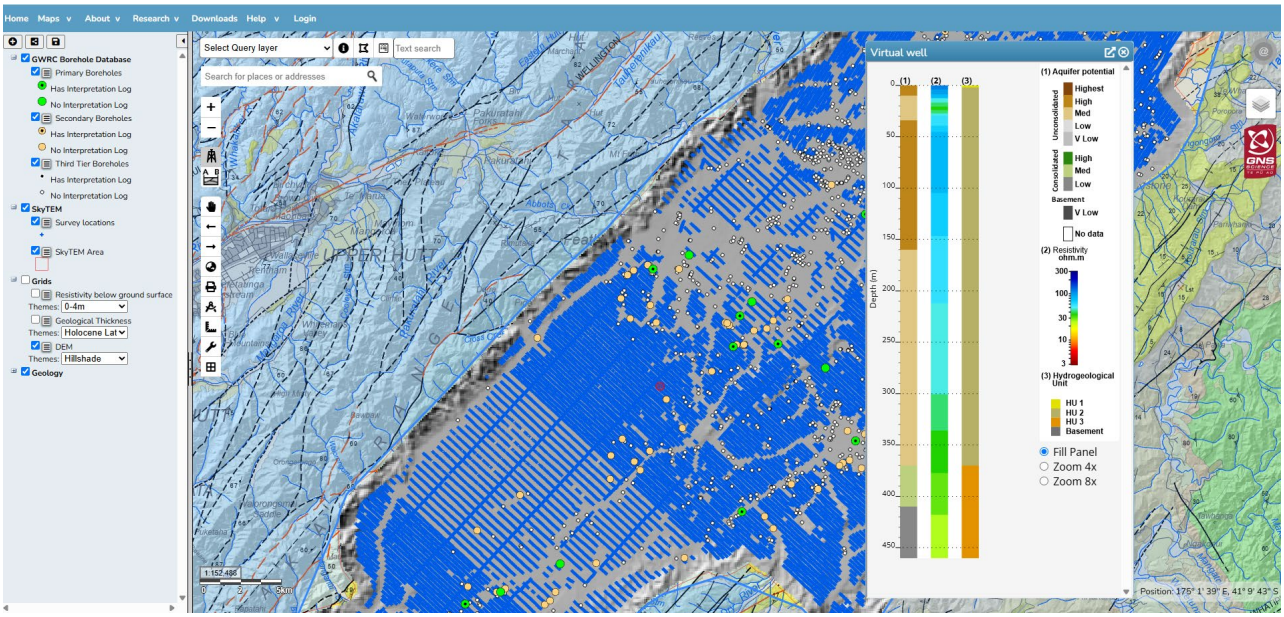

Figure 7.5 Greater Wellington Regional Council Ruamāhanga JavaScript Map Server interface. A pseudo-borehole is presented as an inset window.

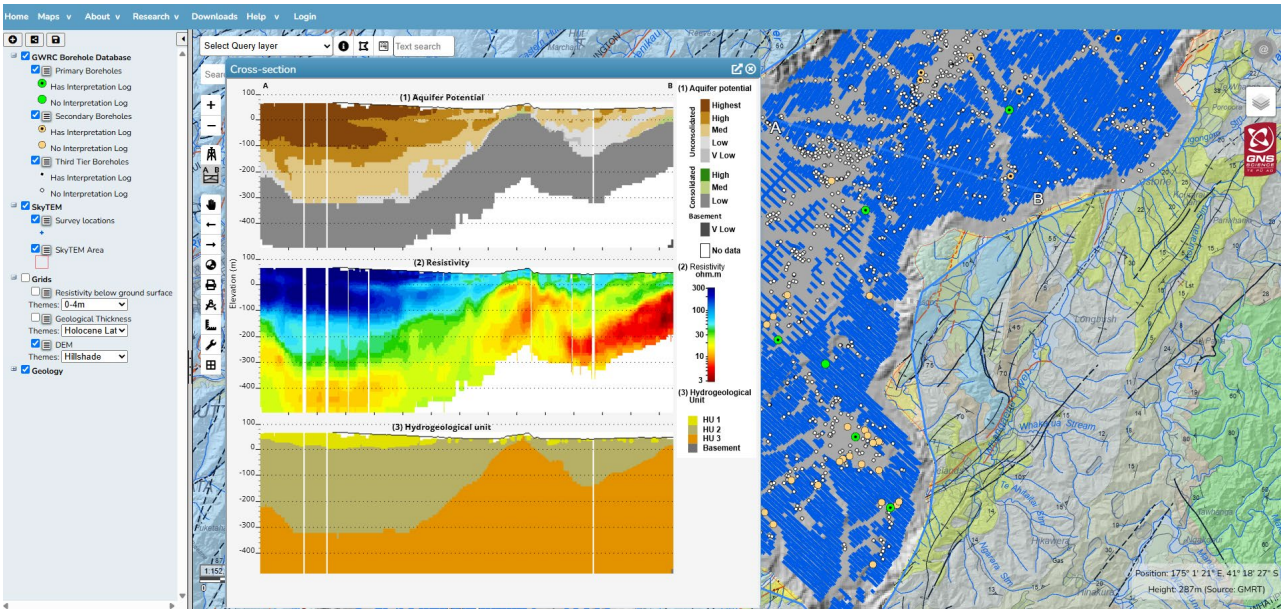

Figure 7.6 Greater Wellington Regional Council Ruamāhanga JavaScript Map Server interface. A cross-section is presented as an inset window.

8.0 Conclusions

Phase 2 of the Ruamāhanga Airborne Aquifer Mapping Project comprised the following tasks:

- Task 1: Review of the geology of the Wairarapa Valley focussed on hydrogeology.
- Task 2: Construction of a layered 3D hydrogeological model (broad scale) and a point- and grid-based 3D hydrogeological model (fine scale).
- Task 3: Delivery of a model on a publicly accessible viewer (JS Map Server).

Task 1 was completed using a series of workshops and a compilation of the existing geological and hydrogeological maps, cross-sections and 3D models.

In Task 2, GNS combined the resistivity model, delivered in Phase 1 (Kellett et al. 2024), with supporting geoscience data to build a series of cross-sections that map the distribution of key horizons and faults across the Ruamāhanga Catchment. Three main horizons were interpreted to guide the development of a conceptual layered model (Base Holocene/Upper Pleistocene, Base Quaternary, Top greywacke basement). GNS held a series of workshops that presented this model to GWRC with a focus on key cross-sections in the Pirinoa, Martinborough, Parkvale, Te Ore Ore and northwest Waingawa areas (see Figure 1.2 for locations). These horizons have been delivered in ASCII grids and a Leapfrog viewer file.

GNS developed a finer-scale hydrogeological model by dividing the SkyTEM resistivity model into four hydrogeological units:

- HU-1 is the Holocene and Late Pleistocene gravel and fine-grained age equivalents (sand, silt, clay, loess and soil)
- HU-2 is the Quaternary gravel, sand, silt and clay. It includes the early and middle Pleistocene unconsolidated units.
- HU-3 is the consolidated lithological formations in the Pliocene and Miocene. It may include some early Pleistocene consolidated units. These rock types are conglomerate, sandstone, mudstone and limestone.
- Basement is the Mesozoic greywacke sandstones and mudstones that crop out in the ranges and in parts of the valley. The greywacke basement underlies the entire area.

Resistivity facies discrimination based on the outcrops in surface geology, and the lithologies in the borehole logs, was the primary method used to map the SkyTEM resistivity into geological facies. A hydrogeological model that captures the resistivity, hydrogeological unit and the AP at each depth interval has been developed at the individual SkyTEM model points (147,601 locations) and an interpolated 3D model (100 x 100 m grid). These large datasets have been delivered as ASCII text files. The Leapfrog 3D viewer that contains all of the models has also been delivered.

In Task 3, the 3D hydrogeological model was presented in a web-based mapping package (JS Map Server). The web-based mapping application also displays key geological information, such as the QMAP geological layer, the thickness of the hydrogeological layers (HU-1 and HU-2) and the distribution of boreholes. The JS Map Server tool allows the hydrogeological model to be presented as pseudo-boreholes or user-defined cross-sections. As part of Task 3, a pilot area was built and a public workshop was held to gather feedback on the JS Map Server product. This feedback focused on reducing the complexity of the information delivered and adjusting some of the colour schemes to clarify the presented material.

Some areas of the model were mapped with greater certainty than others, depending on the density of SkyTEM models, the resistivity characteristics of the subsurface and the availability of supporting geoscience data to calibrate the interpretations.

This report provides the supporting material that will allow a user of the 3D hydrogeological model to understand the data that is in the model and the methods used to build the model.

The majority of the GIS layers and resistivity models have been delivered to GWRC in Phase 1 of the project (Kellett et al. 2024). The following products are delivered as part of Phase 2:

- GIS Layers of key surfaces and grids (H1, H2, Basement, HU-1, HU-2, HU-3).
- Resistivity facies models.
- Aquifer Potential models.
- A LeapFrog viewer file containing the products above.
- A live link to the JS Map Server.

9.0 Recommendations

The hydrogeological model developed in this project is a continuation of the models developed in earlier studies (Gyopari and McAlister 2010a, 2010b, 2010c). It has incorporated the previous information and increased the level of complexity based on the availability of the SkyTEM resistivity data. The resistivity models derived from the SkyTEM data show a good correlation with the geological data available in boreholes, surficial mapping and previous interpreted cross-sections. However, some areas of the SkyTEM models are still poorly constrained due to the following:

- Incomplete coverage caused by infrastructure (towns, railway, road and powerline corridors).
- Lack of resistivity contrasts between different geological units. For example, Holocene gravel, Pleistocene gravel, sandstone and limestone all produce similar responses in the SkyTEM data, but likely have different hydrogeological properties.
- The shallow layers (0–4 m) can include partially saturated intervals that are not well imaged by the SkyTEM system.
- The resolution of the SkyTEM system decreases with depth, so thin aquifers or aquitards can be missed in the modelling.

Some of this uncertainty could be addressed by focussing on smaller areas and incorporating a more detailed correlation with the geology, hydrogeology, groundwater chemistry and aquifer properties. A more quantitative assessment of uncertainty could be considered using a common risk mapping approach that includes distance from calibration points and sensitivity of the SkyTEM models.

The distribution of deep boreholes (>100 m) with detailed geological information is poor. Additional drilling in areas where the hydrogeological model has identified potential deeper aquifers is needed to support the model. Additional drilling in the coastal area could provide information on preferential pathways for saline intrusion into the aquifers.

Additional data are also required to understand the differences between the different Holocene gravel units on the terraces and the river connected modern gravels, as well as the deeper Pleistocene partially consolidated gravel units. Drilling and higher resolution ground-based geophysical surveys are needed to test these connections.

More detailed analysis of groundwater chemistry, aquifer properties and any other data that provides information of groundwater distribution should be included on the next phase of interpretation of these SkyTEM derived models. The SkyTEM resistivity models and the derived AP values can be farther refined by focussing on the screened intervals of boreholes with pump tests, slug tests and documented consented volumes of groundwater abstraction.

The current model is a good basis for the development of hydrogeological flow models that can support groundwater management. Work undertaken by Rawlinson (2023) has demonstrated how the SkyTEM-derived aquifer potential volumes can be translated into hydraulic conductivity and transmissivity volumes for rapid and reliable flow model construction.

The models produced by Phase 2 of the project should be made available on the JS Map Server to allow a wide range of users to identify areas of interest. The more detailed hydrogeological model data could then be made available for additional analysis. The raw SkyTEM data may be reprocessed in the future using more advanced methods and at a more detailed scale. These raw SkyTEM data should also be available for groundwater professionals to undertake additional work.

10.0 Acknowledgements

This work has been jointly funded by the New Zealand Government's Kānoa – REDIU (formerly the Provincial Development Unit), Greater Wellington Regional Council (GWRC), Masterton District Council, Carterton District Council and South Wairarapa District Council.

Rebecca Poole (Tetratech) has provided careful project management through Phase 2 of this project and maintained key contact with the funding agency Kānoa.

Thank you to Rob van der Raaij, Lindsay Annear, Mike Thompson, Helli Ward, Kerry Charles, Sasha Smith and Pete Huggins of GWRC for their contributions in workshops and public meetings as part of this project.

Thank you to Chris Worts and Kate Osborn for business partnerships support. Thank you to Zara Rawlinson, Rob Reeves and Malcolm Arnot for providing report reviews.

11.0 References

Arnot MJ. 1989. Geology of the Waihora Stream area, western Aorangi Range, Wairarapa [BSc(Hons) thesis]. Wellington (NZ): Victoria University of Wellington. 86 p. + map.

Auken E, Christiansen AV, Kirkegaard C, Fiandaca G, Schamper C, Behroozmand AA, Binley A, Nielsen E, Effersø F, Christensen NB, et al. 2015. An overview of a highly versatile forward and stable inverse algorithm for airborne, ground-based and borehole electromagnetic and electric data. *Exploration Geophysics*. 46(3):223–235. https://doi.org/10.1071/EG13097

Auken E, Boesen T, Christiansen AV. 2017. Chapter two - a review of airborne electromagnetic methods with focus on geotechnical and hydrological applications from 2007 to 2017. In: Nielsen L, editor. *Advances in Geophysics*. [Cambridge (MA)]: Elsevier. p. 47–93. (Advances in Geophysics; 58). https://doi.org/10.1016/bs.agph.2017.10.002

Barnes SL. 1964. A technique for maximizing details in numerical weather map analysis. *Journal of Applied Meteorology and Climatology*. 3(4):396–409. https://doi.org/10.1175/1520-0450(1964)003%3C0396:ATFMDI%3E2.0.CO;2

Begg JG. Date unknown. Notes to accompany cartoon cross sections, Turanganui area, southeast Wairarapa. [Masterton] (NZ): J Begg Geo Ltd. Client Report.

Begg JG. 2020. Groundwater in the Turanganui area: supplementary notes on cartoon profiles. [Masterton] (NZ): J Begg Geo Ltd. Client Report.

Begg JG, Johnston MR, compilers. 2000. Geology of the Wellington area [map]. Lower Hutt (NZ): Institute of Geological & Nuclear Sciences. 1 sheet + 64 p., scale 1:250,000. (Institute of Geological & Nuclear Sciences 1:250,000 geological map; 10).

Begg JG, Brown LJ, Gyopari M, Jones A. 2005. A review of the Wairarapa geology – with a groundwater bias. Lower Hutt (NZ): Institute of Geological & Nuclear Sciences. 34 p. Client Report 2005/159. Prepared for Greater Wellington Regional Council.

Beu AG. 1995. Pliocene limestones and their scallops: lithostratigraphy, pectinid biostratigraphy and paleogeography of eastern North Island Late Neogene limestone. Lower Hutt (NZ): Institute of Geological & Nuclear Sciences. 243 p. (Institute of Geological & Nuclear Sciences monograph; 10).

Bloom AL. 1951. The geology along the south-east flank of the Rimutaka Mountains, New Zealand [Master's thesis]. Wellington (NZ): Victoria University of Wellington. 80 p.

Bowler S. 1998. The gravity signature of the Wairarapa Fault in the Featherston region [abstract]. In: Bassett KN, Nobes DC, editors. *Geological Society of New Zealand, New Zealand Geophysical Society 1998 Joint Annual Conference: programme & abstracts*; 1998 Nov 30–Dec 3; Christchurch, NZ. Wellington (NZ): Geological Society of New Zealand. p. 49. (Geological Society of New Zealand miscellaneous publication; 101a).

Cape CD. 1989. Geophysical profiling of the Wairarapa Basin, New Zealand. Wellington (NZ): Department of Scientific and Industrial Research, Geophysics Division. 40 p. Research Report 227.

Cape CD, Lamb SH, Vella P, Wells PE, Woodward DJ. 1990. Geological structure of Wairarapa Valley, New Zealand, from seismic reflection profiling. *Journal of the Royal Society of New Zealand*. 20(1):85–105. https://doi.org/10.1080/03036758.1990.10426734

Christiansen AV, Auken E. 2012. A global measure for depth of investigation. *Geophysics*. 77(4):WB171–WB177. https://doi.org/10.1190/geo2011-0393.1

Clark KJ, Hayward BW, Cochran UA, Grenfell HR, Hemphill-Haley E, Mildenhall DC, Hemphill-Haley MA, Wallace LM. 2011. Investigating subduction earthquake geology along the southern Hikurangi Margin using palaeoenvironmental histories of intertidal inlets. *New Zealand Journal of Geology and Geophysics*. 54(3):255–271. https://doi.org/10.1080/00288306.2011.562903

Coffey GL, Litchfield NJ. 2023. Ground truthing and preliminary slip rates and recurrence intervals for four newly identified faults in the Wairarapa region. Lower Hutt (NZ): GNS Science. 37 p. (GNS Science report; 2023/39). https://doi.org/10.21420/vyta-3574

Collen JD, Vella P. 1984. Hautotara, Te Muna and Ahiaruhe Formations, middle to late Pleistocene, Wairarapa, New Zealand. *Journal of the Royal Society of New Zealand*. 14(4):297–317. https://doi.org/10.1080/03036758.1984.10421732

Daughney CJ, Guggenmos M, McAlister D, Begg J, Jackson B. 2009. Assessment of groundwater and surface water chemistry in the Upper and Lower Wairarapa Valley. Lower Hutt (NZ): GNS Science. 29 p. (GNS Science report; 2009/21).

Fullagar PK, Hughes NA, Paine J. 2000. Drilling-constrained 3D gravity interpretation. *Exploration Geophysics*. 31(1–2):17–23. https://doi.org/10.1071/EG00017

Gyopari MC, McAlister D. 2010a. Wairarapa Valley groundwater resource investigation: Upper Valley catchment hydrogeology and modelling. Wellington (NZ): Greater Wellington Regional Council. 303 p. (Technical publication; GW/EMI-T-10/74).

Gyopari MC, McAlister D. 2010b. Wairarapa Valley groundwater resource investigation: Middle Valley catchment hydrogeology and modelling. Wellington (NZ): Greater Wellington Regional Council. 371 p. (Technical publication; GW/EMI-T-10/73).

Gyopari MC, McAlister D. 2010c. Wairarapa Valley groundwater resource investigation: Lower Valley catchment hydrogeology and modelling. Lower Hutt (NZ): Greater Wellington Regional Council. 131 p. (Technical publication; GW/EMI-T-10/75).

Hayward BW, Grenfell HR, Sabaa AT, Kay J, Clark K. 2011. Ecological distribution of the foraminifera in a tidal lagoon-brackish lake, New Zealand, and its Holocene origins. *Journal of Foraminiferal Research*. 41(2):124–137. https://doi.org/10.2113/gsjfr.41.2.124

Heise W, Caldwell TG, Bertrand EA, Hill GJ, Bennie SL, Ogawa Y. 2013. Changes in electrical resistivity track changes in tectonic plate coupling. *Geophysical Research Letters*. 40(19):5029–5033. https://doi.org/10.1002/grl.50959

Henderson R. 1999. A geophysical investigation into the structure of the Te Maire ridge area, Wairarapa [abstract]. In: Wallace C, editor. *Geological Society of New Zealand Inc 1999 Annual Conference: programme and abstracts*; 1999 Nov 29–Dec 1; Palmerston North, NZ. Wellington (NZ): Geological Society of New Zealand. p. 59. (Geological Society of New Zealand miscellaneous publication; 107a).

Heron DW, custodian. 2023. Geological map of New Zealand 1:250,000. 4th ed. Lower Hutt (NZ): GNS Science. Scale 1:250,000. (GNS Science geological map; 1).

Hicks SR, Woodward DJ. 1978. Gravity models of the Wairarapa region, New Zealand. *New Zealand Journal of Geology and Geophysics*. 21(5):539–544. https://doi.org/10.1080/00288306.1978.10424083

Holdgate G. 1999a. A review of the geology & geophysics for PEP38334 – East Coast Basin, North Island New Zealand. 42 p. + 2 enclosures. Located at: Ministry of Business, Innovation & Employment, Wellington, NZ. New Zealand Unpublished Petroleum Report 2446.

Holdgate G. 1999b. A review of the geology & geophysics for PEP38338 – Cook Strait – East Coast Basin, New Zealand. 29 p. + 31 enclosures. Located at: Ministry of Business, Innovation & Employment, Wellington, NZ. New Zealand Unpublished Petroleum Report 2464.

Hughes B, Gyopari M. 2014. Wairarapa Valley groundwater resource investigation: framework for conjunctive water management. Wellington (NZ): Greater Wellington Regional Council. Report GW/ESCI-T-14/94. 320 p.

Ingham M. 2014. Magnetotelluric survey of the Chester, Tiffin/Peter Cooper and Gladstone anticlines. 67 p. + 9 enclosures. Located at: Ministry of Business, Innovation & Employment, Wellington, NZ. New Zealand Unpublished Petroleum Report 4962.

Johnson P, Mourot F, Rawlinson ZJ, Tschritter C, Weir J. 2019. New Zealand Groundwater Atlas: 3D groundwater models around new Zealand (a review). Lower Hutt (NZ): GNS Science. 51 p. Consultancy Report 2019/139. Prepared for Ministry for the Environment.

Jones A, Gyopari M. 2006. Regional conceptual and numerical modelling of the Wairarapa groundwater basin. Wellington (NZ): Greater Wellington Regional Council. 79 p. + 6 appendices.

Kellett RL, Begg JG, Brakenrig T, Macdonald N, Boyes AF. 2022. Ground geophysical and geological investigations of aquifer characteristics in southern Wairarapa. Lower Hutt (NZ): GNS Science. 73 p. Consultancy Report 2022/69. Prepared for Greater Wellington Regional Council.

Kellett RL, Kirkby AL, Keats BS, Sanders F, Brakenrig T, Berhe DT, Coup L, Herpe M. 2024. Ruamāhanga Airborne Aquifer Mapping Project: SkyTEM data processing and resistivity models. Lower Hutt (NZ): GNS Science. 96 p. Consultancy Report 2024/60. Prepared for Greater Wellington Regional Council.

Knight R, Smith R, Asch T, Abraham J, Cannia J, Viezzoli A, Fogg G. 2018. Mapping aquifer systems with airborne electromagnetics in the Central Valley of California. *Groundwater*. 56(6):893–908. https://doi.org/10.1111/gwat.12656

Leach BF, Anderson AJ. 1974. The transformation from an estuarine to lacustrine environment in the lower Wairarapa. *Journal of the Royal Society of New Zealand*. 4(3):267–275. https://doi.org/10.1080/03036758.1974.10419394

Lee JM, Begg JG, compilers. 2002. Geology of the Wairarapa area [map]. Lower Hutt (NZ): Institute of Geological & Nuclear Sciences. 1 folded map + 66 p., scale 1:250,000. (Institute of Geological & Nuclear Sciences 1:250,000 geological map; 11).

Lewis MA, Cheney CS, ÓDochartaigh BÉ. 2006. Guide to Permeability Indices. Nottingham (GB): British Geological Survey. Open report CR/06/160N. 20 p.

[LINZ] Toitū Te Whenua Land Information New Zealand. 2011. NZ Topo250 maps. Wellington (NZ): LINZ; [updated 2024 Mar 20; accessed 2024 Jun]. https://data.linz.govt.nz/layer/50798-nz-topo250-maps/

McClymont AF. 2000. A gravity survey of the Wharekauhau Thrust, Palliser Bay, New Zealand. *New Zealand Journal of Geology and Geophysics*. 43(2):303–306. https://doi.org/10.1080/00288306.2000.9514888

Mielke P, Weinert S, Bignall G, Sass I. 2016. Thermo-physical rock properties of greywacke basement rock and intrusive lavas from the Taupo Volcanic Zone, New Zealand. *Journal of Volcanology and Geothermal Research*. 324:179–189. https://doi.org/10.1016/j.jvolgeores.2016.06.002

Minsley BJ, Rigby JR, James SR, Burton BL, Knierim KJ, Pace MDM, Bedrosian PA, Kress WH. 2021. Airborne geophysical surveys of the lower Mississippi Valley demonstrate system-scale mapping of subsurface architecture. *Communications Earth & Environment*. 2:131. https://doi.org/10.1038/s43247-021-00200-z

Moore C, Gyopari M, Toews M, Mzila D. 2017. Ruamāhanga catchment groundwater modelling. Lower Hutt (NZ): GNS Science. 189 p. Consultancy Report 2016/162. Prepared for Greater Wellington Regional Council.

Morgenstern R, Litchfield NJ, Langridge RM, Heron DW, Townsend DB, Villamor P, Barrell DJA, Ries WF, Van Dissen RJ, Clark KJ, et al. 2024. New Zealand Active Faults Database: the high-resolution dataset v2.0. *New Zealand Journal of Geology and Geophysics.* 1–16. https://doi.org/10.1080/00288306.2024.2427396

Morgenstern U. 2005. Wairarapa Valley groundwater: residence time, flow pattern and hydrochemistry trends. Lower Hutt (NZ): Institute of Geological & Nuclear Sciences. 36 p. (Institute of Geological & Nuclear Sciences science report; 2005/33).

Nicol A, Van Dissen R, Vella P, Alloway B, Melhuish A. 2002. Growth of contractional structures during the last 10 m.y. at the southern end of the emergent Hikurangi forearc basin, New Zealand. *New Zealand Journal of Geology and Geophysics*. 45(3):365–385. https://doi.org/10.1080/00288306.2002.9514979

O'Dea T, Donaldson IG, King M, Martin GN, Thorpe HR, Wilshere DS, Wilson DD. 1980. Wairarapa groundwater study: report by scientific advisory group. [Masterton] (NZ): Wairarapa Catchment Board. 89 p.

Palacky GJ. 1987. Resistivity characteristics of geologic targets. In: Nabighian MN, editor. *Electromagnetic methods in applied geophysics. Volume 1: theory*. Tulsa (OK): Society of Exploration Geophysicists. p. 53–130. https://doi.org/10.1190/1.9781560802631.ch3

Rawlinson Z. 2013. A review of the most effectual and economical geophysical techniques for characterising groundwater within New Zealand. Lower Hutt (NZ): GNS Science. 90 p. (GNS Science report; 2013/38).

Rawlinson ZJ. 2023. Hawke's Bay 3D Aquifer Mapping Project: 3D hydrogeological models from SkyTEM data in the Heretaunga plains. Lower Hutt (NZ): GNS Science. 69 p. Consultancy Report 2023/57. Prepared for Hawke's Bay Regional Council.

Rawlinson ZJ, Foged N, Westerhoff RS, Kellet RL. 2021. Hawke's Bay 3D Aquifer Mapping Project: Heretaunga Plains SkyTEM data processing and resistivity models. Wairakei (NZ): GNS Science. 90 p. Consultancy Report 2021/93. Prepared for Hawke's Bay Regional Council. https://www.hbrc.govt.nz/assets/Document-Library/Reports/Hawkes-Bay-3D-Aquifer-Mapping-Project-Heretaunga-Plains-SkyTEM-data-processing-and-resistivity-models.pdf

Rawlinson ZJ, Sahoo TR, Kellett RL, Cameron SG. 2024. Hawke's Bay 3D Aquifer Mapping Project: hydrogeological interpretation of the SkyTEM-derived resistivity models within the Poukawa and Otane basins. Wairakei (NZ): GNS Science. 96 p. Consultancy Report 2021/12. Prepared for Hawke's Bay Regional Council.

Sahoo TR, Rawlinson ZJ, Kellett RL. 2023. Hawke's Bay 3D Aquifer Mapping Project: delineation of major hydrological units within the Heretaunga Plains from SkyTEM-derived resistivity models. Lower Hutt (NZ): GNS Science. 55 p. Consultancy Report 2022/30. Prepared for Hawke's Bay Regional Council.

Seebeck H, Van Dissen R, Litchfield N, Barnes P, Nicol A, Langridge R, Barrell DJA, Villamor P, Ellis S, Rattenbury M, et al. 2022. New Zealand Community Fault Model – version 1.0. Lower Hutt (NZ): GNS Science. 97 p. (GNS Science report; 2021/57). https://doi.org/10.21420/GA7S-BS61

Stagpoole V, Caratori Tontini F, Fukuda Y, Woodward D. 2022. New Zealand gravity reference stations 2020: history and development of the gravity network. *New Zealand Journal of Geology and Geophysics*. 65(2):362–373. https://doi.org/10.1080/00288306.2021.1886120

Toews MW, Donath F. 2015. Capture zone delineation of community supply wells and State of the Environment monitoring wells in the Greater Wellington Region. Lower Hutt (NZ): GNS Science. 63 p. (GNS Science report; 2015/06).

Toews MW, Daughney CJ, Cornaton FJ, Morgenstern U, Evison RD, Jackson BM, Petrus K, Mzila D. 2016. Numerical simulation of transient groundwater age distributions assisting land and water management in the Middle Wairarapa Valley, New Zealand. *Water Resources Research*. 52(12):9430–9451. https://doi.org/10.1002/2016WR019422

Van der Raaij R. 2024. Parkvale groundwater quality investigation 2023–2024. Wellington (NZ): Greater Wellington Regional Council. Publication GW/KI-G-24-09. 70 p.

Vella P. 1963. Upper Pleistocene succession in the inland part of Wairarapa Valley, New Zealand. *Transactions of the Royal Society of New Zealand: Geology*. 2(4):63–78.

Warnes PN. 1992. Last interglacial and last glacial stage terraces on the eastern side of Wairarapa Valley between Waiohine and Waingawa rivers. *Journal of the Royal Society of New Zealand*. 22(4):217–228. https://doi.org/10.1080/03036758.1992.10420817

Wells PE. 1989. Late Neogene stratigraphy of the Carrington area, western Wairarapa, North Island, New Zealand. *Journal of the Royal Society of New Zealand*. 19(3):283–303.

White PA, Moreau M, Mourot F, Rawlinson ZJ. 2019. New Zealand Groundwater Atlas: hydrogeological-unit map of New Zealand. Rev. 2022. Wairakei (NZ): GNS Science. 97 p. Consultancy Report 2019/144. Prepared for Ministry for the Environment.

Woessner WW, Poeter EP. 2020. Hydrogeologic properties of earth materials and principles of groundwater flow. Guelph (ON): The Groundwater Project. https://doi.org/10.21083/978-1-7770541-2-0

1 Fairway Drive, Avalon 5011
PO Box 30368, Lower Hutt 5040

gns.cri.nz